ISTANBUL TECHNICAL UNIVERSITY ★ GRADUATE SCHOOL OF SCIENCE ENGINEERING AND TECHNOLOGY

PRELIMINARY DESIGN OF AN ELECTRIC PROPULSION SYSTEM FOR LUNAR NANOSATELLITE MISSION

M.Sc. THESIS

Emine ÇALIK

Department of Aeronautics and Astronautics Engineering

Aeronautics and Astronautics Engineering Programme

DECEMBER 2019

ISTANBUL TECHNICAL UNIVERSITY ★ GRADUATE SCHOOL OF SCIENCE ENGINEERING AND TECHNOLOGY

PRELIMINARY DESIGN OF AN ELECTRIC PROPULSION SYSTEM FOR LUNAR NANOSATELLITE MISSION

M.Sc. THESIS

Emine ÇALIK
(511171108)

Department of Aeronautics and Astronautics Engineering

Aeronautics and Astronautics Engineering Programme

Thesis Advisor: Prof. Dr. Alim Rüstem ASLAN

DECEMBER 2019

ISTANBUL TEKNİK ÜNİVERSİTESİ ★ FEN BİLİMLERİ ENSTİTÜSÜ

NANO UYDULU AY GÖREVİNDE KULLANILACAK BİR ELEKTRİK İTKİ SİSTEMİNİN ÖN TASARIMI

YÜKSEK LİSANS TEZİ

Emine ÇALIK
(511171108)

Uçak ve Uzay Mühendisliği Anabilim Dalı

Uçak ve Uzay Mühendisliği Programı

Tez Danışmanı: Prof. Dr. Alim Rüstem ASLAN

ARALIK 2019

Emine ÇALIK, a M.Sc. student of ITU Graduate School of Science Engineering and Technology student ID 511171108, successfully defended the thesis entitled "PRELIMINARY DESIGN OF AN ELECTRIC PROPULSION SYSTEM FOR LUNAR NANOSATELLITE MISSION", which she prepared after fulfilling the requirements specified in the associated legislations, before the jury whose signatures are below.

Thesis Advisor :	**Prof. Dr. Alim Rüstem ASLAN** İstanbul Technical University	.....
Jury Members :	**Dr. Öğr. Üyesi Cuma Yarım** Istanbul Technical University	.....
	Prof.Dr. Emrah Kalemci Sabancı University	.....

Date of Submission : 15 November 2019
Date of Defense : 17 December 2019

To my family and my dreams,

FOREWORD

I owe my family and my friends a debt of gratitude for supporting and encouraging me in my all experience. I would like to give my endless thanks everyone and everything that inspire me and increase my curiosity in astronautical engineering field. I would like to thank my thesis supervisor who was always ready to help me during my entire study and the valuable jury members for their valuable comments.

I hope that the preliminary design of the nanosatellite propulsion system provided in this study will be an inspiration and basis for future studies and I hope that this preliminary design will be improved and used someday.

December 2019

Emine ÇALIK
(Astronautical Engineer)

TABLE OF CONTENTS

Page

FOREWORD ..... **ix**
TABLE OF CONTENTS ..... **xi**
ABBREVIATIONS ..... **xiii**
SYMBOLS ..... **xv**
LIST OF TABLES ..... **xix**
LIST OF FIGURES ..... **xxi**
SUMMARY ..... **xxiii**
ÖZET ..... **xxvii**
1. INTRODUCTION **1**
2. BACKGROUND **5**
2.1 Chemical Propulsion Systems 5
2.1.1 Liquid propellant propulsion systems 5
2.1.1.1 Hydrazine propellant thrusters 5
2.1.1.2 Non-toxic or green propellant thrusters 6
2.1.2 Gas propellant propulsion systems 8
2.1.3 Solid propellant propulsion systems 9
2.2 Electric Propulsion Systems 9
2.2.1 Resistojet thrusters 10
2.2.2 Ion thrusters 11
2.2.3 Electrospray thrusters 12
2.2.4 Pulsed plasma thrusters 13
2.2.5 Vacuum arc thrusters 14
2.2.6 Hall-effect thrusters 14
3. A LUNAR NANOSATELLITE MISSION ANALYSIS **17**
3.1 Specification of the Nanosatellite for Lunar Mission 20
3.1.1 Structure and mass limitations 22
3.1.2 Power limitation 24
3.2 Transfer Trajectory to the Moon 27
3.2.1 Direct transfer from LEO to LLO 27
3.2.2 Direct transfer from GTO to LLO 28
3.2.3 Spiral transfer 30
3.2.4 Weak stability boundary 31
3.3 Prediction of Lunar Mission Requirements 32
3.4 Selection of Propulsion System Type Due to the Mission 32
4. PROPULSION SYSTEM DESIGN FOR LUNAR MISSION **37**
4.1 Conceptual Design of the Propulsion System 39
4.1.1 Ionization chamber 40
4.1.2 Ion optics 42
4.1.3 Power processing unit 43
4.1.4 Propellant tank 43
4.1.5 Mass flow control unit 43
4.1.6 RF generator 44

4.1.7 Neutralizer 44
4.2 Preliminary Design of the Propulsion System 44
4.2.1 RF plasma ionization 44
4.2.2 Preliminary design of the ion optics 48
4.2.2.1 Determination of grid parameters 48
4.2.2.2 Determination of grid potentials 51
4.2.3 Thrust 53
4.2.4 Specific impulse 56
4.2.5 Power consumption 57
4.2.6 Efficiency 58
4.2.7 Propellant selection 59
4.2.7.1 Mercury 59
4.2.7.2 Xenon 60
4.2.7.3 Argon 61
4.2.7.4 Iodine 61
4.2.7.5 Krypton 62
4.3 Performance Calculations of the Propulsion System 67
4.4 Structural and CAD Design of the Propulsion System 75
4.5 Summary 82
5. CONCLUSIONS AND RECOMMENDATIONS 85
REFERENCES 89
APPENDICES 97
CURRICULUM VITAE 99

ABBREVIATIONS

3D : Three Dimensional
ADCS : Attitude Determination and Control System
ADN : Ammonium Dinitramide
CAD : Computer-aided Design
CC : Carbon-Carbon Composite
CCP : Capacitively Coupled Plasma
CDHS : Command and Data Handling System
CNAPS : Canadian Nanosatellite Advanced Propulsion System
COMM : Communication System
DC : Direct Current
DSSP : Digital Solid State Propulsion
EPS : Electrical Power System
ESA : European Space Agency
EURECA : The European Retrievable Carrier
GEO : Geosynchronous Earth Orbit
GHz : Gigahertz
GTO : Geostationary Transfer Orbit
HAN : Hydroxyl Ammonium Nitrate
IAPS : Ion Auxiliary Propulsion System
ICP : Inductively Coupled Plasma
ISRO : Indian Space Research Organization
JAXA : Japan Aerospace Exploration Agency
KHz : Kilohertz
LEO : Low Earth Orbit
LLO : Low Lunar Orbit
MarCO : Mars Cube One
MEMS : Microelectromechanical Systems
MFCU : Mass Flow Control Unit
MHz : Megahertz
MIT : Massachusetts Institute of Technology

MLI **:** Multi-layer Insulation

NASA **:** National Aeronautics and Space Administration

NSTAR **:** NASA Solar Technology Application Readiness

PPU **:** Power Processing Unit

PTFE **:** Polytetrafluoroethylene (Teflon)

RF **:** Radio Frequency

RFG **:** Radio Frequency Generator

RIT **:** Radio Frequency Ion Thruster

RX **:** Receiver

SCCM **:** Standard Cubic Centimeters per Minute

SERT-1 **:** Space Electric Rocket Test -1

SFL **:** Space Flight Laboratory

SLS **:** Space Launch System

SMAP **:** Soil Moisture Active Passive

SOI **:** Sphere of Influence

SPT **:** Stationary Plasma Thruster

SSO **:** Sun Synchronous Orbit

SSTL **:** Surrey Satellite Technology Ltd.

TCS **:** Thermal Control System

TLI **:** Trans Lunar Injection Maneuver

TMI **:** Trans Mars Injection Maneuver

TRL **:** Technology Readiness Level

TX **:** Transmitter

VASIMR **:** Variable Specific Impulse Magnetoplasma Rocket

UK **:** United Kingdom

UTIAS **:** University of Toronto Institute for Aerospace Studies

US, USA **:** United States of America

XIPS **:** Xenon Ion Propulsion System

SYMBOLS

E	**:** Energy, electrical field
K	**:** Kinetic energy
U	**:** Potential energy
v	**:** Orbital velocity
m	**:** Total mass of planetary satellite
M	**:** Mass of planetary object
g	**:** Gravitational acceleration
G	**:** Universal gravitational constant
r	**:** Radius of orbit of satellite
F	**:** Force, thrust
μ	**:** Standard gravitational parameter
a	**:** Acceleration
ΔV	**:** Delta-V, change of velocity
$\boldsymbol{B_z}$	**:** Magnetic field
N	**:** Number of turns of RF coil
I	**:** Current
μ_0	**:** Vacuum permeability
$\boldsymbol{\omega}$	**:** Cyclic frequency
$\boldsymbol{f}$	**:** RF frequency
$\boldsymbol{n_e}$	**:** Plasma electron density
$\boldsymbol{n_i}$	**:** Plasma ion density
$\boldsymbol{e}$	**:** Electron charge
q	**:** Particle charge
$\boldsymbol{k_B}$	**:** Boltzmann constant
T	**:** Thrust, temperature
$\boldsymbol{T_i}$	**:** Ideal thrust
$\boldsymbol{I_t}$	**:** Total impulse
$\boldsymbol{v_e}$	**:** Electron thermal speed, exhaust velocity
$\boldsymbol{v_{ei}}$	**:** Ideal exhaust velocity

v_{Bohm} : Bohm velocity

m_e : Electron mass

m_{ion} : Ion mass

λ_D : Debye Length

ρ_{coil} : Resistivity of coil

l_{coil} : Length of coil

$A_{cross-sec}$: Cross-sectional area of coil

R_{coil} : Resistance of coil

$\mathbf{Z}$: Impedance

R_{cpl} : Resistance of coil-plasma

L_{cpl} : Inductance of coil-plasma

$\mathbf{C}$: Capacitance

d_s : Screen grid aperture diameter

d_a : Acceleration grid aperture diameter

d_d : Deceleration grid aperture diameter

t_s : Thickness of screen grid

t_a : Thickness of acceleration grid

t_d : Thickness of deceleration grid

l_e : Plasma sheath thickness

l_g : Gap between screen grid and acceleration grid

l_{cc} : Center-to-center distance of apertures

V_T : Total voltage

V_N : Net voltage

V_B : Beam voltage

V_s : Screen grid voltage

V_a : Acceleration grid voltage

V_d : Deceleration grid voltage, discharge voltage

V_{coil} : RF coil voltage

$\mathbf{J}$: Current density

J_{max} : Maximum current density, Child-Langmuir current density

ε_0 : Vacuum permittivity

I_b : Ion beam current

I_s : Screen grid current

I_a : Acceleration grid current

I_{RF} : RF coil current

γ : Thrust correction factor

α : Doubly charged ion correction factor

F_t : Ion beam divergence correction factor

I^+ : Singly charged ions

I^{++} : Doubly charged ions

θ : Half angle of the ion beam divergence

η_m : Mass utilization efficiency

η_e : Electrical efficiency

η_{th} : Thruster efficiency

η_T : Total efficiency

η_{RFG} : Radio frequency generator efficiency

η_d : Ion production efficiency

Isp : Specific impulse

Isp_i : Ideal specific impulse

$\dot{m}$: Mass flow rate

$\dot{m}_i$: Ion mass flow rate

Q : Propellant particle flow rate in sccm

P_e : Exit pressure

P_0 : Free stream pressure

A_e : Exit area

P_{in} : Input power

P_{out} : Output power

P_{RF} : RF power

P_{IO} : Ion optics power

P_{jet} : Jet power

P_{DC} : Direct current power to RFG

P_d : Discharge power

P_n : Neutralizer power

P_{MFCU} : Mass flow control unit power

D : Diameter of grids

P_{max} : Maximum perveance

A_{hex} : Hexagonal area of grid apertures

A_{circle} : Circular area of grid apertures

A_t : Total active area of grid apertures

Φ : Transparency of grids

LIST OF TABLES

Page

Table 2.1 : Example of Hydrazine propellant thrusters. 6
Table 2.2 : Examples of non-toxic or green propellant thrusters. 7
Table 2.3 : Examples of cold gas propellant thrusters. 8
Table 2.4 : Examples of solid motors. 9
Table 2.5 : Examples of the resistojet thrusters.. 11
Table 2.6 : Examples of ion engines. 12
Table 2.7 : Examples of electrospray thrusters. 13
Table 2.8 : Examples of pulsed plasma thrusters. 13
Table 2.9 : Examples of vacuum arc thrusters. 14
Table 2.10 : Examples of Hall-effect thrusters. 15
Table 3.1 : The list of several orbital launch systems [36, 37]. 19
Table 3.2 : Satellite mass classification [38]. 20
Table 3.3 : Masses of all subsystems.. 23
Table 3.4 : Power budget of the satellite. 26
Table 3.5 : Electrical properties of the CubeSat. 26
Table 3.6 : Propulsion system type trade study [12, 14, 16, 17, 20, 25, 28, 29]. 35
Table 3.7 : Lunar mission analysis summary. 36
Table 4.1 : Ion optics parameters. 51
Table 4.2 : Grid potentials. 53
Table 4.3 : The list of Mercury ion thrusters. 60
Table 4.4 : The list of Xenon ion thrusters. 61
Table 4.5 : The list of Argon ion thrusters. 61
Table 4.6 : The list of Iodine ion thrusters. 62
Table 4.7 : The list of Krypton ion thrusters. 62
Table 4.8 : Properties of these elements for standard temperature and pressure. 64
Table 4.9 : Grid potentials of two versions of the thruster. 68
Table 4.10 : Current densities and currents of two versions of the thruster. 69
Table 4.11 : Thrust values of two versions of the thruster. 69
Table 4.12 : Specific impulse value of two versions of the thruster. 70
Table 4.13 : Exhaust velocity value of two version of the thruster. 70
Table 4.14 : Flow rates of two versions of the thruster. 71
Table 4.15 : Power consumptions of two versions of the thruster 73
Table 4.16 : Efficiencies of two versions of the thruster. 74
Table 4.17 : Preliminary designed Krypton RF ion thruster specifications. 82

LIST OF FIGURES

Page

Figure 3.1 : CubeSat standard sizes [40]. 21
Figure 3.2 : Representation of the subsystems in 6U CubeSat. 23
Figure 3.3 : Representation of solar panel configuration. 25
Figure 3.4 : Direct transfer from LEO to LLO (Revised image) [47]. 28
Figure 3.5 : Direct transfer from GTO to LLO (Revised image) [47]. 29
Figure 3.6 : Spiral transfer from GEO to LLO (Revised image) [51]. 30
Figure 3.7 : Representation of Weak Stability Boundary transfer from Earth to Moon [52]. 31
Figure 4.1 : Thrust Generation Schematic. 39
Figure 4.2 : Operation Schematic of RF Thruster [66]. 40
Figure 4.3 : Conductively coupled plasma discharge schematic [68]. 41
Figure 4.4 : Inductively coupled plasma discharge cylindrical and planar respectively [69]. 42
Figure 4.5 : Grid set configurations [65]. 42
Figure 4.6 : Circuit diagram of the system [73]. 47
Figure 4.7 : Illustration of the ion optics [64]. 49
Figure 4.8 : Plasma sheath thickness, le (Revised image) [64]. 49
Figure 4.9 : Geometrical relationship between different example grid sets [65]. 50
Figure 4.10 : Grid Potentials (Revised image) [101].. 52
Figure 4.11 : Graph of relationship between Isp and Vb for different ηm and Xenon propellant. 53
Figure 4.12 : Beam voltage vs. atomic mass graph. 63
Figure 4.13 : Beam voltage vs. thrust graph for different propellants. 65
Figure 4.14 : Beam voltage vs. specific impulse graph for different propellants 66
Figure 4.15 : Beam voltage vs. exhaust velocity graph for different propellants. 66
Figure 4.16 : Flow chart for Krypton gas version. 73
Figure 4.17 : Flow chart for Xenon gas version. 74
Figure 4.18 : CAD design of the discharge chamber. 76
Figure 4.19 : CAD design of the screen, accel. and decel. grid respectively. 77
Figure 4.20 : CAD design of the grids and spacers. 78
Figure 4.21 : CAD design of the RF coil. 78
Figure 4.22 : CAD design of the whole thruster. 79
Figure 4.23 : CAD design of propellant tank of the system. 81
Figure 4.24 : CAD design of the whole propulsion system. 81
Figure 4.25 : 3D drawing of the Lunar mission 6U CubeSat with designed propulsion system. 83

PRELIMINARY DESIGN OF AN ELECTRIC PROPULSION SYSTEM FOR LUNAR NANOSATELLITE MISSION

SUMMARY

In these days, as we celebrate the 50th anniversary of mankind's step on the Moon, human beings have set their sights on the Moon with the knowledge and high-tech products they have developed in the last 50 years. Nowadays, many of the space agencies and large-scale corporation agendas necessarily include the lunar missions. Small-scale companies and universities support these studies, such as the development of subsystems that can be used for lunar missions, ground testing or testing in space with a nanosatellite. Using nanosatellites for interplanetary missions increased its popularity due to its advantages and propulsion system became a necessary subsystem for this type nanosatellite missions. These situations constitutes the main motivation of this study. The aim of the study determined as developing a propulsion system used for transport 6U CubeSat to Low Lunar Orbit from parking orbit.

The propulsion systems, which are currently used or planned to be used in small satellites, were formed by miniaturization of propulsion systems of large spacecrafts. In order to design a mission-based propulsion system, the types of the propulsion system that can be used in small satellites should be recognized and their benefits should be exemplified. In this study, the small satellite propulsion systems have been researched and explained to know and to have an idea about studies of small satellites propulsion system in the future by given examples.

A concept lunar mission was created to determine the required performance values of the propulsion system to be preliminary designed. In this study, the concept lunar mission was determined as a 6U CubeSat separated from the launch vehicle can reach the Low Lunar Orbit by using a propulsion system. After orbiting, lunar surface observation is performed by using its payload which is hyperspectral camera. Required subsystems of the satellite to be designed for these purposes were identified and were scaled to fit in the 6U CubeSat. As a result of the literature review, size and mass limitations of the propulsion system were determined. After specification of the size and mass limitations, another important issue, power limitation of propulsion system was calculated by considering the power generation of solar panel and power consumption of other subsystems. The deployable rotating panel configuration was selected in order to utilize more advantage of solar energy. It is expected that the deployable rotating solar panels can generate approximately 80W. Power budget of the satellite was formed after literature review of other subsystems power consumptions. Using this power budget, the amount of power that can be allocated for the propulsion system is expected to be around 50-60 W. The size, mass and power limitations of propulsion system were used as preliminary inputs in the design. In addition to these limitations, the trajectory determination is necessary to calculate required delta-V value for mission and to decide type of propulsion system to be used

in this transfer. For this purpose, several transfer methods have been compared including their advantages and disadvantages. In this study, direct transfer from LEO, direct transfer from GTO, spiral transfer from GEO and weak stability boundary methods were examined and compared. Spiral transfer method, which is appropriate for CubeSat mission, has been chosen due to its benefits such as less fuel and power consumption. As a result, a propulsion system design was planned for 6U CubeSat, which would be located to GEO by launch vehicle and then transferred to LLO by spiral transfer method. According to this scenario, the delta-V value was predicted as approximately 3.6 km/s. Considering the maximum mass of 6U CubeSat and fuel mass that propulsion system can have, specific impulse and exhaust velocity that the system must produce in order to achieve this delta-V value were calculated as approximately 3420 sec and 33,540 m/s respectively. The most appropriate propulsion system type, which can be compatible with the limitations and can provide these performance values, was selected by using trade study method. As a result of this trade study, the type of propulsion system to be designed for the concept mission was determined by getting the highest score of ion thruster propulsion systems belonging to electric propulsion systems family.

Literature researches have been made on ion thruster propulsion systems and examples have been examined. As a result of these studies, it has been observed that ion engine propulsion systems have four categories. RF ion thruster type have been chosen because they do not have cathodes and thus do not have cathode erosion, as their lifetime is longer. RF ion propulsion system generally has thruster, power supply unit, fuel tank, flow control unit, RF generator and neutralizer. In this study, thruster design is made in detail. RF ion thusters basically consist of the discharge chamber where the fuel is ionized, the RF coil carrying the RF signals that enable the ionization of the fuel, the ion optics used to accelerate the ionized particles. At the beginning of the design process, the necessary steps to generate thrust and the underlying physics were explained. For ion optics design, a geometric relationship was established between the diameter of the apertures, the thickness of the grids, and the distance of the grids to each other. Formulas were given for performance values such as thrust, specific impulse, power consumption and efficiencies. Based on this information, the dimensions of the discharge chamber, grids, RF coil and whole thrust system have been determined. The propellant selection, which is one of the most important factors affecting the performance values of the thruster, was performed. Comparisons have been made between Mercury, Xenon, Argon, Iodine and Krypton propellants, which have been used in electrical propulsion systems for many years or still being tested. As a result, it was decided to experimentally use Krypton gas, the noble gas having the highest atomic mass after Xenon, as propellant in the system. In order to make comparisons and to offer two different propellant alternatives for propulsion system, it was decided to use Xenon gas, which has traditionally been proven as performance and safety.

After the decision of the propellant types, beam voltage, net voltage and potentials of grids could be calculated for two versions of propulsion systems. Based on the Child-Langmuir equation and the geometric properties of the grids, the current density of the plasma was also calculated. The current values were determined by using the diameter of the active surface of the grids and the diameter of the apertures. These current values are important for calculating the power requirements of the system. By calculating the beam current, acceleration voltage and current density, the thrust values were calculated for the Xenon gas and Krypton gas versions of the designed propulsion

system. Xenon gas is able to produce more thrust force than Krypton gas. Both versions were found to provide targeted specific impulse and exhaust velocity values. Burn times of Xenon and Krypton versions were found as approximately 180 days and approximately 443 days respectively. Power consumption is one of the most important performance values for electrical propulsion systems. For this reason, the electrical power consumed by the system while producing the thrust must be calculated. PPU of the system should provide DC power to ion optics to accelerate charged particles and to RF generator to convert it to RF power to ionize the propellant. In addition to the RF generator and ion optics, the neutralizer and mass flow control unit must also be powered to operate. The sum of all these power requirements indicates the amount of electrical power the system needs to operate. As a result of the power calculations, it was found that the Krypton gas version needed approximately 51 W to generate the desired thrust. This power consumption is very reasonable considering the power values that the satellite can provide to the propulsion system. On the other hand, the Xenon gas version requires approximately 84 W. This value is greater than generated nominal power by solar panels. Hence, either panel configuration should be changed or CubeSat size should be enlarged to enable usage of the Xenon gas version of propulsion system. After the power calculations, electrical, mass utilization, thruster and total efficiencies of the systems were calculated to compare two version of the system. As a result, the efficiency of the Xenon gas version resulted higher than the Krypton gas version. However, the use of the Krypton gas version has come to the fore since the fuel cost and power consumption is much lower than the Xenon gas version.

The 3D design of the thruster and other subsystems has been done with the help of the CAD program. Since the detailed design of the thruster is based on the calculations, the 3D design is reproduced with a detailed sizing. It was decided to store the propellant as liquid in a cryogenic tank in order to fit the 6U CubeSat appropriately, since required propellant amount is high and densities of the Krypton and Xenon is quite low. Material selection and required thermal measures were decided by taking into account this situation. Materials discharge chamber, RF coil, ion optics and shell were selected in order to decrease harmful effects of radiation and to provide thermal control. The 3D design of the other components of the propulsion system is representative of the dimensions of commercially available components. The designed propulsion system was shown in the satellite, which is planned to use in lunar mission. Hence, preliminary 3D design of propulsion system and 6U CubeSat were represented.

The detail design of each component of this propulsion system, improving the design by concentrating on plasma calculations, testing on ground and completion of final design of the propulsion system are expected as future works. 3D design, material selection, thermal and radiation measures may change in next phases of the design because requirements of the components and their performance values, which can be provided by system, may be changed.

NANO UYDULU AY GÖREVİNDE KULLANILACAK BİR ELEKTRİK İTKİ SİSTEMİNİN ÖN TASARIMI

ÖZET

İnsanoğlunun Ay'a ayak basışının 50. yılını kutladığımız bu günlerde, insanoğlu geçen 50 yılda arttırdığı bilgi birikimi ve geliştirdiği yüksek teknolojili ürünleri ile gözünü yeniden Ay'a dikmiş durumdadır. Öyle ki, birçok uzay ajansı ve büyük ölçekli şirket ajandalarında Ay görevine mutlaka yer vermektedir. Küçük çaplı şirketler ve üniversiteler bu çalışmalara ay görevlerinde kullanılabilecek alt sistemlerin geliştirilmesi, test edilmesi ya da küçük bir uydu ile uzayda denenmesi gibi destekler vermektedir. Ay görevleri popülerleşirken, nano uyduların gezegenler arası ve derin uzay görevlerinde kullanımısına yönelik çalışmalar yaygınlaşmıştır. Bu tarz görevlerde kullanılan nano uydular itki sistemlerine ihtiyaç duymaktadırlar. Tüm bu sebepler bu çalışmanın motivasyonunu oluşturmuş ve çalışmanın amacı Alçak Ay Yörüngesinde görevini icra etmek için yola çıkan 6U formunda bir küp uyduyu hedef yörüngesine ulaştıracak bir itki sisteminin geliştirilmesi olarak belirlenmiştir.

Küçük uydularda kullanılan ya da kullanılmak üzere geliştirilme süreci devam eden itki sistemleri büyük itki sistemlerinin miniyatürleştirilmesi ile oluşturulmuştur. Göreve özel itki sistemi tasarlayabilmek için küçük uydularda kullanılabilecek itki sistemi tiplerinin tanınması ve sağlayabileceği faydaların örneklendirilmesi gerekmektedir. Kullanılabilecek itki sistemlerini tanıma ve gelecekte küçük uydu itki sistemleri üzerinde yapılacak çalışmalar hakkında fikir sahibi olmak amacı ile küçük uydu itki sistemleri araştırılmış ve bu çalışmada örneklendirilerek anlatılmıştır.

Tasarlanacak itki sisteminin sağlaması gereken performans değerlerinin belirlenmesi için konsept bir Ay görevi oluşturulmuştur. Küp uydunun park yörüngesine ulaşmasını sağlayabilecek fırlatma araçları araştırılmış ve uygun bulununanlar listenmiştir. Bu ay görevinde fırlatma aracından ayrılan 6U formundaki bir küp uydunun itki sistemi kullanarak Alçak Ay Yörüngesi'ne ulaşması ve Alçak Ay Yörüngesi'nde sahip olduğu kamera ile jeolojik ve topografik incelemeler yapılabilmesine yönelik bir görev kurgusu belirlenmiştir. Bu amaçlarla tasarlanacak bir küp uyduda olması gereken alt sistemler belirlenmiş ve 6U formundaki küp uyduya uygun olacak şekilde boyutlandırılmıştır. Yapılan literatür araştırmaları sonucunda alt sistemlerin uydu içerisinde kaplayacağı boyutlar ve kütleler belirlenmiştir. 6U formundaki bir küp uydunun standart olarak 12 kg olması ve 10 cm x 22.6 cm x 36.6 cm boyutlarında olması beklendiği için itki sistemi için ayrılabilecek maximum yer ve kütle belirlenmiştir. İtki sistemi için ayrılabilecek yer ve kütle belirlendikten sonra diğer bir önemli konu olan itki sistemi için ayrılabilecek elektriksel gücün kaç Watt olduğunun hesaplaması yapılmıştır. Küp uydunun alt sistemlerinin etkili bir şekilde çalışıp görevlerini icra edebilmeleri için gerekli olan güç, uydunun güneş panelleri aracılığıyla üretilmektedir. Bu çalışmada katlanabilir ve dönebilir güneş panelleri kullanılarak güneş enerjisinden daha fazla yararlanılması sağlanmıştır. Güneş

panellerinin uydu üzerindeki yerleşimi yapılan 3D tasarım ile gösterilmiştir. Yapılan analizler sonucunda yerleşimi verilen güneş panellerinin yaklaşık olarak 80 W değerinde nominal güç üretebileceği hesaplanmıştır. Yine yapılan literatür araştırmaları sonucunda kullanılan alt sistemlerin harcayacağı güç değerleri belirlenip uydunun güç bütçesi oluşturulmuştur. Oluşturulan bu güç bütçesi sayesinde itki sistemi için ayırılabilecek güç miktarının yaklaşık olarak 50-60 W civarı olması beklenmektedir. İtki sistemi için belirlenen boyut, kütle ve güç kısıtları itki sisteminin tasarımında öncül girdiler olarak kullanılmıştır. İtki sistemi küp uydunun başlangıç noktasından hedef yörüngesine taşınması için kullanılacağından dolayı itki sistemi tipini ve gerekli olan delta-V miktarını belirlemek için uydunun hangi transfer yolunu izleyeceğini belirlemek önemlidir. Bu hedefle bir kaç transfer yöntemi avantajları ve dezavantajları ile karşılaştırılmıştır. Bu çalışmada Alçak Dünya Yörüngesi'nden doğrudan transfer, Yer Sabit Transfer Yörüngesinden Alçak Ay Yörüngesine doğrudan transfer, Yer Sabit Yörünge'den spiral transfer ve Zayıf Stabilite Sınırı transfer metodları incelenmiş ve karşılaştırılmıştır. Her bir transfer yöntemi için kullanılabilecek fırlatma araçları belirtilmiştir. Bu inceleme sonucunda sağladığı faydalar, yakıt ve güç sarfiyatı gibi konular sebebi ile küp uydulu görev için uyumlu olacak spiral transfer metodu seçilmiştir. Sonuç olarak fırlatma aracı ile Yer Sabit Yörünge'ye bırakılacak buradan da Alçak Ay Yörüngesi'ne taşınacak bir 6U formundaki küp uydu için itki sistemi tasarımı planlanmıştır. İtki sisteminin bu görevi başarılı bir şekilde uygulanabilir kılması için sağlaması gereken delta-V değeri spiral metod ile hesaplanmıştır. Bu senaryoya göre uydunun ihtiyaç duyduğu delta-V değeri yaklaşık olarak 3.6 km/sn olarak öngörülmüştür. İtki sisteminin sahip olabileceği maksimum kütle ve yakıt kütlesi göz önüne alınarak sistemin bu delta-V değerini sağlayabilmesi için üretmesi gereken özgül itme ve egzoz hızı sırasıyla yaklaşık olarak 3420 sn ve 33540 m/sn olarak hesaplanmıştır. Görevin gerçekleştirilebilmesi için gereken performans değerlerinin de belirlenmesi ile birlikte bu özellikleri sağlayabilecek itki sistemi tipinin seçimi için gerekli olan parametreler belirlenmiştir. Background kısmında detayları verilen farklı küçük uydu itki sistemlerine ait örneklerden küp uydu formu için uygun olabilecekler arasında getir-götür analizi yapılmıştır. Getir-götür analizinde itme kuvveti, özgül itme, güç tüketimi, yakıt tipi, kütle, boyut ve teknoloji hazırlık seviyeleri değerlendirme kriteri olarak kullanılmıştır. Yapılan bu getir-götür analizinde elektrik itki sistemleri ailesine ait iyon motorlu itki sistemleri en yüksek puanı alarak göreve özel olarak tasarlanacak itki sisteminin tipi belirlenmiştir.

İyon motorlu itki sistemleri üzerine literatür araştırmaları yapılmış ve örnekler incelenmiştir. Bu araştırmalar sonucunda iyon motorlu itki sistemlerinin kendi içerisinde çalışma prensiplerine göre doğru akım elektron boşalımlı iyon motoru, Kaufman iyon motoru, Radyo frekansı iyon motoru ve mikrodalga iyon motoru olmak üzere 4 kategoriye ayrıldığı görülmüştür. Yapılan karşılaştırma sonucunda katota sahip olmadığı ve bu sayede katot erozyonuna sahip olmadığı için dayanım ömrü daha uzun olduğu belirtilen RF iyon motorları seçilmiştir. RF iyon motorları temel olarak yakıtın iyonize edildiği boşaltma odası, yakıtın iyonize olmasını sağlayan RF sinyallerini taşıyan RF bobini, iyonize edilmiş taneciklerin hızlandırılması için kullanılan iyon optikler, iticinin bu çalışmaları yapabilmesi için sisteme dahil olması gereken güç sağlama ünitesi, yakıt tankı, akış kontrol ünitesi, RF jeneratörü ve nötürleyiciden oluşmaktadır. Bu çalışmada detaylı olarak itici tasarımı yapılmıştır. Tasarım yapılırken itki üretmek için gerekli olan aşamalar ve temelinde yatan fizik incelenmiştir. İyon optiklerin 3lü ızgara sisteminden oluşmasına karar verilmiş ve tasarımı yapılmıştır. Daha önce başarılı bir şekilde kullanılan ızgaralı itki sistemlerinin

ızgaralarının sahip olduğu açıklıkların çapı, ızgaraların kalınlıkları, ızgaraların birbirine olan uzaklıkları arasında geometrik bir ilişki kurulmuş ve bu çalışmada NSTAR itki sisteminde kullanılan ızgaralar arasındaki ilişki temel alınmıştır. Bu ilişkiden yola çıkarak iticinin iyon optik parametreleri hesaplanmıştır. İtme kuvveti, özgül itme, güç tüketimi, verim gibi hesaplanması gereken performans değerleri için formüller verilmiştir. Bu bilgilerden yola çıkılarak boşaltım odasının, ızgaraların, RF bobinin ve bütün halde itki sisteminin sahip olacağı boyutlar belirlenmiştir. Bütün olarak 4.7 cm çapında 4.2 cm uzunluğunda olacak iticinin performans değerlerini etkileyen en önemli faktörlerden biri olan yakıt seçimi gerçekleştirilmiştir. Yıllardır elektrik itki sistemlerinde kullanılmış, kullanılmaya devam eden ya da kullanımı değerlendirilen Civa, Ksenon, Argon, İyot ve Kripton yakıtları arasında karşılaştırmalar yapılmıştır. Elektrikli itki sistemlerinin yeni yeni kullanılmaya başlandığı yıllarda yaygın olarak kullanılan Civa, yüksek toksiklik seviyesi sebebi ile uzayda uyduya zarar verdiği ve yer testlerinde çalışan personellerin sağlığını olumsuz yönde etkilediği için daha sonrasında uygun bulunmamıştır. Uzun yıllardan beri geleneksel olarak kullanılan ve günümüzde halen kullanımı devam eden Ksenon gazı kullanımı performans açısından en ideal yakıtlardan biridir. Ancak Ksenon gazının sınırlı kaynaklar sebebi ile çok pahalı olması ve kaynakların gittikçe azalması sebebiyle maliyet artışı öngörüldüğü için ksenon gazı yerine kullanılabilecek alternatifler olan Argon, İyot ve Kripton gazları da değerlendirilmiştir. Bu dört yakıt seçeneğinin itme kuvveti, özgül itme, çıkış hızı vb. gibi performans grafikleri çıkarılmış ve Ksenon gazına performans olarak en yakın performansı, doğada katı halde bulunan, İyot yakıtının sağladığı görülmüştür. Halihazırda İyot'un Lunar IceCube uydusunda itki sistemi olarak kullanılacak Busek firmasına ait BIT-3 itki sisteminde kullanılması planlanmaktadır. İyot'un Kripton'a kıyasla daha toksik olması sebebiyle ekstra güvenlik ekipmanlarına ihtiyaç duyulacaktır. Dolayısıyla tasarlanan itki sisteminde Kripton gazının yakıt olarak kullanılmasına karar verilmiştir. Kıyaslama yapabilmek ve itki sistemine iki farklı yakıt alternatifi sunabilmek için geleneksel olarak kullanılan, kendini performans ve güvenlik olarak ispat etmiş Ksenon gazının ve deneysel olarak kullanımı planlanan Ksenon'dan sonra en yüksek atomik kütleye sahip soygaz olan Kripton gazının kullanılmasına karar verilmiştir.

Yakıt tiplerinin belirlenmesinin ardından, itki sisteminin sağlaması gereken özgül itme ve egzoz hızı değerlerinden yola çıkılarak ızgaralara verilmesi gereken gerilim değerleri hesaplanmıştır. Child-Langmuir plazma kılıfı denkleminden ve ızgaraların geometrik özelliklerinden yola çıkılarak plazma kılıfının kalınlığı hesaplanmış ve bu sayede plazmanın sahip olduğu akım yoğunluğu hesaplanmıştır. Izgaraların aktif yüzeyinin çapı ve sahip oldukları açıklıkların çapından yola çıkılarak akım değerleri bulunmuştur. Bu akım değerleri sisteme verilmesi gereken gücün hesaplanabilmesi için önemlidir. Işın akımı, akselerasyon voltajı ve akım yoğunluğunun hesaplanması ile birlikte, tasarlanan itki sisteminin Ksenon gazlı ve Kripton gazlı versiyonları için itme kuvveti hesaplanmıştır. Ksenon gazının Kripton gazına oranla daha fazla itme kuvveti üretebildiği görülmüştür. Her iki versiyonun da hedeflenen özgül itme ve çıkış hızı değerlerini sağladığı görülmüştür. Kütle akış kontrolcüsünün bu itme kuvvetini sağlayabilmek için sisteme vermesi gereken akış hızı ve sistemin iyon akış hızı hesaplanmıştır. Bu değerlerden yola çıkılarak sistemin bünyesinde bulunan yakıtı ne kadar süre etkili olarak kullanabileceği hesaplanmıştır. Ksenon gazlı versiyon yaklaşık olarak 180 günde yakıtı tüketirken Kripton gazlı versiyon yaklaşık olarak 443 günde yakıtı tüketmektedir. Güç tüketimi elektrikli itki sistemleri için en önemli performans değerlerinden biridir. Bu sebeple sistemin itme kuvveti üretirken tüketmiş olduğu elektriksel gücün hesaplanması gerekmektedir. İticiye boşaltım odasındaki yakıtı

iyonize ediebilmesi için RF gücü verilmesi gereklidir. Güneş panelleriyle üretilen DC güç, itki sistemi komponentlerinden biri olan RF jeneratörü tarafından RF gücüne çevirilerek sisteme verilmektedir. Yüklü parçacıkların hızlandırılabilmesi için iticinin iyon optiklerine DC gücünün verilmesi gerekmektedir. Farklı aşamalarda ihtiyaç duyulan bu elektriksel güç, güç dağıtım ünitesi tarafından komponentlere ulaştırılmaktadır. Sisteme girdi olarak verilen RF ve iyon optik güçlerine ek olarak nötürleyiciye de çalışabilmesi için güç verilmesi gerekmektedir. Tüm bu güçlerin toplamı sistemin çalışabilmek için ihtiyaç duyduğu elektriksel güç miktarını ortaya koymaktadır. Sistemin ürün olarak ortaya koyduğu hızlandırılmış parçacıklardaki elektriksel güç ise çıkış gücünü göstermektedir. Sistemin ürettiği itme kuvveti ile de jet gücü hesaplanır. Güç hesaplamaları sonuncunda, Kripton gazlı versiyonun itki üretebilmek için yaklaşık olarak 51 W değerinde güce ihtiyacı olduğu bulunmuştur. Uydunun itki sistemine sağlayabileceği güç değerleri düşünüldüğünde bu güç tüketimi oldukça makuldür. Diğer taraftan, Ksenon gazlı versiyon yaklaşık olarak 84 W güce ihtiyaç duymaktadır. Bu değer, güneş panellerinin üretebileceği nominal güç miktarından fazladır. Dolayısı ile, Ksenon gazlı versiyonun kullanımının mümkün kılınabilmesi için panel konfigürasyonunu değiştirilip üretilen güç miktarını arttırılması gereklidir. Tüm bu güç hesaplamalarının ve diğer performans hesaplamalarının ardından sisteminin verimi bir kaç yönden hesaplanır. Sistemin kullandığı elektrik gücüne karşılık ne kadar itme kuvveti üretebildiğini gösteren elektriksel verim, kullandığı yakıt kütlesinin ne kadarı etkin olarak itme kuvveti üretiminde kullandığını gösteren kütle faydalanma verimi, ürün olarak ortaya konulan çıkış gücünün ne kadarının itme kuvveti üretiminde kullanıldığını gösteren itici verimi ve son olarak elektriksel ve kütle faydalanma veriminin kombinasyonu olan toplam verim hesaplanmıştır. Sonuç olarak Ksenon gazlı versiyonun verimi Kripton gazlı versiyondan daha fazla çıkmıştır. Ancak Kripton gazlı versiyonun yakıt maliyetinin ve güç tüketiminin Ksenon'a kıyasla çok daha düşük olması sebebi ile Kripton gazlı versiyonun kullanımı ön plana çıkmıştır.

Boyutları belirlenen itici ve diğer alt sistemlerin 3D tasarımı CAD programı aracılığıyla yapılmıştır.İhtiyaç duyulan yakıt miktarının fazla olması ve yakıtların düşük yoğunluklara sahip olması sebebi ile yakıtın 6U formundaki küp uyduya uygun bir şekilde sığdırılabilmesi için krayojenik tank içerisinde sıvılaştırılarak depolanmasına karar verilmiştir. Malzeme seçimi ve gerekli olan termal önlem bu durum göz önünde bulundurularak yapılmıştır. İticinin detaylı tasarımı hesaplamalara dayandırılarak yapıldığı için 3D tasarımı buna uygun olarak yapılmıştır. İticinin boşaltım odası, RF bobini, iyon optiklerinin ve kabuğunun malzeme seçimi, yapılan literatür araştırmaları doğrultusunda, termal kontrole ve radyasyonun zararlı etkilerini önlemeye çalışacak şekilde seçilmiştir. İtki sisteminin diğer komponentlerinin 3D tasarımı piyasada mevcut olan komponentlerin boyutlarından yola çıkılarak temsili olarak yapılmıştır. Son olarak tasarlanan itki sisteminin uydu içerisindeki yerleşimi verilerek Ay görevinde kullanılacak olan 6U formundaki küp uydunun alt sistemleri ile birlikte öncül 3D tasarımı ortaya çıkarılmıştır.

Konsept ay görevinde kullanılmak üzere ön tasarımının yapıldığı bu itki sisteminin her bir komponentinin tasarımının detaylandırılması, plazma hesaplamalarına yoğunluk verilerek tasarımın geliştirilmesi ve test düzeneklerinin kurulup gerekli testlerin yapılması ile birlikte gelecekte son tasarım evresinin tamamlanması beklenmektedir. Tasarımın ilerleyen fazlarında itki sistemi komponentlerinin ihtiyaçları ve sağladıkları performans değerleri değişebileceği için 3D tasarımı, malzeme seçimi, alınan termal ve radyasyon önlemleri değişebilir.

1. INTRODUCTION

Throughout the human history, space has been filled with mysteries and has always been curious and wanted to be discovered. For this reason, it has always been one of the most popular research areas both for the people of the ancient world and modern world. The production of measuring equipments, which are used in space researches to understand the working of the universe, and later the production of more complex devices and spacecrafts for these researches, have created space engineering field. In our recent history, in 1957, Sputnik 1 became a first man-made spacecraft to launch into space thanks to increasing knowledge in space researches [1]. The launch of Sputnik 1 into the space by the Soviet Union has also begun a space race between the USSR and the US, which will last for about 18 years. During this time, space science, performing a manned flight into the space and going to the Moon were always among the most important topics of the world agenda. The Soviet Union has achieved such successes as launching the first artificial satellite into space, sending Laika, which was a dog for the first time, and launching the first manned flight with Yuri Gagarin into orbit of the Earth [2]. However, their main aim was performing a manned flight to the Moon. In USSR side, while such successful projects were being carried out, America, which founded NASA on the one hand, was trying to get ahead by following these developments on the other hand. For this purpose, they have started to Mercury and Gemini space programs [3]. The USSR, which sent the first spacecraft into lunar orbit and accomplished the first unmanned landing on to lunar surface, was approaching their target confidently. Meanwhile, the United States launched the Apollo program, which would achieve great success later. The United States, which made its first manned flight to the Lunar orbit with Apollo-8, increased its experience and accelerated its work in this field, and in 1969, Neil Armstrong became the first human on the Lunar surface [1,2,3]. In the face of this historical development, USSR continued to work, but gave up the manned landing to Moon idea and they began to work with the United States to build a space station in 1975 [2]. Thus, the space race is over, but as always, mankind's desire to explore space remains. By using know-how

from the space race, space researches were continued by the space agencies and universities, which were established by countries.

Exploring the universe or observing the Earth surface with an eye outside the Earth has increased the popularity of satellites due to their benefits. Military and civil communication satellites and ground observation satellites accelerated the space researches after the space race thanks to their benefits in daily life. For long years, large-scale spacecrafts, which have high production cost and long design, production and test time, have been used for these space researches. Due to their high cost, the design, production and testing were long, they were not expendable. Thus, subsystems, which were proved themselves in ground tests for many times, were generally used in these type satellites. A space mission was used to serve more than one purpose due to factors that prevented to perform of the space mission frequently. Space missions should be designed to serve multiple purposes, such as testing an experimental subsystem in space while performing the main task of the mission. Governments, space agencies and large-scale companies could only implement these high-cost and taking long time space programs. In time, development of small satellites became important to reduce cost, shorten design, production and testing times, and make space researches accessible. In 1999, in collaboration with California Polytechnic State University and Stanford universities, the first CubeSat idea for educational purposes was introduced and designed [4]. It has established itself as a solid place since it allows universities to contribute to space research inexpensively. It provided access to space not only for universities but also for small budget companies and organizations. They have increased the number of space studies due to their much lower cost, short design, production and testing times, and expendability compared to the large satellites. CubeSats, which were used for educational purposes before 2013, were used for non-academic purposes after 2013. For this reason, the number of CubeSat has increased considerably in 2013 [5]. Today, it is used for governmental, educational and commercial purposes.

At the beginning, CubeSats were used for communication, remote sensing and technology demonstration missions. However, today, they are used for academic, remote sensing, communication purposes as well as science-proof concept validation and deep space and interplanetary missions. With the increase in the number and usage of CubeSat, propulsion systems have been used to maneuver and control the spacecraft

during their missions. For many years, propulsion systems have been actively used in large satellites for transfers or orbital maneuvers. After, these systems were tried to miniaturized to enable the usage in small satellites. Today, propulsion systems are effectively used in small satellites for purposes of orbit raising and adjustment, station keeping, attitude control, repositioning, deorbiting, deep space mission and constellation management. In 2018, the success of the MarCO project, which was successfully transferred to Mars using two CubeSat with propulsion systems, proved that CubeSats can be used effectively in deep space missions and accelerated the mission studies with CubeSat [6]. On the other hand, it has popularized the development of propulsion systems that can be used to transfer the satellite from one point to another in an interplanetary or deep space mission. This study, which is a step forward for manned flight to Mars, which is among the targets of space agencies and large-scale space companies such as SpaceX, has had widespread media coverage. On the other hand, the space agencies, companies, countries and universities have set their sights on the Moon before manned mission to Mars. In these years, the lunar missions have become very popular as in the 1960s. Almost every space agency has the lunar mission in their calendars. One of the most important reasons for this is the manned space program Artemis, which will be performed as a pre-flight rehearsal to Mars [7]. NASA supports large and small lunar missions to gather more information. Looking at the world, Japan, China, India and ESA have performed many lunar missions. Against the United States, which has achieved success in setting foot on the Moon, these countries have performed these missions to test the systems they have developed. The SMART-1 satellite, designed and manufactured by ESA, has allowed some sub-systems such as ion propulsion engines to be tested in space [8]. China, performing another successful lunar mission, became popular with Chinese Lunar Exploration Program. Nowadays, Chang-E 2 performs its mission successfully [9]. Another country, which attaches importance to lunar exploration, is India. Designed and manufactured by ISRO, the Chandrayaan-1 spacecraft attracted attention because it discovered water traces on the Moon surface. This time, India, which wanted to be fourth country landing on the Moon surface, started to work for Chandrayaan-2 space mission. In September 2019, the Vikram module, which was separated from the Changrayaan-2 spacecraft and was expected to land on the Moon surface, was disconnected 400 m before the surface and the space mission failed unfortunately [10]. The failure of this mission, which has been studied for more than 10 years, has made

a significant contribution to the lunar missions in order to learn from the mistakes that are made. From the beginning of human space adventure, not to give up in the face of difficulties, always try again and always make improvements is the most important and constant way to successful space missions. While India has learned from failure of its major work, China is the US's biggest rival with lunar missions.

SLS-1 rocket, which is planned to carry into space Artemis Space Program of NASA, is planned to carry 13 CubeSats in 6U forms to be used in cislunar missions as secondary payloads [11]. Cubesats, which are used for interplanetary or deep space missions, requires propulsion system for transfer, control and orbital maneuvers. The CubeSats, which has propulsion system and specific lunar mission motivate this study. With this motivation, it is aimed to design a propulsion system that is planned to transfer 6U CubeSat to Low Lunar Orbit in a concept lunar mission. In order to make this study possible, the investigation of the propulsion systems, evaluation of the transfer options to be transferred to the Low Lunar Orbit, selection of the transfer type and determination of the approximate delta-V requirement and elaborating of the features of CubeSat allows the determination of some important parameters for the propulsion system to be designed. In the light of this information, the performance values and design characteristics that the propulsion system must provide are determined. Structural design and CAD design of the system is made in this study.

2. BACKGROUND

In order to design a propulsion system for nanosatellites, it is necessary to have knowledge about propulsion systems used in nanosatellites or currently being developed. Propulsion systems can be divided into two main categories as chemical propulsion systems and electrical propulsion systems according to their working principles. In this section, general information about chemical and electrical propulsion systems used for nanosatellites is given to provide a basis.

2.1 Chemical Propulsion Systems

Chemical propulsion systems burn the fuel they contain and break the molecular bonds of the fuel to produce chemical energy and convert this chemical energy into thrust. These systems have been very successfully used in large space vehicles for many years and then miniaturized to be used in small satellites. Recently, they are effectively used for small satellites. This type of propulsion systems is generally ideal for space missions that require low delta-V, requiring impulsive burns, since they produce low specific impulse (<300 sec) and high thrust (>1N) compared to other systems. This type of propulsion system can be subdivided into liquid, gas and solid propellant propulsion systems depending on the state of the fuel used.

2.1.1 Liquid propellant propulsion systems

Liquid propulsion systems can be examined under two main categories according to the toxicity of the liquid fuel used.

2.1.1.1 Hydrazine propellant thrusters

The most popular and effective propellant of chemical propulsion system, hydrazine has been widely used to control attitude, correction maneuvers and station keeping for missions which have large spacecrafts over 60 years. Due to characteristics of the propellant hydrazine, this propulsion system is adapted to small size spacecrafts. It can be used to perform high thrust maneuvers as main propulsion system of the small spacecrafts. The hydrazine thruster is generally used for attitude, trajectory and orbit

control of small and mid-size satellites. From 1N class, MR-103 thruster of New Horizon for attitude control application can be used to generate main thrust for small spacecrafts. The thruster of Moog Space and Defense Group, MONARC-5 was used in Soil Moisture Active Passive (SMAP) spacecraft of NASA in 2015 [12]. Examples of hydrazine propellant thruster are given in Table 2.1 with their Technology Readiness Level that is explained in Appendix A.

Table 2.1 : Example of Hydrazine propellant thrusters.

Thruster	Thrust (N)	Specific Impulse(sec)	TRL	Company	Ref.
MPS-120	0.25-1.25	206-217	TRL 8	Aerojet Rocketdyne	[13]
MONARC-1	1.0	227.8	TRL 8	Moog Space and Defense Group	[14]
MONARC-5	1.0	226.1	TRL 9	Moog Space and Defense Group	[12,14]
1 N Thruster	0.320-1.1	220	TRL 9	Ariane Group	[15]

As a disadvantage of this monopropellant, system is that hydrazine is a highly toxic and dangerous propellant. It needs quite challenging material selection to improve performance and lifetime of spacecrafts. This type of liquid propellant propulsion system must deal with the storage problem and operational pressure of propellant. Addition to these problems, it has a risk of contamination in laboratory and space environment. Considering all of these, hydrazine and other toxic propellants caused to research of propulsion systems that are used non-toxic propellants. MPS-120, MONARC-1 and 1 N Thruster of Ariane Group given in Table 2.1 may be used in CubeSat form. These examples can ve evaluated for nanosatellite lunar mission.

2.1.1.2 Non-toxic or green propellant thrusters

Recently, non-toxic propellant is developing to reduce the risk of contamination, vapor pressure and to provide safety for ground test personnel as compared to toxic propellant. Thanks to this type of propellant, there is less need to safety equipment. In addition to these, this type of propellants provides better performance such as high thrust and specific impulse and higher density due to the better physical properties.

Therefore, non-toxic propellants are developed and tested by some research centers recently. The most popular non-toxic propellants are AF-M315E also known as hydroxyl ammonium nitrate (HAN) based and LMP-103S also known as ammonium dinitramide (ADN) based that are developed by US Air Force Research Laboratory and Busek. The micro propulsion system that increases lifetime of CubeSats has examples MPS-130, HPGP and BGT-X5 that are designed for 0.5U up to 2U CubeSats [12, 16, 17]. Examples of non-toxic propellant thruster are given in Table 2.2.

Table 2.2 : Examples of non-toxic or green propellant thrusters.

Thruster	Thrust (N)	Specific Impulse (sec)	Propellant	TRL	Company	Ref.
GR-1	0.26-1.42	231	HAN	TRL 6	Aerojet Rocketdyne	[12]
GR-22	5.7-26.9	248	HAN	TRL 5	Aerojet Rocketdyne	[12]
HPGP	0.25-1	204-235	ADN based LMP-103S	TRL 8	ECAPS	[12,18]
HYDROS	0.2-0.6	258	Liquid Water	TRL 5	Tethers Unlimited, Inc.	[12]
BGT-X5	0.5	220	HAN based AF-M315E	TRL 5	Busek	[12,19]
MPS-130	1.5	240	HAN based AF-M315E	TRL 6	Aerojet Rocketdyne	[20]

As disadvantages, this type of propulsion systems cause challenge in selection of materials because of the very high combustion temperature and increased power consumption. Taking into account mass and size of the non- toxic/green propellant thruster examples, 1 N HPGH, HYDROS, BGT-X5 and MPS-130 thrusters may be used in CubeSats.

2.1.2 Gas propellant propulsion systems

Cold and warm gas propellants for propulsion system has been sufficiently used for large spacecrafts over the years that it designed for missions with large spacecrafts. In this type of chemical propulsion system, a compressed gaseous or liquid ejects to nozzle in a controlled manner purposing to generate thrust. Required thrust is only generated from the compressed gaseous or liquid. It has no combustion, combustion chamber and oxidizer; it consists of only valve, nozzle and propellant storage tank basically. Architecture of this type of propulsion system is simple and light. By taking into account those, it adjusted to small spacecrafts properly. This simple and light design reduces the required power and needs less safety equipment. This is a very important advantage to expand the lifetime of spacecrafts. Besides, it can be used both pulsed and continuous operations [12, 16].

The cold gas propulsion system manufactured by UTIAS, CNAPS was used in CanX-4 and CanX-5 to demonstrate formation flying in 2014. Surrey Satellite Technology Ltd. (SSTL) manufactured the Butane Propulsion System. This propulsion system was used within small spacecraft missions successfully [12, 16]. Other examples of cold gas thruster are given in Table 2.3 [12].

Table 2.3 : Examples of cold gas propellant thrusters.

Thruster	Thrust	Specific Impulse	Propellant	TRL	Company	Ref.
MicroThruster	0.05-2.36 N	65 sec	Nitrogen	TRL 9	Moratta	[12,21]
Butane Prop. Sys.	0.5 N	80 sec	Butane	TRL 9	SSTL	[12]
POPSAT-HIP1	0.083 mN	32-43 sec	Argon	TRL 8	Micro Space	[12,16]
CNAPS	12.5-40 mN	40 sec	SF6	TRL 9	UTIAS/ SFL	[12,22]
CPOD	25 mN	49 sec	R134a	TRL 6	Vacco	[12]

Taking into account mass and size of the cold gas thruster examples, Micro Thruster, CNAPS, POPSAT-HIP1 and CPOD thrusters may be used for CubeSat form.

2.1.3 Solid propellant propulsion systems

The solid motor propulsion system generates thrust by burning solid propellant, which is located in combustion chamber. It consists of combustion chamber that holds the solid propellant and igniter and nozzle. This conventional propulsion system is well known with its generation of high thrust and moderate specific impulse. It can be miniaturized for small spacecrafts and can be used for orbit insertion and other impulsive orbital maneuvers. In other words, it is suitable for high delta-V operations in small spacecraft missions. Solid rocket propulsion system needs safety equipment to handle with the temperature. This system is not a mature propulsion system that is still testing in ground and space. CAPS-3 developed by Digital Solid State Propulsion (DSSP) is at TRL 8, which states that the system is completed and flight qualified. Examples of solid motor are given in Table 2.4 [12, 16].

Table 2.4 : Examples of solid motors.

Thruster	Thrust (N)	Specific Impulse(sec)	Propellant	TRL	Company	Ref.
CAPS-3	0.3	<900	HIPEP-501A	TRL 8	DSSP	[12,16]
ISP 30 spec motor	37	187	Al and Ammonium perchlorate	TRL 7	ISP	[12]
STAR 4G	258	277	Ammonium perchlorate	TRL 6	Orbital ATK	[12]
CDM-1	76	226	AP/HTPB	TRL 6	DSSP	[12]

Taking into account mass and size of the solid motor examples, Micro Thruster, CAPS-3 of DSSP and ISP 30 spec motor of ISP thrusters may be used for CubeSat form.

2.2 Electric Propulsion Systems

Electric propulsion systems convert electrical energy into kinetic energy to obtain thrust. The idea of using electrical energy to produce thrust was first introduced in 1906 by Robert H. Goddard. Later, Eduardovich Tsiolkovsky was also studied about

electric propulsion systems in 1911. In the following years, due to the acceleration of studies on chemical propulsion systems, both of them canalized to chemical propulsion systems [23]. In the 1950s, electric propulsion systems came back to the agenda as they could be good alternatives to chemical propulsion systems and studies speeded up again. Finally, electric propulsion systems were effectively used in the 1990s. They can be easily adapted to small satellites since they are more miniaturized than chemical propulsion systems and have been used for small satellites effectively. Electrical propulsion systems produce much higher specific impulse (>300 sec) and low thrust (<1 N) compared to chemical propulsion systems. Since the thrust is continuous, it is suitable for long periods use. Due to these features, it is ideal for space missions requiring high delta-V. Its efficiency is high, as it requires less fuel consumption compared to chemical propulsion systems [12].

Electric propulsion systems are worse than chemical propulsion systems in countering Earth gravity. They work more efficiently in low gravity and vacuum environment. This type of propulsion systems can be used for attitude control, constellation management, interplanetary and deep space missions.

2.2.1 Resistojet thrusters

Resistojet has simple architecture and is very easy to control. It can produce relatively high thrust compared to other electric propulsion systems but provides less specific impulse. It is possible to produce with low budget. As disadvantage, these systems have some problems such as heat loss and nozzle erosion. Due to the impulse and specific impulse values it provides, it can be used in attitude control and orbit insertion of LEO missions. Resistojet of Surrey Satellite Technology Ltd. has reached TRL 9, which means it has been successfully deployed in a space mission, but is not yet available for CubeSats [12, 16]. The current status of some resistojets that can be used for small satellites is given in Table 2.5.

Taking into account mass, size and power consumption of the resistojet examples, Micro Resistojet, CHIPS and PUC thrusters may be used for CubeSat form.

Table 2.5 : Examples of the resistojet thrusters.

Thruster	Thrust	Specific Impulse	Propellant	TRL	Company	Ref.
Resistojet	100 mN	30-50 sec	Xenon, butane	TRL 9	SSTL	[12]
CHIPS	30 mN	52-76 sec	R134A	TRL 6	CU/VACCO	[12,24]
Micro Resistojet	10 mN	80-150 sec	Ammonia	TRL 5	Busek	[12,25]
PUC	4.5 mN	70 sec	SO2	TRL 6	CU/VACCO	[12,26]

2.2.2 Ion thrusters

Ion engines decompose the fuel contained in ions and use it in the production of impulse. The thrust is generated by accelerating charge particles of ionized propellants. It utilizes the voltage difference of its grids to accelerate the charged particles to obtain thrust. It provides quite high specific impulse and low thrust. Because of this feature, it provides more efficiency compared to other electrical propulsion systems. Due to subatomic particles, it can work in near vacuum environments. Therefore, they can be used for station keeping maneuvers in some GEO satellites, deep space and interplanetary space missions [12, 16].

The first ion thruster was produced by NASA, launched and tested successfully into space under the name Space Electric Rocket Test (SERT-1) [23]. This type of propulsion system used in NASA's Deep Space 1 spacecraft as the main propulsion system for the first time. The ion propulsion system used in this spacecraft is called NSTAR [23]. In the following process, several governments including Japan and Germany sent the spacecraft using ion engines to the space and successfully performed the missions. Nowadays, due to its high efficiency and miniaturization, it is very suitable for small satellites, especially nanosatellites. Although there is no nanosatellite ion propulsion system in the market that has reached technology readiness level 9, this type of nanosatellite propulsion system will have flight heritage thanks to Lunar IceCube CubeSat, which is planned to be launched into space with SLS-1 in 2020 and the use of ion engines for nanosatellites will increase its popularity

[12]. The current status of some ion engines being developed by some companies and universities is given in Table 2.6.

Table 2.6 : Examples of ion engines.

Thruster	Power (W)	Thrust (mN)	Specific Impulse	Propellant	TRL	Company	Ref.
BIT-1	10	0.1	2250 sec	Xenon	TRL 5	Busek	[27]
BIT-3	60	1.4	3500 sec	Xenon-Iodine	TRL 6	Busek	[12,28]
I-COUPS	-	0.3	1000 sec	Xenon	TRL 7	University of Tokyo	[12]
RIT-μX	50	50-500	300-3000 sec	Xenon	TRL 5	Airbus	[12]
MiXI	14-50	0.4-1.5	3100 sec	Xenon	-	JPL	[17]

Taking into account mass, size and power consumption of the ion engine examples, all the examples given in Table 2.6 are suitable for use in CubeSats.

2.2.3 Electrospray thrusters

Electrospray thrusters are a member of electrostatic propulsion systems. This propulsion system generates thrust by accelerating ions just as ion engine, but this type do not need gas ionization. This is because electrospray thrusters use ionic liquid as propellants [12, 16].

Massachusetts Institute of Technology (MIT) developed the first electrospray thruster S-IEPS [29]. After MIT, several companies were starting to develop these type of thrusters for commercial purposes. Busek has amount of examples and they are developing a fully integrated electrospray propulsion system for CubeSats. The current status of some electrospray thrusters being developed by some companies and universities is given in Table 2.7 [12].

Taking into account mass, size and power consumption of the electrospray thruster examples, all the examples given in Table 2.7 are suitable for use in CubeSat form.

Table 2.7 : Examples of electrospray thrusters.

Thruster	Power (W)	Thrust	Specific Impulse	TRL	Company	Ref.
S-IEPS	1.5	0.074 mN	1150 sec	TRL 6	MIT	[12,29]
BET-1	15	0.7 mN	400-1300 sec	TRL 7	Busek	[16]
BET-100	5.5	5-100 μN	1800 sec	TRL 8	Busek	[16]

2.2.4 Pulsed plasma thrusters

Pulsed plasma thrusters, which have an electrodynamic working basis, produce impulse through the interaction of electric field and magnetic field. It has a simple architecture like resistojets. It provides average specific impulse and low thrust compared to other electric propulsion systems. Furthermore, the power requirements are very low and do not require liquid or gas supply systems. They are not suitable for long-term missions because they have short lifespan. This type of electrical propulsion system can be used for missions requiring small delta-V, for example attitude control and technology demonstration missions [12, 16]. The current status of some pulsed plasma thrusters being developed by some companies and universities is given in Table 2.8 [12].

Table 2.8 : Examples of pulsed plasma thrusters.

Thruster	Power (W)	Thrust (μN)	Specific Impulse	Propellant	TRL	Company	Ref.
PPTCUP	2	40	655 sec	PTFE	TRL 6	Mars & Clyde	[12]
NanoSat PPT	5	90	640 sec	PTFE	TRL 5	Mars & Clyde	[12]
BmP-220	1.5	20	536 sec	PTFE	TRL 5	Busek	[12]
MPACS	10	80	827 sec	PTFE	TRL 7	Busek	[12]

2.2.5 Vacuum arc thrusters

Vacuum arc thrusters, which have electrostatic working principle, provide relatively high specific impulse and low thrust. It creates plasma by using the electric arcs in the chamber and accelerates this plasma through the electric field to produce thrust. This propulsion system is as simple as resistojets and pulsed plasma thrusters. Due to this simple structure, its mass is lower. They can operate at low voltages. Despite these good properties, their low efficiency and heat losses are among the disadvantages [12, 16]. The current status of some vacuum arc thrusters being developed by some companies and universities is given in Table 2.9.

Table 2.9 : Examples of vacuum arc thrusters.

Thruster	Power (W)	Thrust (μN)	Specific Impulse	Propellant	TRL	Company	Ref.
μ-CAT	2-14	1-50	2500-3000 sec	Titanium	TRL 7	Gwu and USNA	[12,17]
μ-BLT	4	0.054	-	Aluminum	-	University of Ilinois	[17]

Taking into account mass, size and power consumption of the vacuum thruster examples, all the examples given in Table 2.9 are suitable for use in CubeSat form.

2.2.6 Hall-effect thrusters

Hall-effect thrusters, like ion engines, primarily ionize fuel. Then, this ionized fuel is accelerated by the effect of the electric field and the magnetic field perpendicular to each other and consequently produces thrust. Usually, Xenon is preferred as propellant for this propulsion system. This system generates low thrust and high specific impulse. They can be used for high delta-V missions such as interplanetary transfers. It has a successful flight heritage for large spacecraft, but is not suitable for CubeSats without redesigning, as it requires very, very high power consumption for nanosatellites. Many universities and companies work to adapt Hall-effect thrusters to nanosatellites and produce prototypes [12, 16]. The current status of some Hall Effect thrusters for small satellites being developed by some companies is given in Table 2.10.

Taking into account mass, size and power consumption of the Hall-effect examples, only the HT100 thruster of SITEL is suitable for use in CubeSat 8U, 12U and 27U due to power consumption.

Table 2.10 : Examples of hall-effect thrusters.

Thruster	Power (W)	Thrust (mN)	Specific Impulse	Propellant	TRL	Company	Ref.
BHT-200	200	13	1390 sec	Xenon, Iodine	TRL 8	Busek	[12,30]
BHT-600	600	39	1500 sec	Xenon, Iodine	TRL 6	Busek	[31]
HT100	175	5-15	<1350 sec	Xenon	TRL 6	SITEL	[12]

3. A LUNAR NANOSATELLITE MISSION ANALYSIS

Since it is the closest celestial object to the Earth, the Moon has always aroused curiosity for human beings and created a desire to learn more about it. Therefore, one of the first goals of humankind in space adventure is to go to the Moon. So much so that the space race, an important part of the Cold War between 1957 and 1975, was based on going to the Moon and landing people on the Moon. Governments were obsessed with reaching the Moon to establish superiority over each other. On July 16, 1969, US was the first to achieve the goal of going to the Moon with Apollo 11 space mission. This Moon landing, which is an incredibly big event in that time, will have an important place in the memory of human history. The large part of information about the Moon that known about it comes from the Apollo Program of NASA. In these days when we celebrated the Fiftieth anniversary of the Apollo 11 space mission, it became very popular to perform lunar missions and manned flights to the Moon again. Currently, several space agencies and companies perform a lunar mission or planned in their work calendar. The Chinese Chang'e lunar mission, which takes the Chinese name from the lunar goddess, has detailed the lunar surface map and contributed to what is known about the lunar. Chandrayaan lunar missions developed by the Indians have also made a very important discovery by tracing the water resources on the lunar surface [32]. In addition to these missions, SMART-1 lunar orbiter carried out by ESA also contributed to the testing of important technologies such as experimental ion engine and telecommunication system to be used in deep space missions. In addition to that, it collected data on geology and topography of the Moon to get more information about it [8]. Today, Chandrayaan-2, Artemis, Lunar Reconnaissance Orbiter, Chang'e-3 and Chang'e-4 spacecrafts are proceeding their activity on their lunar missions [33].

One of the biggest handicaps of lunar missions is that the used spacecrafts are very large and these large spacecrafts need high amount of fuel and consequently cost of the mission becomes very high. Taking into account cost of fuel and cost of launch vehicle service that is required to launch the spacecraft into space, only space

organizations can meet the requirements of this type space missions. However, in recent years, it is seen that nanosatellites can carry on scientific missions with very low budget compared to others. The use of nanosatellites shortens project and allows rapid progress as it reduces the cost of the mission. In next years, seven of 13 CubeSats that are carried by Artemis 1 Program will perform specific lunar missions. Some of these CubeSats are Lunar Flashlight of JPL, Skyfire of Lockheed Martin, Lunar IceCube of Morhead State University, LunaH-Map of Arizona State University, Cislunar Explorers of Cornell University, EQUULEUS of JAXA and OMOTENASHI of JAXA [34]. This shows that not only the space agencies but also the universities can contribute to the lunar missions with the CubeSats.

This study aims propulsion system preliminary design for a CubeSat that perform a low-budget specific lunar mission as CubeSats listed above designed by universities. Mission profile of the CubeSat was determined as lunar orbiter. In order for the propulsion system to be designed specifically for the mission, it is necessary to know the mission details and determine the requirements. This satellite is intended to settle in Low Lunar Orbit. The aim of the satellite was determined as lunar surface observation. Hence, the satellite will capture images from the lunar surface with a hyperspectral camera and transmit these images to the Earth for detailed analysis.

The CubeSat, which is designed for the lunar mission, produced and passed several ground tests, is launch into space by a launch vehicle to perform its missionToday, many countries have designed such a vehicle and successfully launched into space. These countries include US, Russia, ESA member states, India, Spain, Japan, China, South Korea and many others [36, 37]. These launch vehicles are used on the purpose of carrying more than one payload to their mission orbits or determined altitude. The largest fuel and energy consumption occurs while defying the gravity of the Earth and leaving the Earth's surface. This is the difficult and quite costly part of the mission. Robert A. Heinlein has a famous saying about this situation: “Once you get to Earth Orbit, you're halfway to anywhere in the Solar System!” [35]. Therefore, multiple spacecrafts are launched into space to perform their space missions by same launch vehicle on the purpose of reduction the cost of mission. Among the planned orbital launch vehicles, a selection can be made according to the transfer trajectory within the scope of lunar mission. Several planned launch operations in the coming years are listed in Table 3.1.

Table 3.1 : The list of several orbital launch systems [36, 37].

Orbital Launch Vehicle	Country	Company	Capability	Date of Flight
Alpha	United States	Firefly Aerospace	1000 kg to LEO, 600 kg to SSO	2020
Angara 1.2	Russia	Khrunichev	3500 to LEO, 2400 to SSO	2020
Ariane 6 A64	Europe	Ariane Group	21650 to LEO, 11500 to GTO, 5000 to GEO, 8500 to TLI	2020-2021
Starship and Super Heavy	United States	SpaceX	150000 to LEO, 100000 to TMI	2020
Space Launch System Block1	Unite States	NASA/Boeing	95000 to LEO, 26000 to TLI	2020
Long March 8	China	CALT	7600 to LEO, 2500 to GTO, 4500 to SSO	2021
OmegA	United States	NG Navigation	10100 to GTO, 7800 to GEO	2021
Soyuz-5	Russia	TsSKB-Progress RSC Energia	18000 to LEO, 2500 to GEO	2022
Minotaur 5	United States	Northrup Grumman Innovation Systems	630 kg to GEO	-
Electron	United States	Rocket Lab	225 kg to LEO	-

A CubeSat that will perform lunar mission can be launched into space with one of these orbital launch vehicles as secondary payload. In addition to these ride-share opportunities, dedicated launchers, which are designed for small satellites to carry them into space as primary payload, are rising trend recently. These launchers can be also seen in the Table 3.1. The launch vehicle can be selected in accordance with the

transfer trajectory options of the CubeSat. Launch vehicle selection and transfer trajectory selection are two important interconnections. Taking into account the delta-V requirements for the satellite, selection of launch vehicle for planned transfer trajectory will be made in the following sections.

3.1 Specification of the Nanosatellite for Lunar Mission

Generally, satellites are classified according to their missions, orbits and masses. Satellite classification due to their masses is given in Table 3.2. CubeSat from nanosatellites class was selected for lunar surface observer satellite that orbits in Low Lunar Orbit. CubeSat form was selected due to low cost and easy to production.

Table 3.2 : Satellite Mass Classification [38].

Class	Mass
Large satellites	>1000 kg
Medium satellites	500-1000 kg
Minisatellites	100-500 kg
Microsatellites	10-100 kg
Nanosatellites	1-10 kg
Picosatellites	100 g- 1 kg
Femtosatellites	10 g – 100 g
Attosatellites	1 g – 10 g
Zeptosatellites	0.1 g – 1 g

In 1999, CubeSats were designed and produced by California Polytechnic University and Stanford State University collaboration to allow university students to participate easily in space programs. Until 2013, it was used for university education and small-scale research. After this date, large-scale space companies and space agencies of governments started to use CubeSat in their space missions [4, 5]. Therefore, number of space mission with CubeSat was increased dramatically. The factors such as Low cost of the design, production and test processes of CubeSats, very quick production process, having lots of launch opportunities, enabling new systems to be tested in space quickly and expandability in any risk situation make CubeSats preferable. Nowadays, they are quite popular and being studied by great number of groups and organizations

because they required very low budget compared to others. Before 2013, almost all of the CubeSats were produced for academic purposes. However, almost half of the CubeSats are produced for non-academic purposes recently [4]. Some of the intended purposes of these CubeSats are education, communication, remote sensing, technology demonstration, navigation, military and Earth observation. They provide important contributions to scientific researches. Since the CubeSats proved themselves in a wide variety of missions and can be produced with low budget, the CubeSat form was preferred for this type lunar mission.

The CubeSat architecture consists of U forms whose size and mass are determined by generally accepted standards that are mentioned in CubeSat Design Specification documents. The standard 1U (single unit) CubeSat is 10 cm x 10 cm x 11.35 cm in size and has mass about 1.33 kilograms [39]. Some CubeSat architectures, which are created by these single units, are given in Figure 3.1.

Figure 3.1 : CubeSat standard sizes [40].

MarCO, which has the name of the first CubeSat used in deep space and the first CubeSat to go to Mars successfully and Lunar Flashlight, Lunar IceCube and others, which will be launched with SLS Block 1 and perform a specific lunar mission, have 6U CubeSat architecture. [41] For this reason, 6U cube satellite form was considered suitable for such lunar mission. This 6U CubeSat form requires thermal control subsystem (TCS), attitude determination and control subsystem (ADCS), electrical power subsystem (EPS), communication subsystem (COMM), command and data handling subsystem (CDHS), structure, payload and propulsion subsystem to perform

this space mission. If briefly mentioned about duties of these subsystems, TCS is required to keep the temperature of the subsystem at desired level. ADCS determines the attitude of the instruments and payloads and corrects the attitude of them. EPS consists of battery, solar panels and power management board. It generates power and stores the power in battery for subsystems. COMM enables to make data transfer and communication between the satellite and the ground control station. CDHS coordinates the subsystems and enables to operate them effectively. Propulsion system that is preliminary designed in this study allows transferring the satellite to mission orbit. To keep these subsystems together, satellite need a structure. In addition, antenna instruments for communication and solar panels are needed to generate electrical power. Hence, a 6U form is ideal to perform this lunar mission effectively.

For this concept lunar mission, payload of the satellite is a hyperspectral camera It is expected that the camera to be used will make hyperspectral shots and collected data about geology and topography of the Moon is transmitted to the Earth to contribute scientific researches.

3.1.1 Structure and mass limitations

After determining the CubeSat form to be used for mission and designing the necessary subsystems and payload details, it is necessary to calculate the maximum size that can be reserved for the propulsion system required to perform this mission. To estimate the structure limitation of propulsion system, the dimensions of subsystems and payloads need to be detailed. If considering the whole structure of 6U Cubesat, it is 100 mm x 226 mm x 366 mm in size and approximately 12 kg according to the 6U CubeSat Design Specification document [42]. 1U of this 6U satellite must be reserved for payload because the selected camera can fit in a 1U structure and it has a mass of 1.3 kg [43]. Looking at the ADCS's on the market, the average size of it is 0.5 U - 0.75 U and weighs about 1-1.25 kg. COMM is approximately 0.75 kg and almost 0.25 U - 0.5 U. On Board Computer of CubeSat is 0.2 U and 200 g. The battery occupies the largest space in EPS, approximately 0.5 U. The total EPS can be considered as 0.7U and about 2.5 kg. The structure, which frames the subsystems, is almost 1.75 kg and [44]. In the light of this information, the representation of the subsystems within the satellite is given in Figure 3.2.

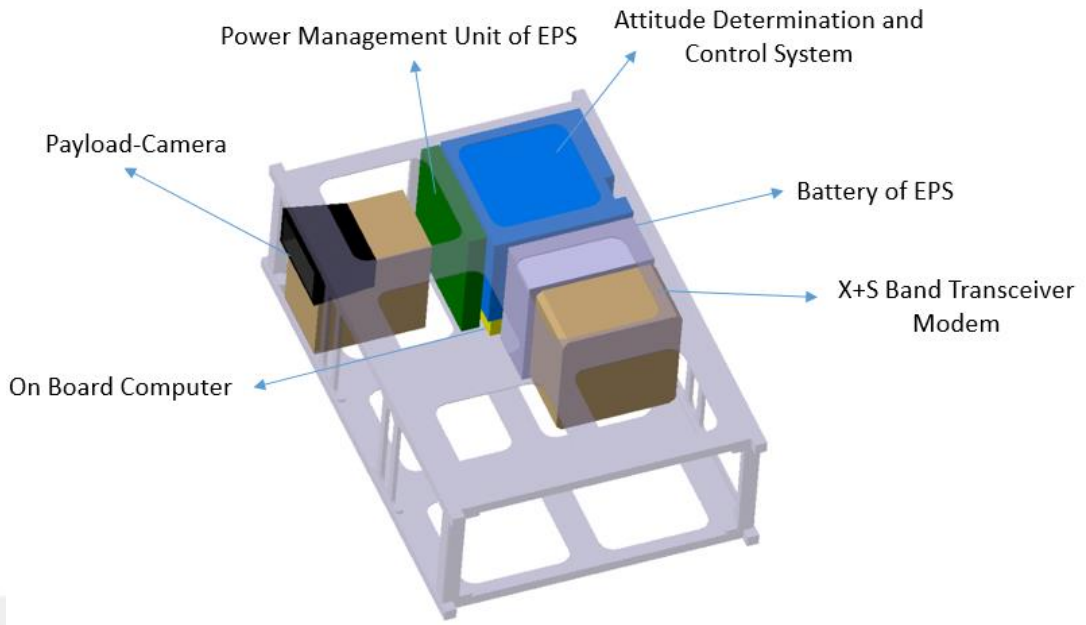

Figure 3.2 : Representation of the subsystems in 6U CubeSat.

As shown in Figure 3.2, the maximum space that can be reserved for the propulsion system, including the propellant tank and thermal equipment, is maximum 3U. The approximate mass of the subsystems and the estimated mass of the propulsion system are given in Table 3.3.

Table 3.3 : Masses of all subsystems.

Subsystem	Mass [kg]
Command and Data Handling Sys.	0.2
Communication Sys.	0.75
Structure & Mechanisms	1.75
Attitude Determination and Control Sys.	1.25
Electrical Power System	2.5
Payload - Camera	1.3
Propulsion Sys.	3
Total	***10.75***
10% Margin	***11.825***

Taking into account masses of other subsystems and instruments, the mass of the propulsion system should be about 3 kg in order to meet standards. In the propulsion system design phase, wet mass and dry mass of the system are assumed 3 kg and 1.75 kg respectively.

3.1.2 Power limitation

The satellite panels provide the energy required by the satellite subsystems to perform their duties. The panels become active when they receive sunlight and start to generate power. A large part of this generated power is currently used for operation subsystems. After the subsystems power needs are met, the remaining power must be stored in the batteries to use it lack of sunlight. The power requirements of satellites vary according to the size of the satellites, their subsystems, and the mission they will perform. The power, which can be generated by panels, varies due to the panel configuration, whether the panels are fixed to the body or deployable, and how often and how long they can benefit from sunlight during the term of the mission. Body fixed solar panels can generate limited energy due to the size of solar area facet directions. Panels cannot be exposed to sunlight at the same time in fixed panel configuration. The deployable panel configuration is generally preferred so that allowing all panels to be exposed to sunlight simultaneously. In the deployable panel option, the panel layout can be adjusted to provide the amount of power needed and the power that the satellite can generate can be optimized. In this study, in order to utilize the advantage of providing as much power as possible for the propulsion system, the panel layout that will maximize the power produced by the panels is preferred. A 6U CubeSat can approximately generate power of 20-30W with body-mounted solar panels. However, this power can be increased up to 120 watts by using the multiple deployable rotating panels [45]. The designed panel layout for this lunar mission is shown in Figure 3.3.

As a result of the analysis, it was found that each of the panels produced approximately 19W peak power during the transfer. The deployable rotating solar panels have sun sensor on themselves and they rotate according to the Sun position. Consequently, the satellite generates approximately nominal 80 W and peak 125 W of power in this panel configuration.

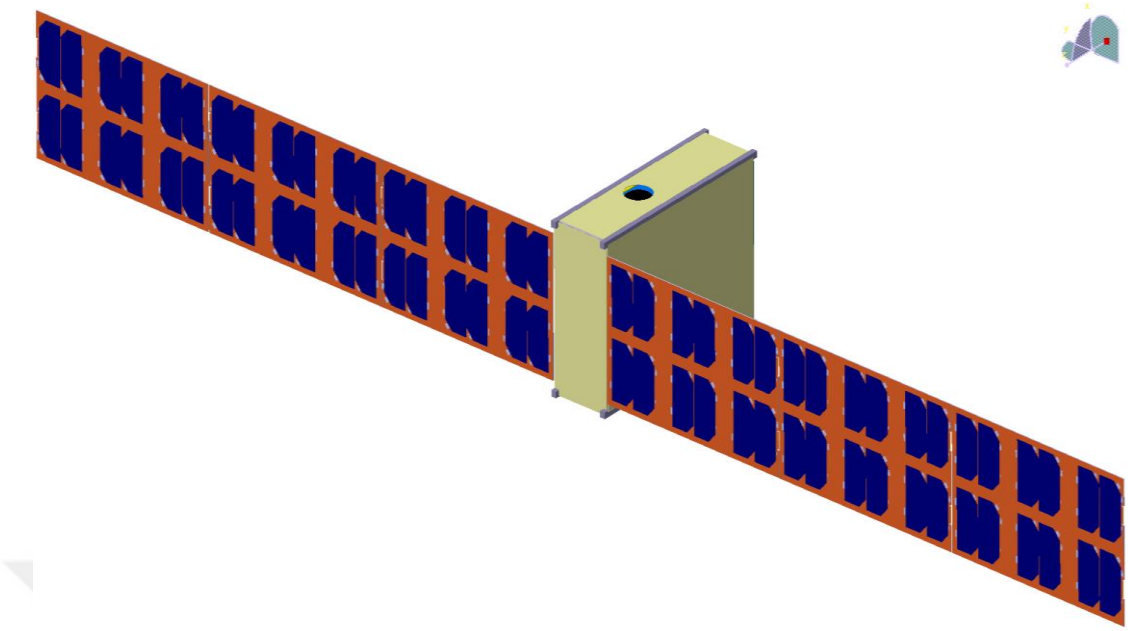

Figure 3.3 : Representation of solar panel configuration.

In order to find the maximum power that can be provided for the propulsion system, firstly it is determined which other subsystems will be operational on the satellite where the propulsion system is actively operated, in other words the power requirement peaks. Then, it is determined how much power these subsystems require when the propulsion system is actively operated and how much of the power generated by the panels can be reserved for the propulsion system. The approximate power budget of the satellite during operation of propulsion system is given in Table 3.4.

Allocated power for the propulsion system is assumed as 57 W. The power consumption for the propulsion system designed is expected to be between 50 and 60 W. In addition to the power budget of the CubeSat, electrical properties of the CubeSat is given in Table 3.5.

Table 3.4 : Power budget of the satellite.

Subsystems	Power Cons. *(W)*	Working Perc.	*Total Cons. (W)*	*Bus Voltage*
Command and Data Handling Sys.	1.5	100%	1.5	3.3V, 5V
Communication RX (S-Band)	3.5	100%	3.5	5V
Communication TX (X-Band)	45	10%	4.5	12V
Electrical Power Sys.	0.5	100%	1,00	3.3V
Attitude Determination & Control	3.5	100%	3.5	
Payload - Camera	11	15%	1.1	
Thermal Control & Mechanisms	15	25%	3.75	
Propulsion Sys. (Max)	57	100%	57	
Propulsion Sys. (Idle)	10,00	0%	0,00	
Power Consumption (W)		75.35		
Power Cons. (W) + Margin [%5]		79.1175		
Power Generation (W)		80		
Net Power Margin (W)		4.65	*5.81%*	

Table 3.5 : Electrical properties of the CubeSat.

CubeSat Electrical Properties	
Power generation	80 W (Min. Ave.),>125 W (Peak)
Power consumption of subsystems	19.3 W
Output (BUS) voltages	3.3V, 5V, 12V and Vbat
Battery configuration	8S1P
Battery capacity	77 Wh, 2.6 Ah
Supply voltage	0-35 V
Battery voltage	24-33.6 V
Heater power	6W
Operational temperature	-40 / +85 °C

3.2 Transfer Trajectory to the Moon

In order to reach to Moon successfully, appropriate transfer trajectory should be determined according to the mission. Lifetime of the satellite and planned duration of the mission, regarding the budget and the aim of the mission play a major role in determining of the transfer trajectory. The time of arrival to the lunar orbit varies considerably depending on the path used and the thrust type provided by the propulsion system. The cost of mission is also absolutely affected. This can be considered as transporting a package by airline transport in a shorter time rather than transporting it by road transport in a longer period. As a matter of course, the cost substantially differs between these two transportation options. On the other hand, the aim of the mission is important to determine final orbit of the spacecraft. In this study, since the aim of the mission is to make lunar surface observation, the appropriate final orbit will be Low Lunar Orbit.

The satellite, which is separated from the surface of the earth by a launch vehicle, is placed into its parking orbit by means of the launch vehicle. The launch vehicle can be selected in accordance with a particular transfer trajectory or the transfer trajectory can be determined according to the capacity of the launch vehicle. In this study, various transfer trajectories that can be used to reach the low orbit of the Moon are mentioned and the most appropriate path is chosen according to the mission requirements. Therefore, after roughly determining the appropriate transfer trajectory, the launch vehicles that can be placed in the parking orbit are evaluated.

In order to select propulsion system type and to design this system for a nanosatellite, which will be used in lunar mission, approximate delta-V, value should be calculated. For the calculation of required delta-V, transfer trajectory, which is path to reach to Moon, should be determined. Several transfer trajectory options that can be used to reach the Moon are examined in this section. It should be noted that these trajectories are simply designed. It can be elaborated in the future for more detailed lunar mission.

3.2.1 Direct transfer from LEO to LLO

The first transfer trajectory type is the direct transfer option, which is always considered the most basic and traditional in interplanetary transfer. This type of transfer was used in the years when space research gained momentum and countries' desire to establish superiority over space was extremely high. In that period, this

transfer trajectory was preferred in many space missions including the Apollo space mission. In this transfer, the satellite is placed in Low Earth Orbit by means of launch vehicle. Ariane 6 A64, Starship, SLS, Soyuz, Minotaur 5 and Electron can carry the satellite to LEO from Table 3.1. The first impulsive maneuver starts from LEO to the Moon, thanks to main engine of the satellite or upper stage of the launch vehicle. This maneuver is called Translunar Injection (TLI) and it needs high thrust value. This Lunar Transfer can be considered as Hohmann Transfer for delta-V calculation, but midcourse correction is needed to do not miss the Moon in the middle of the lunar transfer way. For cislunar missions, the upper limit of this correction maneuver is generally considered to be 0.05 km/s [46]. According to information from previous flight experience, Translunar injection is expected to require a delta V of about 3.1 km/s [46]. Once the satellite has entered the Moon's gravitational field, a lunar orbit insertion maneuver is performed to enter in an orbit at the low lunar orbit. The delta-V need of this mission is nearly 0.8 m/s. The delta-V has additive property. Therefore, the total velocity change required to achieve direct transfer trajectory maneuvers and to reach the Moon is approximately 3.180 km/s [46]. The maneuvers for this type of transfer requires high thrust and thrust in generated by impulsive burn. These impulsive burns can be achieved using chemical propulsion systems. By using direct transfer, the satellite can reach to the LLO in approximately 3 to 5 days [47]. High amount of propellant is needed to perform this transfer in this transfer time. A sketch of this transfer type is given in Figure 3.4.

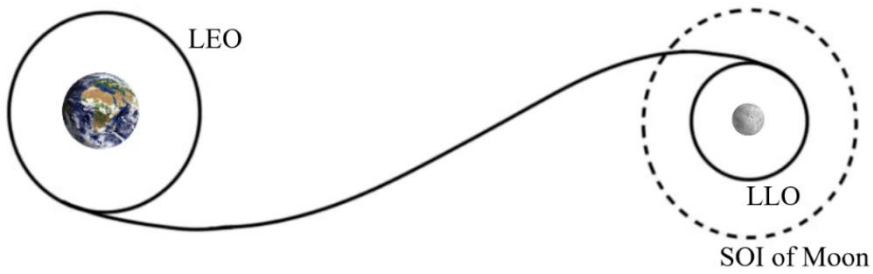

Figure 3.4 : Direct transfer from LEO to LLO (Revised image) [47].

3.2.2 Direct transfer from GTO to LLO

As the lunar transfer to the Moon can be accomplished from Low Earth Orbit, it is also possible to transfer to the Moon by using the Geostationary Transfer Orbit that is used

to reach the Geostationary Orbit. Since the Geostationary Transfer Orbit has much more energy than the LEO and the transfer from GTO to the Moon consumes less fuel than the LEO. Since it is desirable to save fuel and reduce costs, it is preferable to transfer from GTO to the Moon. The GTO and lunar orbit are not directly aligned for the translunar trajectory because they are not located on the same plane. However, the GTO and the orbit of the Moon align twice a year [46]. At this time, it is possible to reach the GTO by direct transfer without the need to plane change maneuver. In this case, it can be reached to the Moon in a shorter time, but it is necessary to use a high-thrust chemical propulsion system. If the angle difference between the two planes is small, the angle difference can be closed by performing midcourse correction on the direct transfer without the need for a plane change maneuver. During the rest of the year, satellite must perform a plane change maneuver to capture the Moon because the GTO is in the equatorial plane, an angle difference of 18.26 degrees to 28.54 degrees between the lunar orbit and GTO [48]. Fuel consumption is very high when direct plane change maneuver and translunar injection are performed at large angles. In order to save fuel, the GTO apogee is increased up to approximately 1 million km, the velocity is very low at this height and it can capture the lunar orbit with short translunar injection and plane change maneuver from this point [46]. By using this fuel-saving method, transfer to the lunar orbit can take approximately 50-60 days [46]. A sketch of this transfer type is given in Figure 3.5.

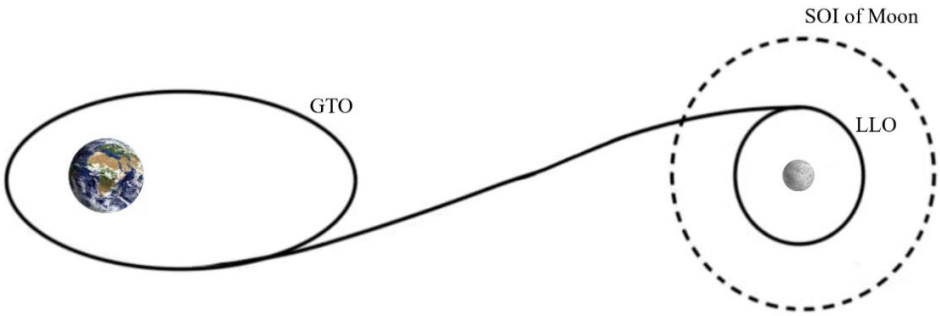

Figure 3.5 : Direct transfer from GTO to LLO (Revised image) [47].

Ariane 6 A64, Long March 8 and OmegA launch vehicles can carry the satellite to geosynchronous transfer orbit from Table 3.1 as secondary payload.

3.2.3 Spiral transfer

In addition to these two high impulsive transfer method, there is an alternate option for providing low thrust systems. This transfer type is called spiral transfer or low-thrust spiral transfer. From any circular orbit, radius of orbit or altitude is increased gradually by applying small and constant thrust parallel to the velocity vector. The satellite can be reached from low Earth orbit or Geostationary Earth Orbit to the Moon. This transfer method increases delta-V requirement and reduces fuel consumption considerably [49]. For this reason, it is mostly used for small satellites with electric propulsion systems.

Using spiral transfer, there are two basic transfer trajectories. In first option, the spacecraft is reached to the Earth-Moon libration point 1 by spiraling out or climb from an orbit around the Earth. After enter the gravitational field of the Moon, the spacecraft spiral in until final target orbit of the Moon. In second option, the altitude of the orbit around the Earth is increased gradually until reaching to the orbit of the Moon around the Earth. After the spacecraft reaches the desired altitude around Moon, the orbit is circularized and the spacecraft reaches its final orbit. These two options need inclination change in addition to the spiral transfer to catch the Moon. The inclination change requirement changes due to the initial orbit [50].

This transfer method is suitable for the missions that do not need to reach the Moon in a short time because delta-V requirement of this method is quite high and burn is non-impulsive that provides not instantaneous velocity change. By using spiral transfer, the satellite can reach to the Moon in 9 to 12 months [50].

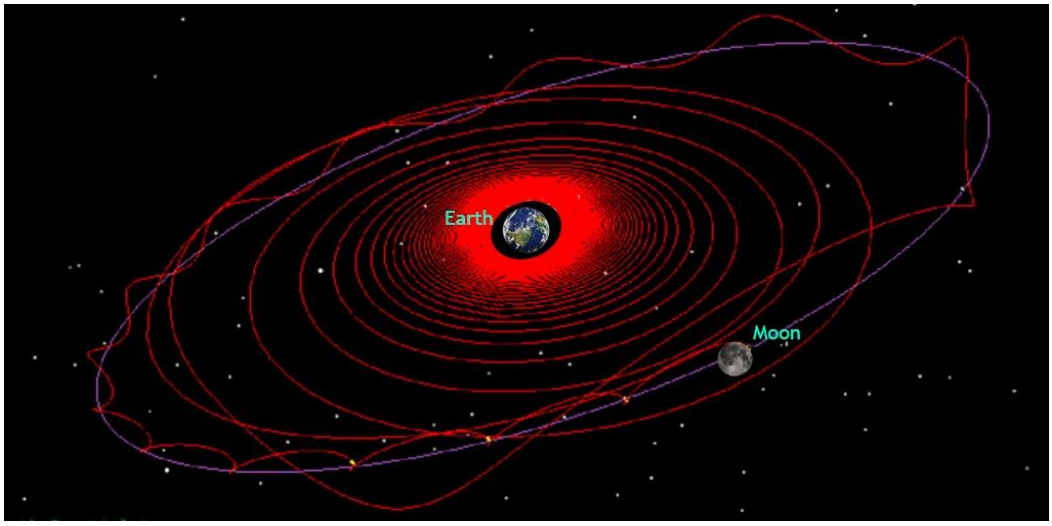

Figure 3.6 : Spiral transfer from GEO to LLO (Revised image) [51].

Ariane 6 A64, Soyuz 5, OmegA and Minotaur 5 launch vehicles from Table 3.1 can carry the satellite to GEO.

3.2.4 Weak stability boundary

In addition to the previously mentioned transfer methods, there is a weak stability boundary transfer to the Moon based on the weak stability boundary theory. This transfer method is also known as ballistic capture transfer to Moon or low energy transfer to the Moon. Earlier this transfer method was successfully used in Japan's Hiten and ESA's SMART-1 space missions [52]. In this transfer method, with the gravity assist at the Lagrange points, the transfer is directed and performed without spending any energy or with very little energy at these points. Due to this feature, it provides a very high amount fuel saving compared to other transfer methods. Example Earth - Moon weak stability transfer representation is shown in the Figure 3.7.

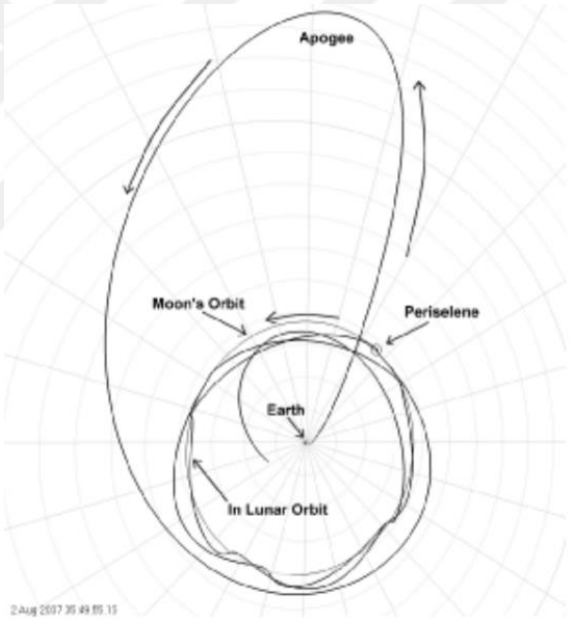

Figure 3.7 : Representation of Weak Stability Boundary transfer from Earth to Moon [52].

In order to reach to the Moon, in this transfer method, it is necessary to travel approximately 4 times the distance traveled to reach the Moon by direct transfer method [47]. In order to use the advantage of the Lagrange points, the satellite goes far from the Earth. This situation increases the amount of power required for communication. In this study, since it is desired to provide as much power as possible for the propulsion system, this transfer method is not preferred as the mission for which the propulsion system is designed.

As a result of the evaluation of the transfer types, considering the propellant and power consumption, the propulsion system to be designed is planned to be used for the transfer of the Moon by spiral transfer method. The propulsion system will be designed considering the requirements of spiral transfer from GEO to LLO.

3.3 Prediction of Lunar Mission Requirements

In this section, delta-V requirement of low thrust spiral transfer from GEO to LLO is preliminary analyzed to use for selection of propulsion type and designing of propulsion system of the nanosatellite. The predicted delta-V requirement of this lunar mission can be calculated from low-thrust mission preliminary anlysis equations [55]. The total delta-V requirement of this lunar mission is about 3.6 km/s. After prediction of required delta-V value for the mission, specific impulse or exhaust velocity can be forecasted by making estimation for fuel consumption of the thruster. This assumption can be made by using Tsiolkovsky rocket equations given in equations 3.1 and 3.2.

$$\Delta V = v_e ln \frac{m_{full}}{m_{empty}} \tag{3.1}$$

$$\Delta V = Isp g_0 ln \frac{m_{full}}{m_{empty}} \tag{3.2}$$

In structure and mass limitations section, the maximum mass of propulsion system was found 3 kg with propellant. Based on this fact, the mass of propellant can be assumed approximately 1.25 kg. Hence, the estimated specific impulse of the propulsion system is 3420 sec. In the same way, exhaust velocity of the thruster should be nearly 33540 m/s. By using these predictions, preliminary design of the thruster can be started.

3.4 Selection of Propulsion System Type Due to the Mission

In order to design a propulsion system for the lunar mission, the type of propulsion system to be designed must first be determined. In the Background chapter, the types of thrust systems are mainly introduced and state-of-the-art of small satellite propulsion systems is given. Before assessing the suitability of these systems for the lunar mission, the requirements of the mission should be briefly summarized. The maximum size that can be reserved for the propulsion system in a 6U CubeSat is 3U, and for the satellite, which is expected to be 12 kg, the propulsion system is expected

to have an average mass of 3 kg. Peak power can be provided for the propulsion system in power budget review is around 60W while the propulsion system is actively operating. With the spiral transfer method, the delta-V value required was found to be around 3.6 km/s for low-budget transfer from geostationary earth orbital to low lunar orbit. The specific impulse value is 3420 sec and the exhaust velocity is of 33540 m/s were determined by using the possible dry and wet mass of the propulsion system and this delta-V value. Based on all this information, the type of propulsion system can be determined with the help of a trade study. In order to represent the average status of each type of propulsion system, an example was determined from each type and a trade study was conducted between these examples.

In order to perform a trade study to determine the type of propulsion system, evaluation criteria and weight factors, which are the ratings of the importance of these evaluation criteria, should be determined. Evaluation criteria for thrust system selection are thrust, specific impulse, power requirement, propellant type, mass, size and TRL. Briefly, why these features are identified as evaluation criteria, each space mission requires a different thrust value level and thrust is one of the important criteria in determining the suitability of propulsion systems. Specific impulse, which is also a measure of the efficiency of the system, is one of the important criteria. Since the power, mass and structure can provide the propulsion system, it is essential to select a system that can be adapted to a 6U satellite. For this reason, these characteristics are the evaluation criteria that must be selected in the propulsion system selection for defined satellites form. Some propulsion systems are named according to the types of propellant they use, such as the Hydrazine Propellant system and the green propellant system. This is due to the change in safety equipment and the complexity of the system with respect to the propellant used. The main reason for this change is the toxicity of the propellant or the possibility of damaging the spacecraft due to its chemical properties. Therefore, it is one of the propellant evaluation criteria. Technology Readiness Level should be included in the evaluation criteria since it is an indicator of the level of system proving itself. TRL is an evaluation criterion because in this study it is desirable to select a propulsion system type that has proven itself in a space mission and to design a propulsion system for the mission to be included in the class of that propulsion type.
Weight factors are and indicator of the importance of evaluation criteria and they are determined as a percentage. For this trade study, thrust, specific impulse and TRL are

the most important evaluation criteria and therefore have 20 percent weight factors. Mass and size are as important as thrust, specific impulse and TRL, but since they are the criteria that affect each other, it is appropriate to give 10 percent weight factors to each of them. For propellant type and power requirement criteria, 10 percent weight factors are determined.

After the evaluation criteria and weight factors have been determined, normalization scale is determined for scoring. Considering the mission profile in this study, it is seen that the use of a system with a high specific impulse is essential. It must have a thrust of mN grade with high specific impulse. In propellant selection, systems that do not require toxic propellant need to score higher. In this mission, since the size, mass and power values that can be provided for the propulsion system are almost certain, scoring is made considering these values. Since the propulsion system, which has a level below TRL 5, does not participate in this study, a gradual scoring from 5 to 9 can be made.

As seen in Table 3.6, BIT-3 propulsion system of Busek has the highest score. Since this propulsion system belongs to the class of ion engine propulsion system, the most suitable propulsion system for this mission is determined as ion engine propulsion system.

After the selection of the thrust system type, the defining characteristics of the thrust system to be designed were determined. As a result, the characteristics and mission profile that are decisive in propulsion system design are summarized in Table 3.7.

Table 3.6 : Propulsion system type trade study [12, 14, 16, 17, 20, 25, 28, 29].

Product	Company	Propulsion Type	Thrust		Specific Impulse (sec)		Power (W)		Propellant		Mass (kg)		Size		TRL		Total
Weight Factors			20%		20%		10%		10%		10%		10%		20%		
MONARC-1	MSDD	Hydrazine	1 N	2	227.5	2	>18	4	Hydrazine	1	Dry 0.38	5	13x0.5cm LxD	4	TRL 5	1	2,40
MPS-130	Aerojet Rocketdyne	Non-Toxic	0.25-1.25 N	3	206-235	2	>17	4	AF-M315E	5	2.76	1	2U	3	TRL 6	2	2,70
Nanoprop 6U	GomSpace NanoSpace	Cold Gas	4-40 mN	4	60 -110	1	<8	5	Butane	4	0.9	5	1U	4	TRL 7	3	3,40
CAPS-3	DSSP	Solid Motor	0.3N	3	<300	2	N/A	3	HIPEP-501A	2	2.33	3	N/A	3	TRL 8	4	2,90
Micro Resistojet	Busek	Resistojet	10 mN	4	150	2	15	4	Ammonia	3	1.25	4	1 U	4	TRL 5	1	2,90
BIT-3	Busek	Ion Engine	1.4 mN	5	3500	5	60	3	Xenon-Iodine	4	2.5	3	2U	3	TRL 7	3	**3,90**
S-IEPS	MIT	Electrospray	74 µN	1	1160	4	1.5	5	Ionic liquid	4	0.1	5	0.2 U	5	TRL 6	2	3,30
MPACS	Busek	Pulsed Plasma	144 µN	1	827	3	10	5	PTFE	4	N/A	3	N/A	3	TRL 7	3	2,90
µ-CAT	Gwu and USNA	Vacuum Arc	1 – 50 µN	1	2500 – 3000	5	2.0-14	5	Titanium	4	0.2	5	200 cm3	3	TRL 7	3	3,50
HT100	SITAEL	Hall Effect	5 – 15 mN	4	<1350	4	175	1	Xenon	4	0.45	5	<0.75U	5	TRL 6	2	3,50

Table 3.7 : Lunar mission analysis summary.

Mission & CubeSat Physical Properties		
1	Mission type	Lunar orbiter
2	Phase using propulsion system	Spiral transfer to LLO
3	CubeSat form	6U
4	Mass of CubeSat	12 kg
5	Payload	Hyperspectral camera
6	Power generation	80W (Min. Av.) >125W (Peak)
7	Power consumption of subsystems	19.3W
8	Output (BUS) voltages	3.3V, 5V, 12V and Vbat
9	Delta-V requirement of the mission	approximately 3.6 km/s
10	Type of propulsion system	Ion engine
11	Maximum size of propulsion system	3 U
12	Maximum wet mass of propulsion system	3 kg
13	Maximum dry mass of propulsion system	approximately 1.75 kg
14	Maximum power budget for propulsion system	50-60W
15	Specific impulse requirement	approximately 3420 sec
16	Exhaust velocity requirement	approximately 33.54 km/s

4. PROPULSION SYSTEM DESIGN FOR LUNAR MISSION

For previously detailed lunar mission, the most appropriate propulsion system was determined as ion engines in the main category of electrical propulsion systems because of the trade study. In the beginning of the study, electrical propulsion systems were preferred to chemical propulsion systems. Because chemical propulsion systems do not provide continuous thrust, this type of propulsion system is not suitable to go to the Moon with spiral transfer method. Electrical propulsion systems enable cislunar missions because of providing continuous thrust, more fuel saving compared to chemical propulsion systems and high delta-V values [56]. As a result of the trade study, ion engines with the highest score for the mission were found suitable because of their high specific impulse and thrust values. It is considered a good option since ion engines are planned to be used in similar space missions and such engines are being developed.

Briefly mentioning about the ion engines, the idea that the propellant can be ionized and produced thrust with the help of electrostatic field was first introduced by Robbert A. Goddard. Only years after Goddard, Eduardovich Tsiolkovsky, who was regarded as the founder of rocket science, studied this type of propulsion system. Later, both of them have made studies in the field of chemical propulsion systems due to the popularization of chemical propulsion systems. In the 1960s, Lewis research center, the first ion engine was designed under the leadership of Kaufman and this type of ion engine is known as Kaufman ion thruster. The first space mission in which ion engines are used is Space Electric Rocket Test 1, SERT-1. The purpose of this study, which was conducted by NASA, was to test ion engines in space, and two ion engines, one of which is mercury and the other is cesium propellant, were sent into space in 1970. The mercury-fueled ion engine, which was successful in this test, accelerated the studies on ion engines. With NASA's use of the NSTAR ion engine as the main propulsion system in the Deep Space-1 space mission, many space agencies have used ion propulsion systems from their space programs [57, 58, 59]. Ion engines that have many flight heritage to this date are the one of most suitable options for interplanetary and deep space missions thanks to continuous thrust, high delta-V and fuel saving.

After many years of successful use in large space vehicles, they became easily adapted to small satellites with the popularization of small-scale satellites thanks to the high miniaturization of this type of propulsion system.

Basically, ion engines ionize the propellant contained in the propellant tank in the discharge chamber and these charged particles are accelerated by passing them through voltage grids that create electrostatic field. In order to avoid the charging of the spacecraft, the positively charged particles, which are rapidly exiting the grids, are neutralized by means of neutralizers. Ion motors are divided into sub-categories according to their propellant discharge methods within the discharge chamber. These types can be categorized as below [60].

- Direct current electron discharge ion thrusters
- Kaufman ion thrusters
- Radio frequency discharge ion thrusters
- Microwave discharge ion thrusters

Radio frequency thruster, RF thrusters, come into prominence thanks to their high specific impulse and low thrust values (in the order of mN). This ion engine type has a quite good flight heritage. RIT-10 ion thruster, which developed by Germany in 1993, was used in EURECA space mission and became the first RF thruster used in a space mission [61]. RF ion engines use MHz radio frequency to ionize the propellant in the discharge chamber. Thus, there is no need for hollow cathode or hot cathode in the discharge chamber. Thanks to this design advantage, it does not have cathode erosion and therefore has a longer life. By means of this situation, this ion engine type is the best option for long term space missions such as long interplanetary and deep space [61]. Furthermore, this type of ion engine has been found suitable for this lunar mission because it requires lower power consumption than direct current electron discharge ion thrusters and Kaufman ion thrusters. Therefore, efficiency is higher than Kaufman ion thrusters and direct current electron discharge ion thrusters [60, 62]. In addition, all these facts, the miniaturization of RF ion thrusters is very high for small satellites. Recently, RF ion thrusters are available for many companies and space agencies that are being developed for nanosatellites. Busek developed one of the most promising ones, BIT-3 RF thruster is planned to be used in Lunar IceCube 6U CubeSat, which will be used in similar lunar mission in this study [63]. For all these reasons, the

RF ion thruster type has been chosen as the type of propulsion system to be designed and used in the lunar mission in this study.

4.1 Conceptual Design of the Propulsion System

In this section, the components of RF ion propulsion system are examined and the configuration of these components is decided because some components have several configurations such as RF antenna and grid set configurations. To decide the components and their configurations, the working principle of the RF ion thruster must be understood.

Classical RF ion thrusters have ionization, acceleration and neutralization processes to generate thrust for spacecrafts as shown in Figure 4.1 These thrusters are called RF ion thrusters because they use RF power to ionize the propellants through RF power.

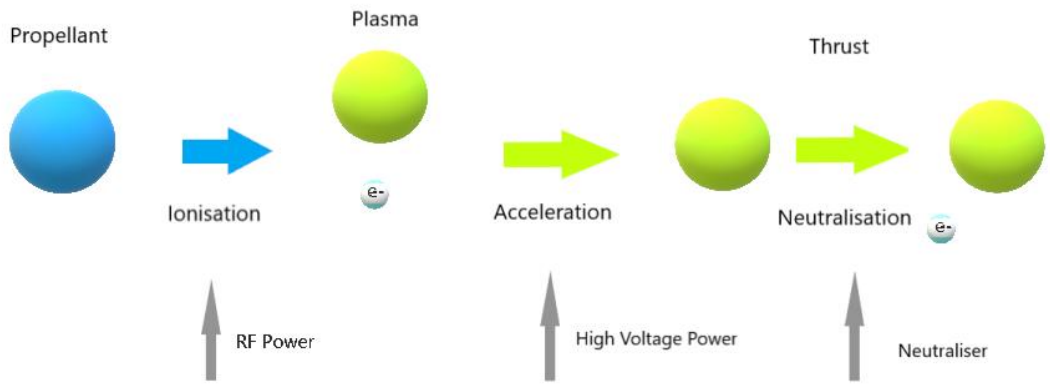

Figure 4.1 : Thrust Generation Schematic.

The propellant in the propellant tank is transferred to the discharge chamber thanks to the propellant feeding system. This propellant is ionized in discharge chamber by RF power. There are several type of usage of this RF power, which is generated in RF generator. This generator converts the DC power, which comes from the PPU of the propulsion system to the RF power. One of these types is wrapping a RF coil around the discharge chamber. Plasma in the discharge chamber is transferred to the grids of the thruster. In grids of the thruster, plasma is accelerated by using electrostatic acceleration method due to positive potential screen grid and negative potential acceleration grid. These grids take their power from PPU of the thruster. In addition to these grids, a third grid, which has no potential, can be used for some advantages. The

ions of the plasma are extracted and accelerated in these grids due to the potential difference and apertures of the grids. The positively charged ion of the beam plume can be charged the spacecraft and thruster; this causes the erosion on the surface of spacecraft and thruster. In order to prevent this undesired situation and extend the lifespan of the thruster, a neutralizer should be placed at end of the thruster. This neutralizer expels the electron to the ion beam plume to neutralize it. The scheme of the working principle of the RF ion thrusters is given in Figure 4.2 [60, 64, 65].

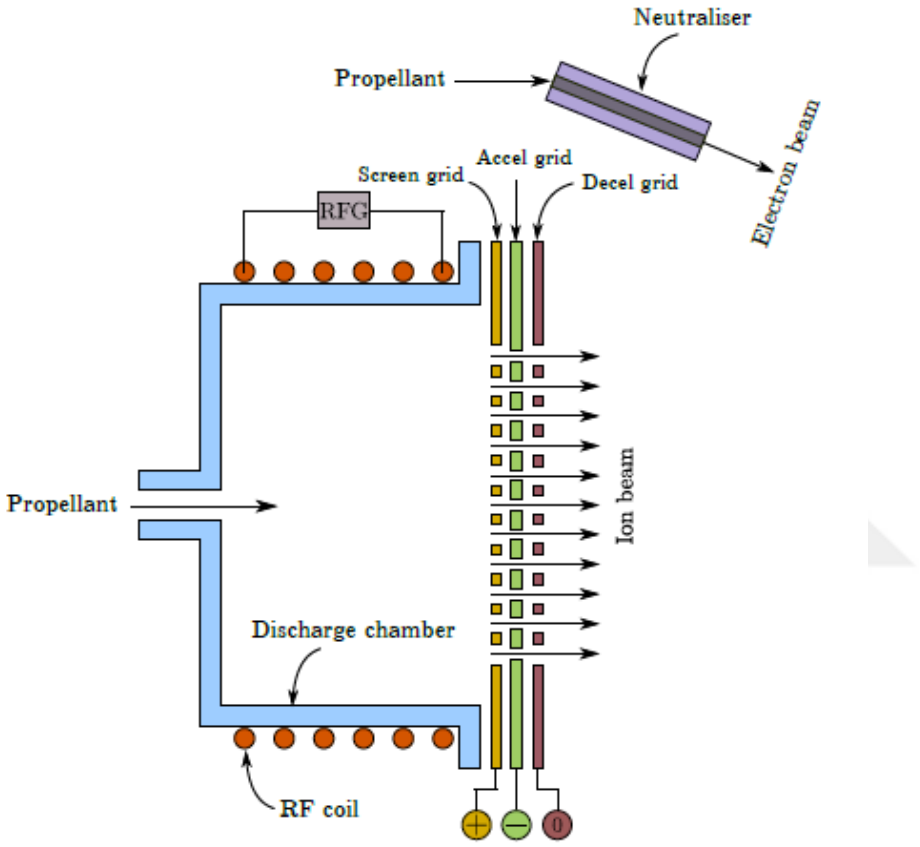

Figure 4.2 : Operation Schematic of RF Thruster [66].

Based on the scheme of the RF ion thruster, conceptual design can be divided in to four as ionization chamber, grids, neutralizer and power supply of the thruster. There are several ways to use RF power to ionize the propellants and configuration of the girds. These ways should be examined to decide which is the most effective method the generate thrust.

4.1.1 Ionization chamber

The propellant is ionized in the discharge chamber, also known as ionization chamber through RF power. There are several ways to use RF power for this purpose. These

ways are capacitively coupled plasma discharge and inductively coupled plasma discharge. Capacitively plasma discharge consists of two planar electrodes and a vacuum chamber. These electrodes are worked by using RF power. In capacitively coupled plasma CCP type discharge, there is no need to magnetic field requirements and architecture of the system is simple. On the other hand, low ion flux and high ion energy are dependent each other and cannot be changed separately [59, 67]. The schematic of the CCP discharge is given in Figure 4.3.

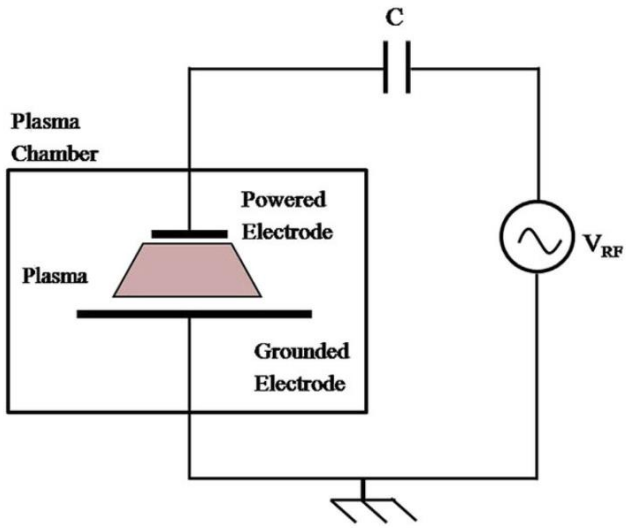

Figure 4.3 : Conductively coupled plasma discharge schematic [68].

The second RF ion discharge type is inductively couples plasma discharge, which couples RF energy to free electrons. RF antenna near the discharge chamber creates an alternative RF magnetic field and induces RF electric fields, which energize electrons that participate in the ionization of gas molecules and atoms at low pressure. By contrast, with CCP discharge, it has low ion energy and it can be controlled independently. This type of discharge provides nonuniform density profile [67]. The ICP discharge has planar or cylindrical coil for generating plasma by using between 100 KHz and 16 GHz radiofrequency waves [59]. The schematic of the ICP discharge types are given in Figure 4.4.

For this thesis, inductively coupled plasma discharge with cylindrical RF coil around the discharge chamber was selected ionization chamber configuration because ICP discharge generates a plasma that has higher density than CCP discharge thanks to inductive coupling between the plasma and RF antenna.

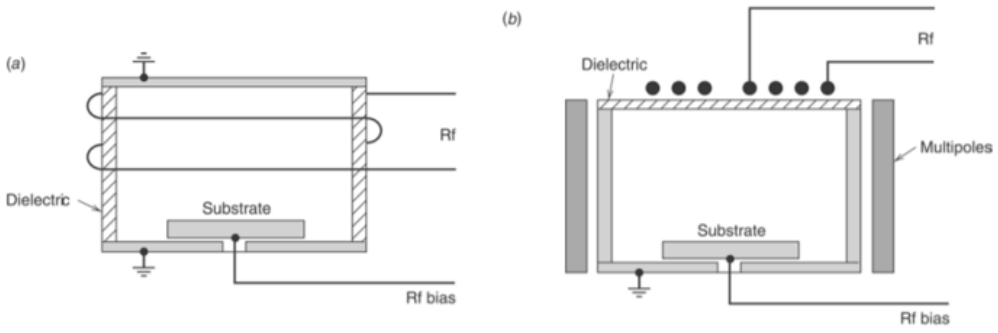

Figure 4.4 : Inductively coupled plasma discharge cylindrical and planar respectively [69].

4.1.2 Ion optics

The grids of the thruster are used to accelerate the plasma particles by using electrostatic-acceleration method. The plasma particles flow through aligned apertures of the grids and acceleration is generated by geometries of the apertures and high voltage applied between two grids. Two different ion optic grids configurations as two-grid system and three-grid system are shown in Figure 4.5.

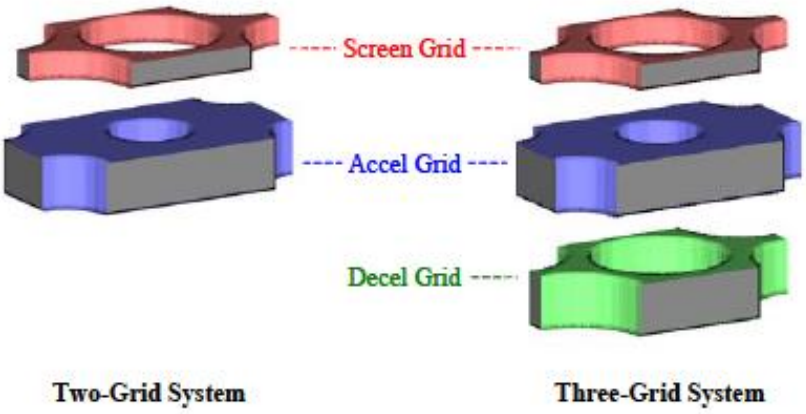

Figure 4.5 : Grid set configurations [65].

The most of the gridded ion thruster examples use two-grid system configuration because this system was designed earlier and simpler than three-grid system [65]. To make choice between the gird sets, the functions of the grid types must be known. The first grid is called screen grid that is biased less positive than plasma. The plasma passes through the first grid and takes ion beam form. This ion beam is accelerated between two high voltage girds and generates thrust. In third-grid system, a third grid,

also known as deceleration grid is placed at the end of the thruster. The purpose of this deceleration grid is to protect the acceleration grid from the back streaming of the ion because the ions pass through the acceleration grid tend to backflow due to the negative voltage of the acceleration grid [64, 65]. This back flowing of accelerated ions decreases the generated thrust of the thruster. The third grid should be used to get rid of this performance-decreasing phenomenon. Besides, this grid does not have a negative impact on power consumption since it does not need potential energy. In this study, three-grid system was chosen to accelerate the ions.

4.1.3 Power processing unit

The power processing unit provides the necessary electrical power to the propulsion system components. It manages the portion of the power generated in the electrical panels allocated to the propulsion system. In propulsion system, power processing unit is primarily responsible for providing and distributing power to the RF generator to generate RF signal for use in plasma production and positive and negative high voltages for to the ion optics for accelerating the particles of ionized plasma. In addition, it supplies required power of mass flow control unit for the controlled release of propellant into the discharge chamber and required power for neutralizer to operate.

4.1.4 Propellant tank

The propellant tank is the component in which the propellant is maintained in suitable conditions for use in propulsion production. The propellant in the propellant tank is delivered to the discharge chamber through the mass flow control unit. The propellant tank is pressurized or not, depending on the state of the propellant in it. For instance, in gas or liquid propellant systems, pressurized propellant tanks are used to prevent the propellant from occupying a lot of space due to the low propellant density. For solid propellants such as Iodine, there is no need to use a pressurized tank.

4.1.5 Mass flow control unit

Mass Flow Control Unit (MFCU) is the unit responsible for the flow of propellant from the propellant tank to the discharge chamber and the neutralizer at the appropriate flow rate. The power supply unit supplies the power required for the MFCU.

4.1.6 RF generator

The RF coil requires RF power to generate magnetic field. This RF power is provided by converting the DC power from the solar panels into RF power in the RF generator. It is one of the most essential part of the RF ion thruster systems. It converts the DC current allocated for plasma production to RF current and transmits the RF current to the RF coil, enabling plasma production. They cannot convert all the power they receive from the PPU to RF power; they usually operate with 70-80% efficiency. However, there are advanced versions that run at 90% efficiency [45,60,70].

4.1.7 Neutralizer

After the ions pass through the deceleration grid and leave the thruster, the spacecraft is negatively charged. Because of this negative charge, the ions are drawn back to the spacecraft. To prevent the occurrence of this situation, a neutralizer that neutralizes the ion plume by means of ejection of electrons should be placed at the end of the thruster as a hollow cathode [59, 64]. If this neutralizer is not used in the space environment, accelerated ions are drawn back to the spacecraft and thrust cannot be generated. Neutralizer cathode also uses propellants to generate electrons. It takes its power from the same power supply unit as the thruster.

4.2 Preliminary Design of the Propulsion System

In Preliminary Design section, the physics behind the propulsion system design is introduced and the necessary formulas for calculating the performance parameters such as thrust, specific impulse, power consumption and efficiency are combined, after specifying the components required for the propulsion system and making the necessary configuration selections in conceptual design section. The prilimanry design of the ion optics and the choice of propellant to be used were made in this section.

4.2.1 RF plasma ionization

The first required process to produce thrust in the propulsion system is the release of the propellant, which is contained in the propellant tank into insulated discharge chamber by means of the mass flow controller and the ionization of the propellant in this ionization chamber. This process is very important because it is the first of the three main stages of thrust generation. The major actors in the RF ionization phase are

the mass flow controller, the insulated discharge chamber in which the propellant is ionized and directly connected to the ion optics, RF antenna, which enables to ionize the propellant in the discharge chamber, and RF source, which provides this RF. As mentioned in the conceptual design section, the ICP discharge model was chosen to work in this study. In this ICP model, the RF coil wrapped around the discharge chamber was preferred as the RF antenna to ionize the propellant. In this section, RF ionization process is mentioned and required formulas are given.

The amount of the electrical power generated by solar panels of the satellite allocated for the propulsion system is transferred to the propulsion system. Some of this transferred electricity as DC is reserved for providing required electricity to operate ion optics and some of this electricity is allocated for ionization process. DC allocated for ionization is transferred to the RF generator to convert direct current to RF current. This RF generator converts the received direct current into RF current and it is transmitted to the RF coil, which is wrapped around the discharge chamber. RF ion thrusters usually use frequency around 1 MHz, as well as the use of 13.56 MHz is common. The magnetic field in the RF coil is induced by the RF current. The time-varying magnetic field formula is as 4.1 [60,62,67,71].

$$B_z = \frac{NI}{\mu_0} e^{i\omega t} \tag{4.1}$$

where N is the number of turn of RF coil around the discharge chamber, I is the RF current, μ_0 is permability of free space and ω is cyclic frequency. This cyclic frequency can be formulated as equation 4.2 with RF.

$$\omega = 2\pi f \tag{4.2}$$

This axial time-varying magnetic field creates azimuthal electrical field, which is perpendicular to magnetic field. The relationship between magnetic field and electrical field is presented by Maxwell equations as 4.3 [60].

$$\nabla \times E = -\frac{\partial B}{\partial t} \tag{4.3}$$

The electric field in the azimuthal direction can also be written as equation 4.4.

$$E_\theta = -\frac{i\omega r}{2} B_{zo}{}^{i\omega t} \tag{4.4}$$

An electromagnetic field is applied inside the disharge chamber. Therefore, free electrons gain energy and are accelerated. The electrons that are activated cause the ionization of the propellant by electron impact ionization. The generated plasma is assumed quasi-neutral ($n_e \approx n_i$). This means that the electron density and the ion density are almost equal [60]. The plasma electron density can be calculated by using equation 4.5.

$$n_e = \omega_p{}^2 \frac{\varepsilon_0 m}{e^2} \tag{4.5}$$

where ω_p plasma frequency, which is equal to $2\pi f_p$. Other important properties related to the plasma is electron temperature of the plasma. Electron temperature can be found from the average kinetic energy of the plasma [67].

$$E = \frac{3}{2} k_B T_e \tag{4.6}$$

where k_B is Boltzmann constant. In normal case, electron temperature is higher than ion temperature for ion thrusters. Electron temperature is 5 eV in RF ion source [60]. In this situation, electron thermal speed can be written as equation 4.7.

$$v_e = \sqrt{\frac{8k_B T_e}{\pi m_e}} \tag{4.7}$$

However, the ions enter the plasma sheath with Bohm velocity before accelerated by ion optics grids and it can formulated as equation 4.8.

$$v_{Bohm} = \sqrt{\frac{k_B T_e}{m_{ion}}} \tag{4.8}$$

Bohm velocity is calculated as 1.9 km/s at 5 eV electron temperature. In addition, for RF ion source to generate plasma, minimum pressure in discharge chamber varies between 10^{-3} torr and 10^{-2} torr according to the literature [60, 72].

Another important quantity of the plasma is Debye length, which is characteristic length of the plasma. This length refers to the distance at which charged particles in the plasma of certain properties can interact. They can sense the effect of each of the particles within this distance [65]. This length can be written as equation 4.9.

$$\lambda_D = \frac{\varepsilon_0 k_B T_e}{e^2 n_e} \tag{4.9}$$

After the plasma properties, the details should be given about the RF coil that enables the RF ionization and the RF current through this coil. RF generator converts DC power to RF power, transfers it to coil and as mentioned before, the typical frequency used in RF ion thruster is about 1 MHz [60, 73]. The simple circuit diagram of this system is as Figure 4.6.

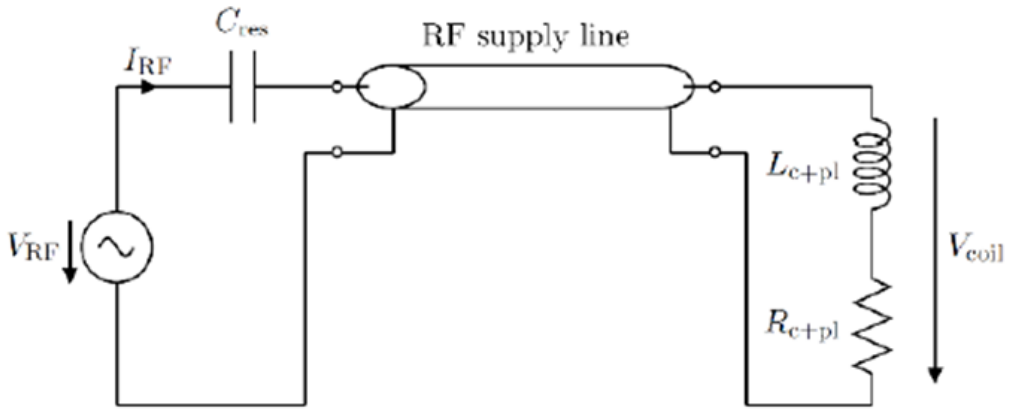

Figure 4.6 : Circuit diagram of the system [73].

Number of turn, length and radius of coil directly affect the coil inductance. This relationship is demonstrated by equation 4.10.

$$\rho_{coil} = \frac{\mu_0 \pi r^2 N^2}{l_{coil}} \tag{4.10}$$

where radius of the coil is r, number of turns is N and length of the coil is l. In addition, the material and the cross-sectional area of the coil are the factors affecting the resistance of the coil [73].

$$R_{coil} = \rho_{coil} \frac{l_{coil}}{A_{cross-section}} \tag{4.11}$$

Total impedance of the thruster coil in conjunction with the inductively coupled discharged plasma is given as equation 4.12 [73].

$$Z = R_{cpl} + L_{cpl} \omega_{RF} i \tag{4.12}$$

RF ion thrusters typically use a short RF supply line with 50 Ω impedance since this value does not generate radiation [71]. It can be used to decrease radiation level of

whole system. Capacitance of the system can be calculated by using output frequency of RF generator [71].

$$C = \frac{1}{(2\pi f_0)^2 L_{cpl}} \tag{4.13}$$

4.2.2 Preliminary design of the ion optics

Ion optics part has substantial role for electrostatic thrusters. After the ionization in discharge chamber, acceleration of charged ions occurs in this part thanks to grids and high voltage of these grids. Ion optics consists of three grids, which are screen grid, acceleration grid and deceleration grid. Design of the ion optics can be examined in two parts as grid sizing and grid potentials.

4.2.2.1 Determination of grid parameters

As decided before, three grids systems is used to accelerate the plasma particles. Plasma in discharge chamber meets with the screen grid firstly and it passes through apertures of this grid. While passing the apertures, the screen grid has to allow occurring Child-Langmuir sheath around apertures of screen grid. After screen grids ion particles in plasma is accelerated into acceleration grid and through acceleration grid apertures. Acceleration grid should has smaller aperture size than screen grid aperture size. Nevertheless, screen grid protect the acceleration grid. Third grid, deceleration grid protects the electrons from back flowing [74]. The aperture size of the deceleration grid has to bigger than the aperture size of the acceleration grid in order not to be an obstacle for accelerated ion particles, which means thrust. The schematic illustration of the grids is given in Figure 4.7.

d_s, d_a and d_d represent the diameter of the screen grid aperture, acceleration grid aperture and deceleration grid aperture respectively. t_s, t_a and t_d represent the thickness of the screen grid, acceleration grid and deceleration grid respectively as well. Plasma sheath thickness should be calculated from Child-Langmuir equation as equation 4.14. A small demonstration of the plasma sheath thickness between two grids is given in Figure 4.8.

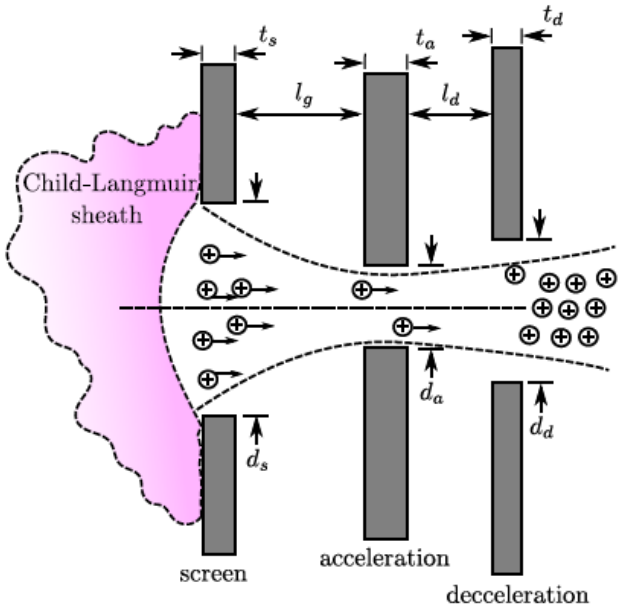

Figure 4.7 : Illustration of the ion optics [64].

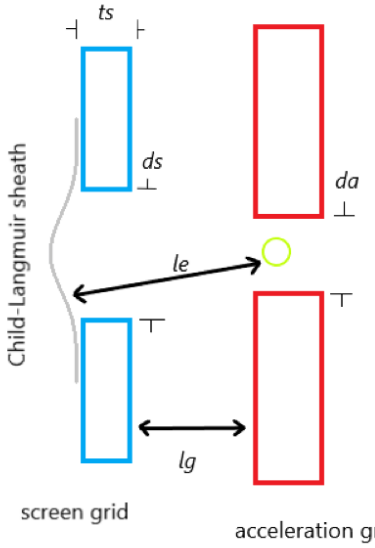

Figure 4.8 : Plasma sheath thickness, l_e (Revised image) [64].

Plasma sheath thickness can be calculated by simple geometrical approach as equation 4.14.

$$l_e = \sqrt{(l_g + t_s)^2 + \frac{{d_s}^2}{4}} \tag{4.14}$$

where l_g is gap distance between screen grid and acceleration grid. Generally, size of these parameters are similar for different gridded ion thrusters. Farnell gathered the

grid set examples and constructed a geometrical relationship between these example grid sets. This geometrical relationship between example grid sets is given in Figure 4.9 [65].

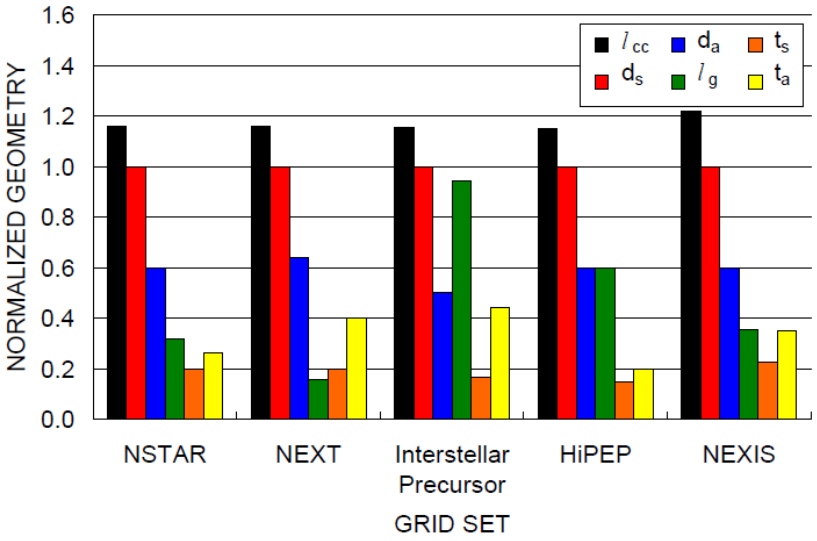

Figure 4.9 : Geometrical relationship between different example grid sets [65].

where l_{cc} center-to-center grid spacing. Figure 4.9 shows that different example of grid sets have similar geometrical shape. If diameter of screen grid aperture d_s is chosen, all other parameters can be calculated by using the ratio these parameters to d_s. According to the literature review most of the screen grid aperture diameter is around 2 mm [58, 61, 64, 65, 75, 76]. Because of the fact that d_s was chosen as 2 mm in preliminary design section. By using the geometrical relationship combination of example grid sets, ion optics parameters of screen grid and acceleration grid were arranged. Most studies do not use deceleration grid or not focus deceleration grid parameters. Deceleration grid parameters were adjusted by using two studies to be proportional to screen and acceleration grids [64,77]. All of the ion optics parameters for this thruster are arranged as given in Table 4.1.

After arrangement of the grid dimensions, sheath thickness length l_e can be found as 1.65 mm. The apertures of the grids are located on center of imaginary hexagonal areas which has side length $\sqrt{3}\, l_{cc}$. By using this hexagonal area and the total active grid area, number of apertures can be found. Total grid active area, which has apertures on itself, should be determined as well since it is necessary to calculate total generated thrust by thruster. Considering the dimensions of the satellite cross sectional area where the thruster head is placed, maximum diameter of the thruster can be found.

This maximum value is almost 7.5-8 cm and the Xenon fueled ion engine can generate 1.5-15 mN between 2.5 and 8 cm interval of grid diameter. However, when considering other components of the propulsion system, such as the neutralizer, propellant tank, this maximum value is decreased to almost half of it. Hence, active grid diameter is determined as 3.5 cm and maximum 202 apertures can be fitted in this active grid area for screen grid. The number apertures in the acceleration is not increased because breaking the aperture alignment has a negative effect on efficient thrust generation. For this active area, transparency of the grids is 0.0653.

Table 4.1 : Ion optics parameters.

Parameter	NSTAR Geometrical Ratio	Value
d_s	$d_s/d_s = 1$	2 mm
d_a	$d_a/d_s = 0.6$	1.2 mm
d_d	-	2 mm
t_s	$t_s/d_s = 0.2$	0.4 mm
t_a	$t_a/d_s = 0.4$	0.8 mm
t_d	-	0.8 mm
l_g	$l_g/d_s = 0.46$	0.92 mm
l_d	-	0.8 mm
l_{cc}	$l_{cc}/d_s = 1.17$	2.34 mm

4.2.2.2 Determination of grid potentials

Grid potentials are essential parameters for acceleration part of the RF ion thrusters. Plasma particles come to the grids with Bohm velocity. Ions are accelerated into grids and through grid apertures both. The grids take their high voltage power from power supply because of the connection. To make acceleration possible, screen grid has positive potential and acceleration grid has negative potential. As mentioned before, deceleration grid is used to prevent the thruster from ion back streaming. Hence, it does not need any power; potential of the deceleration grid is zero. Potentials of the grids are shown in Figure 4.10.

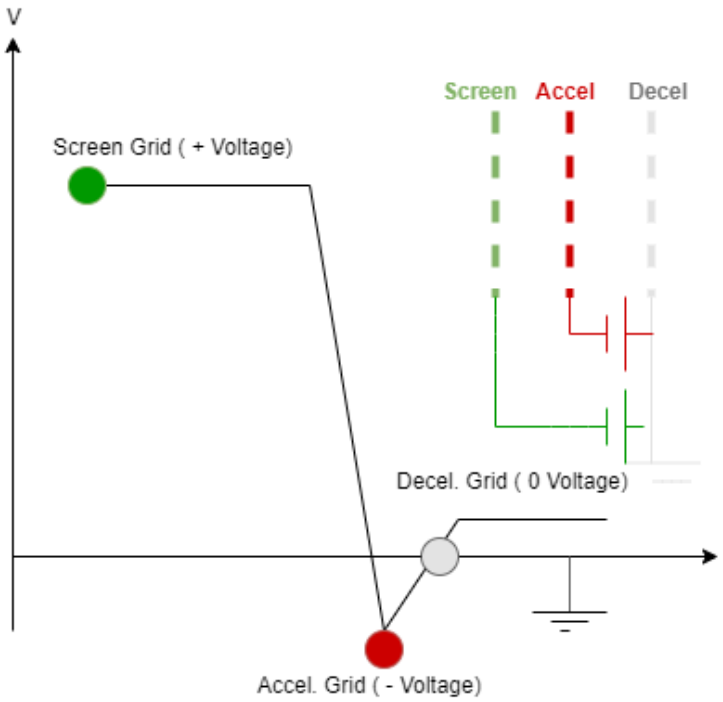

Figure 4.10 : Grid Potentials (Revised image) [101].

Total grids potential is represent the voltage that comes from power supply to screen grid and acceleration grid. It can be formulated as equation 4.15.

$$V_T = V_s + |V_a| \tag{4.15}$$

Maximum current density can found in A/m^2 by using Child-Langmuir Law equation 4.16. [78]

$$J_{max} = \frac{4\varepsilon_0}{9}\sqrt{\frac{2e}{m_{ion}}}\frac{{V_T}^{3/2}}{{l_e}^2} \tag{4.16}$$

The total voltage of the grids is not transmitted to plasma beam fully. Plasma beam voltage is same as net acceleration voltage of the thruster. The ratio of the net acceleration voltage to the total acceleration voltage is indicated by letter R.

$$R = \frac{Net\ acceleration\ voltage}{Total\ acceleration\ voltage} = \frac{V_N}{V_T} = \frac{V_N}{V_s + |V_a|} \tag{4.17}$$

According to the literature search, this ratio corresponds to between 0.85 and 0.9 [60,64,65]. Beam or net acceleration voltage has an effect on specific impulse. Relationship between specific impulse and beam voltage can be found Figure 4.11 for

Xenon gas and different mass utilization efficiency, η_m by assuming thrust correction factor is 0.985.

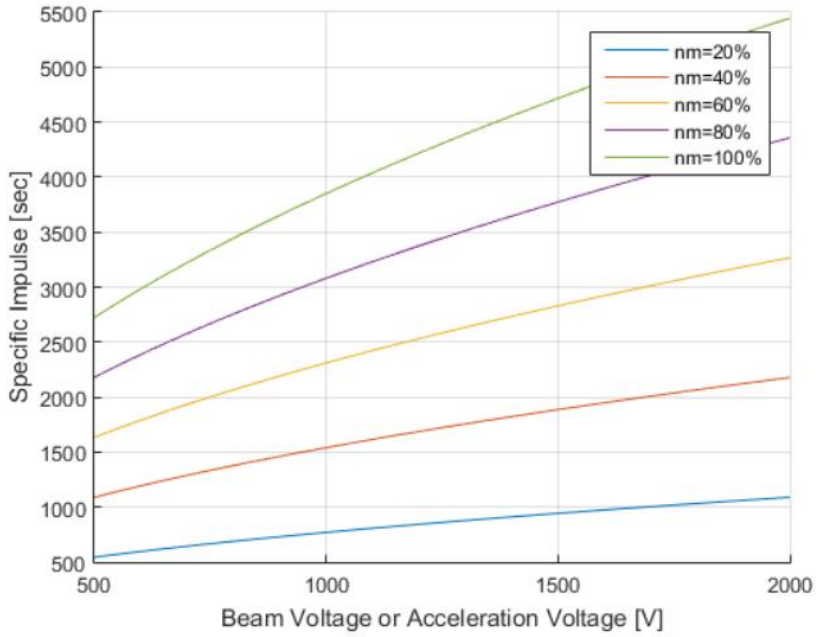

Figure 4.11 : Graph of relationship between Isp and V_b for different η_m and Xenon propellant.

The grid potential values are calculated by assuming 80% mass utilization efficiency as given in Table 4.2.

Table 4.2 : Grid potentials.

Parameter	Potential [V]
V_T	1369.7
V_N, V_b	1232.7
V_s	1219.7
V_a	-150
V_d	0

4.2.3 Thrust

Thrust is one of the main specification for propulsion systems. The value of thrust varies due to the thruster types and size because each space mission and spacecraft needs different capability and sized propulsion system. Large spacerafts has less size and mass limitations than small spacecrafts, and their propulsion systems can generate

higher thrust in comparison with small spacecrafts. Due to physical limitation of small spacecrafts, they have smaller thrusters and propellant tanks. This causes the low thrust generation between millinewtons and micronewtons.

In this part, calculations of thrust for RF ion thrusters are examined. After the selection of the propellant and clear determination of other essential values such as ion beam current, the value of theoretical thrust and predicted thrust can be calculated. Based on general thrust equation, thrust formula can be derived for RF ion thruster.

$$T = \dot{m}v_e + (P_e - P_0)A_e \tag{4.18}$$

Difference between exit pressure and free stream pressure is extremely low and because of that this part can be omit for electric propulsion systems. Thrust equation is rewritten as equation 4.19.

$$T = \dot{m}v_e \tag{4.19}$$

Main principle of the electric propulsion systems is conversion of electrical energy to the kinetic energy as mentioned before. By using this fact, exhaust velocity formula can be derived for ideal thruster.

$$\frac{1}{2}m_{ion}{v_e}^2 = e\,V_b \tag{4.20}$$

where m_{ion} is ion mass of propellant and V_b is beam voltage. This equation is arranged as equation 4.21.

$$v_e = \sqrt{\frac{2qV_b}{m_{ion}}} \tag{4.21}$$

where q is charge of particle. For fully but singly ionized propellant, there is an ion beam current formula given as equation 4.22 [79].

$$I_b = \dot{m}(e/m_{ion}) \tag{4.22}$$

By combining equation 4.19, equation 4.21 and equation 4.22, the theoretical thrust formula, which is maximum thrust value, is derived for ideal ion thruster as given 4.23.

$$T = \sqrt{\frac{2m_{ion}V_b}{q}} I_b \tag{4.23}$$

As can be understood from the theoretical thrust formula, propellant selection is an important effect on thrust value. This formulas belong to ideal ion thruster, but create an ideal thruster is almost impossible in practice. There are some facts such as divergence of ion beam and doubly charged of some ions. These phenomena decrease the thrust value of the thrusters, and they should be into account to calculated predicted thrust value. To make thrust value more realistic, thrust correction factor should be put in the equation 4.23. This thrust correction factor consists of combining two other correction factors, which are beam divergence correction factor and doubly charged ion correction factor. Ion beam divergence correction factor is given as equation 4.24 [60].

$$F_t = cos\theta \tag{4.24}$$

where θ is half angle of the ion beam diverence. The other correction factor, doubly charged ion correction factor can be calculated by using equation 4.25.

$$\alpha = \frac{1 + 0.707\frac{I^{++}}{I^{+}}}{1 + \frac{I^{++}}{I^{+}}} \tag{4.25}$$

To calculate this factor, ratio of doubly charged ions to singly charged ions is needed. The less plasma has doubly charged particles, the higher thrust is generated due to this formula. The thrust correction factor is created with these mentioned factors as equation 4.26.

$$\gamma = F_t\ \alpha \tag{4.26}$$

Finally, thrust prediction formula can be rewritten for non-ideal ion thruster as equation 4.27.

$$T = \gamma \sqrt{\frac{2m_{ion}V_b}{q}} I_b \tag{4.27}$$

These correction factors will be calculated in following section, and predicted thrust can be found.

4.2.4 Specific impulse

The second important specification of the propulsion systems is specific impulse that represents the efficiency of the thruster. Specific impulse of the ion thruster can be derived from general specific impulse formula given as equation 4.28 [80].

$$Isp = \frac{T}{\dot{m}g} \tag{4.28}$$

where g is the acceleration of the gravity and $\dot{m}$ is mass flow rate of the selected propellant. This formula can be represented by using particle flow rate of propellant that is Q in sccm as equation 4.29.

$$Isp = 1.037 \times 10^6 \frac{T}{Q} \tag{4.29}$$

Specific impulse can be expressed with exhaust velocity or exhaust velocity of the ions.

$$Isp = \frac{v_e}{g} = \frac{v_i \eta_m}{g} \tag{4.30}$$

where η_m is mass utilisation efficiency, and formulated as equation 4.31.

$$\eta_m = \frac{\dot{m}_\iota}{\dot{m}} = \frac{I_b m_{ion}}{e\dot{m}} \tag{4.31}$$

As a result of substitution of these formulas, the theoretical specific impulse can be calculated from equation 4.32.

$$Isp = \frac{\eta_m}{g}\sqrt{\frac{2qV_b}{m_{ion}}} \tag{4.32}$$

The difference between ideal thruster and more realistic thruster was discussed in thrust part. Predicted specific impulse can be calculated with the same logic by using equation 4.33.

$$Isp = \frac{\gamma \eta_m}{g} \sqrt{\frac{2qV_b}{m_{ion}}} \tag{4.33}$$

Mass utilization efficiency and the correction factor are directly proportional to the Isp. To increase the efficiency of thruster, which is specific impulse, mass utilization efficiency should be increased.

4.2.5 Power consumption

Nanosatellites have power limitation just as size and mass limitations. Due to the unit numbers, the place, which is reserved for EPS, is decreasing or increasing. In addition to that, the size and capacity of components that can generate power such as solar panels vary. Less power consumption is an indication of the success of the designed propulsion system. Two different powers must be given to the system in order to operate the thruster and generate the thrust. These input powers are radiofrequency power to ionize the propellant in discharge chamber and ion optics power to create electrostatic and accelerate the ionized propellant.

$$P_{in} = P_{RF} + P_{IO} \tag{4.34}$$

where P_{RF} is RF power and P_{IO} is ion optics power. RF power can be calculated from RF current and the coil resistance with simple approach.

$$P_{RF} = R_{cpl} {I_{RF}}^2 = \frac{{V_{coil}}^2}{R_{cpl}} \tag{4.35}$$

This equality gives sufficient results for the preliminary design. However, in cases where RF power needs to be calculated in more detail, Simon and Chabert's articles should be examined and their procedures should be followed [73,81]. Unfortunately, since the RF generator does not operate at 100 percent efficiency, it is wrong to think that the power required to produce plasma with RF is directly RF power. Recently, RF generators operating at 90 percent efficiency are available and it is assumed that the efficiency of RF generators is 90 percent in this study. The required RF power to be added to the input power must be taken into account in this way. Using this data, the thruster input power is calculated. Unfortunately, not all of this power can be used to

generate thrust, losses occur. Output electrical power of the thruster can be considered beam power.

$$P_{out} = I_b V_b \tag{4.36}$$

This output electrical power is converted to the jet power, which is kinetic power.

$$P_{jet} = \frac{1}{2} m_{ion} {v_e}^2 \tag{4.37}$$

Efficiency of the thruster will be examined in next part thanks to these formulas. As a result, total power consumption of the thruster can be calculated from the inputted power to thruster which are RF power and ion optics power, but total power consumption is a bit more than thruster power requirements. There are other input powers to generate some other part of the propulsion system such as propellant ignitor.

4.2.6 Efficiency

Efficiency is a great success measurement of the thrusters. In electric propulsion systems, total thruster efficiency is evaluated by considering electrical efficiency and mass utilization efficiency both because of the working principle of the electric propulsion systems. Electrical efficiency is calculated from ratio of output power-to-input power. Output power and input power mean beam power and given power to the thruster for working such as RF power and ion optics power [59].

$$\eta_e = \frac{P_{out}}{P_{in}} = \frac{P_b}{P_{RF} + P_{IO}} \tag{4.38}$$

whereP_b, P_{RF} and P_{IO} are beam power, RF generator power and ion optics power respectively. RF generator efficiency can be calculated from ratio of the RF power to DC power.

$$\eta_{RFG} = \frac{P_{RF}}{P_{DC}} \tag{4.39}$$

Today, the efficiency of some RF generators is around 90 percent. For this study, RF generator efficiency was accepted as 90 percent. In previous section, mass utilisation efficiency was formulized as equation 4.40.

$$\eta_m = \frac{\dot{m}_\iota}{\dot{m}} = \frac{I_b m_{ion}}{e\dot{m}} \tag{4.40}$$

Ratio of the jet power, which is converted from electrical power to jet (kinetic) power, shows the total thrust efficiency [60].

$$\eta_T = \frac{P_{jet}}{P_{in}} = \frac{T^2}{2\dot{m}P_{in}} \tag{4.41}$$

Total efficiency formula can be written in terms of electrical efficiency and mass utilization efficiency as equation 4.42.

$$\eta_T = \gamma^2 \eta_e \eta_m \tag{4.42}$$

Ion production efficiency, also called ion production cost is found by dividing power of production ion by the currents of ion production.

$$\eta_d = \frac{P_d}{I_b} \tag{4.43}$$

η_d represents discharge loss of the plasma generater. Because of that, smaller η_d is desired to improve the performance of the ion thruster.

4.2.7 Propellant selection

In order to calculate perfomance indicators, propellant selection must be made. Since propellant selection is one of the most important factors affecting performance, cost and safety, it is necessary to make a detailed examination on the types of propellant used and their benefits in order to make propellant selection.

4.2.7.1 Mercury

Many ion engines designed in the early stage used mercury as propellant. Especially, from the 1960s to the late 1970s, the idea of using mercury as propellant for propulsion systems with ion thrusters was very popular [78, 82]. At that time, quite a lot of study was done about mercury ion thrusters and a lot of mercury ion thrusters were develop to use in different space mission scale from orbital control to deep space exploration. SERT I, SERT II and IAP were only a few of them. In progress of time, some propulsion systems, which were originally designed to use mercury as propellant, had

also changed propellant choice as Xenon. These systems are UK-10 thruster of Great Britain, RIT-10 of West Germany and ETS-III of Japan [83, 84]. A small list of mercury ion thruster is given in Table 4.3.

Table 4.3 : The list of Mercury ion thrusters.

Thruster	Date (circa)	Diameter	Specific Impulse (circa)	Country	Ref.
SERT I	1964	10 cm	5000 sec	USA	[85,86]
SERT II	1970	15 cm	4200 sec	USA	[85,86]
SEPST	1970	20 cm	3600 sec	USA	[86]
SIT-5	1972	5 cm	3000 sec	USA	[86]
SEPS	1981	30 cm	3100 sec	USA	[85,86]
IAPS	1983	8 cm	2550 sec	USA	[85,86]

Between 1960s and 1970s, mercury was selected because of its physical advantages such as high molecular weight, storability and low potential requirements for ionization. On the other hand, being high toxicity and harmful for health of workers in ground test made it necessary to take extra safety measures. In 1980s, Xenon began to be preferred over the mercury [83].

4.2.7.2 Xenon

As mentioned before, usage of mercury was replaced by Xenon in time. Since that time, Xenon is the most preferred propellant for ion thrusters due to its properties.

Since Xenon is an inert gas, which is a noble gas, it does not react with the surface of the spacecraft components. It provides more safety. In addition, their chemical and physical properties increase their preferability. Some important properties of Xenon are high atomic mass and low potential energy to ionize. The cost of Xenon is very high due to its limited availability and expensive production process [74, 89-91]. Due to limited resources, price of the Xenon is increasing. Owing to fact that, searching of alternative propellant to Xenon has accelerated by researchers. The list of Xenon ion thrusters are given in Table 4.4.

Table 4.4 : The list of Xenon ion thrusters.

Thruster	Date (circa)	Diameter	Specific Impulse (circa)	Country	Ref.
SCATHA (P78-2)	1979	3.6 cm	350 sec	USA	[58]
XIPS-13	1997	13 cm	2565 sec	USA	[85]
XIPS-25	1998	25 cm	3800 sec	USA	[85]
NSTAR (DP1)	1998	30 cm	1900-3100 sec	USA	[86]
NEXT	2010	36 cm	4190 sec	USA	[87]
I-COUPS	2014	-	1000 sec	Japan	[12]
RIT-μX	2013	2.5 cm	300-3000 sec	Germany	[88]

4.2.7.3 Argon

Argon is the third most common gas in our atmosphere with percentage 0.93. As xenon gas very expensive, consideration of Argon usage as propellant has emerged that can be used as an alternative to the Xenon gas. Because it is inert gas, this gas does not cause any damage to the surface of the spacecraft and does not cause corrosion as well [74, 92]. The list of Argon ion thrusters are given in Table 4.5.

The fact that the cost of Argon gas is 125 times less than the cost of Xenon gas has been attractive for space missions requiring high propellant mass and university education purposes. As disadvantages, atomic mass of Argon is much lower than Xenon and it need to high potential energy for ionization. These facts cause decreasing the efficiency of the thrusters.

Table 4.5 : The list of Argon ion thrusters.

Thruster	Date (circa)	Diameter	Specific Impulse (circa)	Country	Ref.
VASIMR	1979	-	3000-12000 sec	USA	[93]

4.2.7.4 Iodine

In 1990s, Iodine was considered as an alternative to Xenon for ion and Hall Effect thrusters and Iodine is one of the most popular alternative to Xenon recently. Space agencies and some companies developed several thrusters as given in Table 4.6 [74, 94].

Table 4.6 : The list of Iodine ion thrusters.

Thruster	Date (circa)	Diameter	Specific Impulse (circa)	Country	Ref.
BHT-200	2006	3 cm	1390 sec	USA	[30]
BHT-8000	2012	17 cm	2210 sec	USA	[95]
BIT-3	2017	3 cm	2100 sec	USA	[28]

Iodine is in solid form in room temperature, it enables to small propellant tank. Atomic mass and ionization potential energy are closed to the Xenon. Iodine is one of the best alternatives to Xenon. However, Xenon is a slightly toxic propellant compared to Xenon and may require extra safety equipment. It is not the best alternative for Xenon since it is incompatible with many materials.

4.2.7.5 Krypton

Krypton has a much higher cost than Argon. However, the cost is still low compared to Xenon cost. Until this year, there was no flight proven Krypton thruster in space. Krypton thruster was launched into space in Starlink constellation [96]. When the chemical and physical properties of Krypton are examined, it is seen that a pressurized propellant tank is needed to fit into the satellite since it is an inert gas. However, it has the highest density after Xenon among noble gases. With the advantage of being noble gas, Krypton does not need protective equipment because of its good chemical compatibility property. The list of Krypton ion thrusters are given in Table 4.7.

Table 4.7 : The list of Krypton ion thrusters.

Thruster	Date (circa)	Diameter	Specific Impulse (circa)	Country	Ref.
SPT-100	1991	-	1600 sec	USA	[89]
BHT-1500	2008	10 cm	1820 sec	USA	[97]
Thruster of Starlink	2019	-	-	USA	[96]

It is expected to gain a solid place in the coming years with its widespread use and successful use in space missions.Some important properties of these propellants are given in Table 4.8.

In order to evaluate these propellants, it is necessary to examine the effect on the main factors determining the performance of the propulsion system. Figure 4.12 shows a comparison of the required ion beam voltages to achieve the same specific impulse using different propellants. From the voltage difference of the ion beam, the comparison of the amount of power required to the ion optics with respect to the propellant can also be inferred directly proportional. As can be seen from the graph, the Argon has the lowest atomic mass and the voltage required to accelerate is the lowest. The required voltage for Iodine and Xenon compared to Argon is about 3 times. Among all four different propellants, it can be said that Krypton has an average voltage requirement.

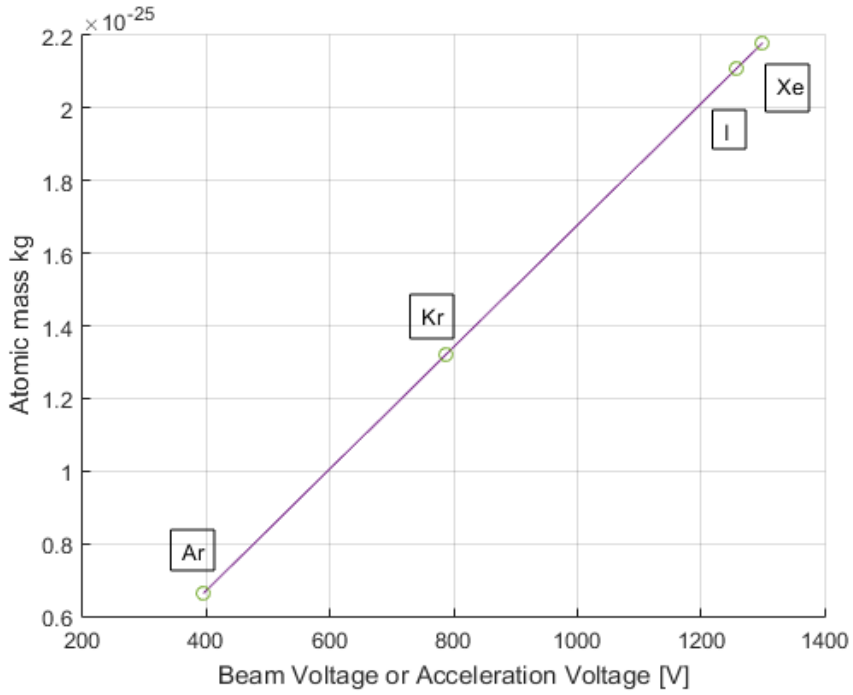

Figure 4.12 : Beam voltage vs. atomic mass graph.

Another factor that needs to be examined is how the thrust value changes with respect to propellants when the same amount of voltage is supplied to the thruster ion optics. The pure effect of the different propellants on the propulsion can be observed in this way. This effect can be examined in Figure 4.13.

Table 4.8 : Properties of these elements for standard temperature and pressure.

Propellant name	Atomic Number	Atomic Mass (kg)	State	Ionization Potential Energy (eV)	Density (g/cm^3)	Melting Point (C)/ Boiling Point (C)	Price ($/100 g)	Ref.
Xenon	54	$2.18\ x10^{-25}$	Gas	12.13	0.0059	-117.8 / -118.09	120	[74,90,98]
Argon	18	$6.63\ x10^{-26}$	Gas	15.76	0.0018	-189 / - 185.7	0.5	[74,90,98]
Iodine	53	$2.107\ x10^{-25}$	Solid	9.3	4.993	113.7 / 184	8.3	[74,90,98]
Krypton	36	$1.319\ x10^{-25}$	Gas	14	0.0037	-157.37 / -153.2	33	[74,90,98]

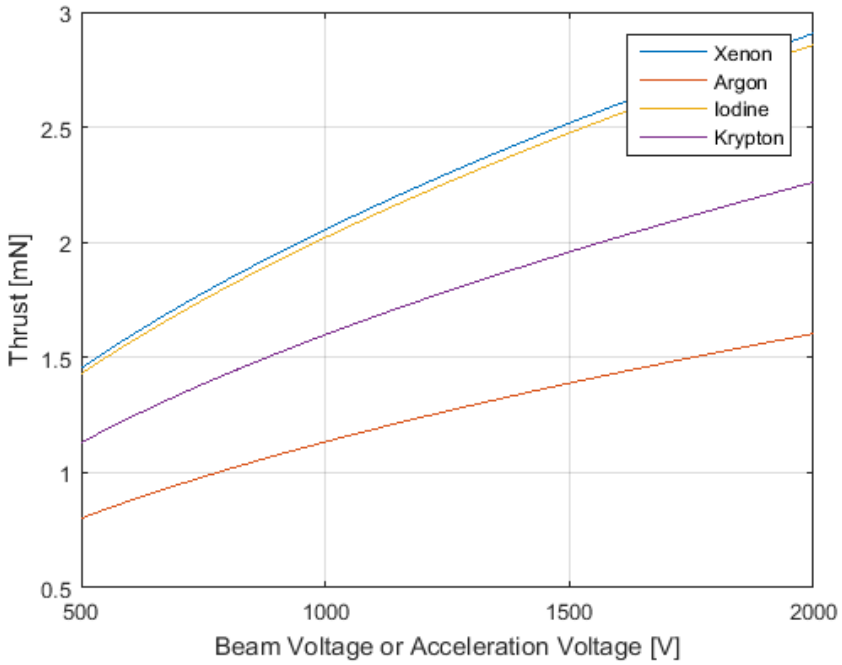

Figure 4.13 : Beam voltage vs. thrust graph for different propellants.

Since ion beam voltages generally vary between 500 and 2000 volts, the graph shows the change in thrust of Xenon, Argon, Iodine and Krypton propellants for this value range. High molecular weight Xenon and Iodine propellants appear to produce higher thrusts. Compared to these propellants, low thrust production of Argon is remarkable. Since the amount of thrust produced has an effect on the transfer time in the use of the propulsion system for transfer, it can be inferred that the mission using the Argon propellant system will be completed in a longer time. Specific impulse values of different propellant types within the same ion beam voltage range can be evaluated by a method similar to the comparison of thrust values with respect to propellant. This evaluation is graphed in Figure 4.14. As shown in the graph, specific impulse values between 2000 and 8000 can be obtained between 500 and 2000 volts. When the acceleration voltage is kept constant, there is an inverse relationship between atomic mass and specific impulse in equation 4.33. Therefore, when Argon gas, which has the lowest atomic weight is used, it is seen that the system provides the highest specific impulse. It is seen that Xenon and iodide provide close and low specific impulse compared to Argon and Krypton due to their close atomic weights. Given the high specific impulse requirement for space missions requiring high delta-V, the Argon and Krypton gases that provide high specific impulse have advantages over Xenon and Iodine.

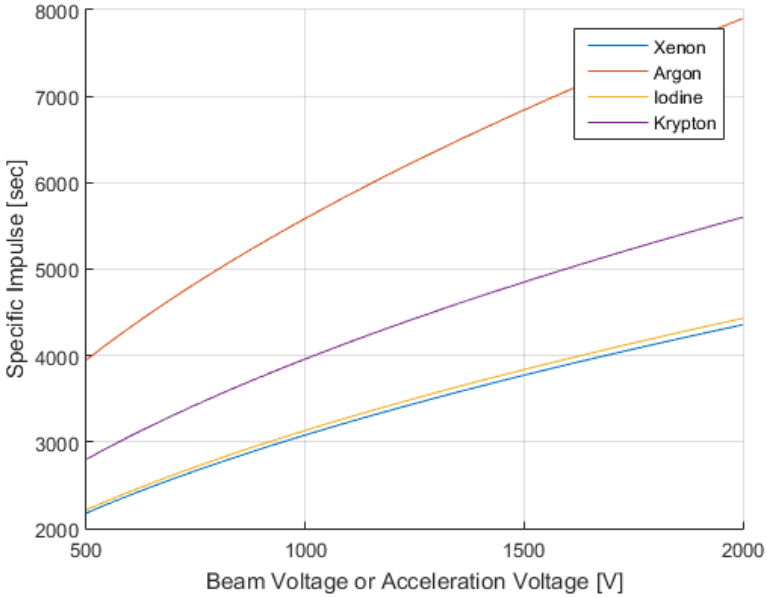

Figure 4.14 : Beam voltage vs. specific impulse graph for different propellants

Likewise, when exhaust velocities for the same ion beam voltage range are compared, it is seen in Figure 4.15 that the highest velocity belongs to the Argon gas with the lowest atomic mass.

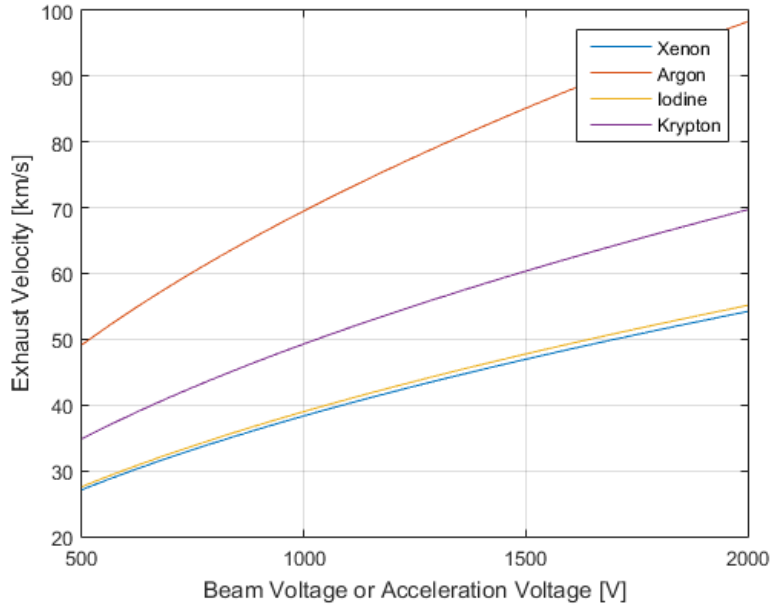

Figure 4.15 : Beam voltage vs. exhaust velocity graph for different propellants.

If Argon is used as an alternative to Xenon gas, the thrust value will be reduced considerably. Since this is undesirable, the use of Argon gas, which is the cheapest in price compared to other options, is not feasible. In all evaluations, Iodine, which

provides the values closest to Xenon, can be considered a powerful alternative to Xenon. In addition, it is the second cheapest propellants among the four propellants and does not require a pressurized propellant tank because it is stored in solid state and this enables it to be placed freely in the space available in the satellite. On the other hand, as mentioned earlier, Iodine is a highly reactive substance and therefore has a chemical incompatibility. Therefore, it needs extra safety equipments. In addition, since Iodine is used in BIT-3 RF ion thruster, which is planned to be used in Lunar IceCube satellite, which is expected to be sent to space in 2020, this study has worked on Krypton gas, which provides optimum values in all evaluations. Krypton can be presented as the most powerful alternative to Xenon, both in terms of the performance values it provides and because it can be supplied at about a quarter of the price of Xenon. In addition, this study has provided motivation to use Krypton as a propellant since a successful Krypton RF ion thruster is not used in space and the use of Krypton in space missions has an evolving flight heritage. It is decided to design Xenon fueled version, in addition to Krypton gas as propellant for the designed propulsion system. In this way, it is aimed to increase the comparability of Xenon gas, which has been used successfully for many years and the developing Krypton gas, which is used for many years.

4.3 Performance Calculations of the Propulsion System

In this section, in the light of the information and formulas given in the previous sections, the performance values of the designed propulsion system and the values of the parameters determining the design are calculated. The performance values of the designed thrust system both experimentally using Krypton gas version and Xenon gas version, which is traditionally used in electric propulsion systems, were calculated based on the same physical design.

As mentioned earlier, the ion optics part of the propulsion system, where thrust is generated by accelerating the charged particles of the ionized propellant in the discharge chamber, is very important for the ion engine propulsion system. Thanks to the positive and negative high voltages given to the grids and the physical properties of the grids, it provides the acceleration of charged particles. Thus, the diameter of the apertures of the grids, the distance of the grids to each other, their thickness and the voltage values given to the grids directly affect the performance values of thruster. In

Preliminary Design section, design parameters of three-grid ion optics system, which is appropriate for this thruster, were given based on Farnell's work in Figure 4.9. Specific impulse and exhaust velocity values were given by taking into account of delta-V requirement of this cislunar spiral transfer and estimated mass propellant, which is compatible with 6U CubeSat form. Using the specific impulse equation 4.33, the beam voltage required to obtain the desired specific impulse was calculated. By calculating the beam voltage, other voltage values were found for the Xenon and Krypton versions as follows with the formulas given in the ion optics design section.

As seen in Table 4.9, the Xenon gas version of propulsion system requires applying more voltages to ion optics of the thruster to achieve same specific impulse with Krypton gas version because of their different atomic masses. To generate same specific impulse and exhaust velocity, which are required for the lunar mission, Xenon gas version needs to apply approximately 1.5 times more voltages than Krypton version.

Table 4.9 : Grid potentials of two versions of the thruster.

Potentials				
Krypton	Beam voltage, net voltage	V_b	786.8	V
	Total voltage	V_T	874.2	V
	Screen grid voltage	V_s	764.2	V
	Accel. grid voltage	V_a	-110	V
Xenon	Beam voltage, net voltage	V_b	1232.7	V
	Total voltage	V_T	1369.7	V
	Screen grid voltage	V_s	1219.7	V
	Accel. grid voltage	V_a	-150	V

Maximum current density, which may occur in ion optics grids of the thruster by using Child-Langmuir equation, which is given in equation 4.16. However, current density of ion beam is below this limit and beam current density can be calculated by replacing total voltage with beam voltage in equation 4.16. By using beam current density and active grid area of the screen grid, beam current can be found. Similarly, by calculating the current passing through the grids, the current density and the passing currents of the system can be calculated for Xenon and Krypton version as given in Table 4.10.

Table 4.10 : Current densities and currents of two versions of the thruster.

Current Densities & Currents				
Krypton	Max. current density	J_{max}	56.2	A/m^2
	Beam current density	J_B	48.0	A/m^2
	Beam current	I_B	0.030	A
	Screen grid current	I_s	0.030	A
	Accel. grid current	I_a	0.011	A
Xenon	Max. current density	J_{max}	88.1	A/m^2
	Beam current density	J_B	75.2	A/m^2
	Beam current	I_B	0.047	A
	Screen grid current	I_s	0.047	A
	Accel. grid current	I_a	0.017	A

As can be seen in Table 4.10, the Xenon gas version of the thruster has more current density. Therefore, it has more ion beam current. The amount of beam current, together with the beam voltage, affects the thrust value generated by the propulsion system. The following table shows the amount of thrust produced by two different types of propellant using beam voltages and beam currents.

Table 4.11 contains the normalized thrust value with the ideal thrust value. The reason in that not all ions are completely attended in thrust production. Ideal thrust, also known as theoretical thrust value, is multiplied by thrust correction factor to find the closest thrust value. In this study, it is assumed that the propellant is singly charged and the thrust correction coefficient is 0.985. The Xenon gas version creates a higher thrust as shown. Higher thrust can shorten transfer time.

Table 4.11 : Thrust values of two versions of the thruster.

Thrust				
Krypton	Ideal Thrust	T_i	1.11	mN
	Thrust	T	1.09	mN
Xenon	Ideal Thrust	T_i	2.72	mN
	Thrust	T	2.68	mN

As mentioned before specific impulse is primary objective to catch the delta-V requirement of the mission, which has certain full mass, and empty mass. The objective specific impulse value was calculated by using Tsiolkovsky rocket equation in Determination of Lunar Mission Requirements part. However, in this part, the specific impulse value is calculated by using ion engine specific impulse formula, which was given equation 4.33. Resultant specific impulse of the systems is given in Table 4.12.

Table 4.12 Specific impulse value of two versions of the thruster.

Specific Impulse				
Krypton-Xenon	Ideal specific impulse	Isp_i	3472	$s$ec
	Specific impulse	Isp	3420	$s$ec
	Total Impulse Capability	I_t	41,925	N-sec

As verified in Table 4.12, voltage values of the Xenon and Krypton version are appropriate for achieving objective specific impulse values. Thus, they reached the same specific impulse even if their atomic mass was different. The ideal specific impulse and normalized specific impulse values are given in Table 4.12 provided by the systems as in Table 4.11. Exhaust velocity can be also found from delta-V requirement of the mission as specific impulse. By means this, exhaust velocity can be considered as secondary objective to design RF ion thruster for specific mission. Exhaust velocity value of two type propellant versions of the thruster as given in Table 4.13.

Table 4.13 : Exhaust velocity value of two version of the thruster.

Exhaust Velocity				
Krypton-Xenon	Ideal exhaust velocity	v_i	34.05	km/s
	Exhaust velocity	v	33.54	km/s

This exhaust velocity value is exactly same with the exhaust velocity objective value, which is calculated before. By using exhaust velocity value and thrust values of Xenon and Krypton versions, required mass flow rates are found to achieve these performance

values. Ion flow rates are calculated from beam current, atomic mass and electron charge. It is required for calculation of mass utilization efficiency. The burn time is the time at which the thruster has run out of propellant using the propellant in its tank with the given mass flow rate. The flow rates and burn times of the systems are given in Table 4.14.

Table 4.14 : Flow rates of two versions of the thruster.

Flow Rates & Burn Time				
Krypton	Mass flow rate	$\dot{m}_p$	3.26E-08	kg/sec
	Ion flow rate	$\dot{m}_{ion}$	2.61E-08	kg/sec
	Burn time	t_b	443	days
Xenon	Mass flow rate	$\dot{m}_p$	8.01E-08	kg/sec
	Ion flow rate	$\dot{m}_{ion}$	6.41E-08	kg/sec
	Burn time	t_b	180	days

Krypton gas version has longer burn time than Xenon gas version due to the higher mass flow rate of the Xenon gas version. These times also show the mission time with active electric propulsion system.

Power consumption is one of the most important evaluation criteria for electrical propulsion systems. In this type propulsion system usage, the most amount of generated power is allocated for propulsion system of satellite. In accordance with the information given in Power Consumption section, power generation of solar panels of satellite is about 80 W, and 50-60 W of this generated power can be allocated for propulsion system. In order to calculate the total power consumption in RF ion thrusters, step by step calculations should be made for the processes need electrical power. The first power-required process is ionization of the propellant in the discharge chamber by using RF power. The required RF power can be calculated from properties of RF coil and RF current, which passes through the RF coil. However in preliminary design, RF power requirements can be assumed from literature researhes. RF power can be assumed as 15W for xenon propellant, which has 12.13 eV/ion ionization potantial energy. Similarly, xenon gas version of thruster requires approximately 15 W RF power. Because the RF generators are 90% efficient in this frequency range, the

PPU should give 18.8 W and 16.6 W DC powers to RF generator for ionization of krypton and xenon respectively [60, 99]. These power values These values were taken into account to calculate required input power for PPU unit of the whole system. Next power required process is the acceleration process of charged particles. Ion optics consume electrical power for this purpose. Another process, neutralization, the power used by the neutralizer should be included in the calculation of power consumption. In this study, the neutralizer power consumption in a similar system is assumed as 5 W for this system since the neutralizer design is not mentioned in detail [50]. Input power requirement is summation of these power values, but output power of the system is ion beam power, which is product of the thruster. The jet power that thruster has produced with thrust is also calculated and given in Table 4.15.

As seen Table 4.15, Krypton gas version of the propulsion system requires approximately 51 W power consumption to generate thrust. This power consumption value is quite appropriate for the system, which has 50-60 W allocated power for propulsion system. In terms of power consumption, usage of the Krypton gas version is reasonable. On the other hand, the Xenon gas version requires much more power consumption than the Krypton gas version to achieve the target specific impulse. As understood from the table, this required power value is almost 84 W. Considering that the total power generated by the current panel configuration of the system is around 80 W, the Xenon gas version does not seem suitable for the 6U CubeSat detailed in the Lunar mission analysis section. However, the power generated by the system can be increased to approximately nominal 120 W by changing the panel configuration for the 6U CubeSat. Another alternative to use the Xenon gas version is to evaluate its usage on satellites larger than the 6U form.

Bus system can supply 3.3V, 5V, 12V and approximately 30V to all subsystems. PPU of the propulsion system distributes these voltages to components of the system. The flow charts of the Krypton and Xenon version of PPU are given in Figure 4.16 and Figure 4.17 respectively.

Table 4.15 : Power consumptions of two versions of the thruster.

Power Consumption				
Krypton	Beam power	P_b	23.6	W
	Screen grid power	P_s	23	W
	Accel. grid power	P_a	1.18	W
	RF power	P_{RF}	17	W
	Neutralizer power	P_N	5	W
	Other Components	P_{other}	3	W
	Input power	P_{in}	51	W
	Output power	P_{out}	23.6	W
	Jet power	P_{jet}	18.3	W
	Ionization cost	ε_b	1698	eV/ion
Xenon	Beam power	P_b	58.0	W
	Screen grid power	P_s	57	W
	Accel. grid power	P_a	2.5	W
	RF power	P_{RF}	15	W
	Neutralizer power	P_N	5	W
	Other Components	P_{other}	3	W
	Input power	P_{in}	84	W
	Output power	P_{out}	58.0	W
	Jet power	P_{jet}	45.0	W
	Ionization cost	ε_b	1797	eV/ion

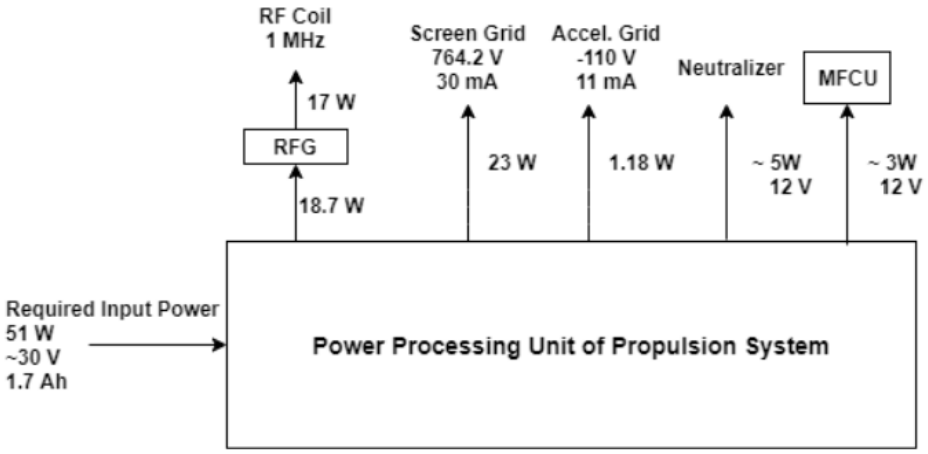

Figure 4.16 : Flow chart for Krypton gas version.

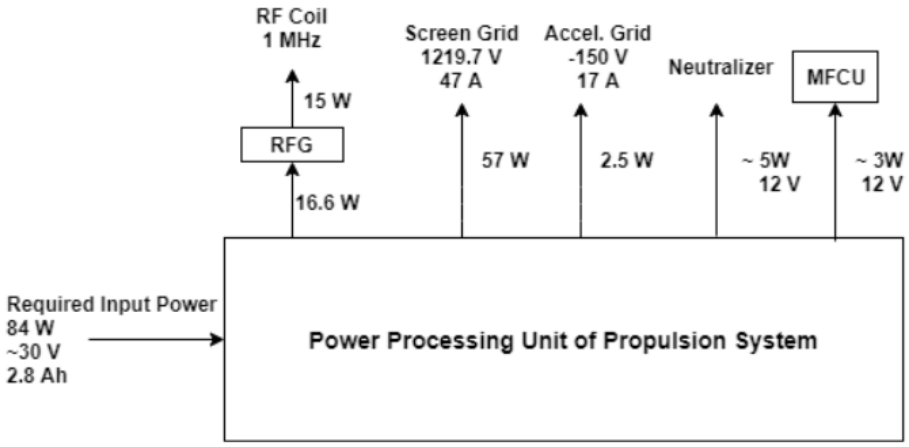

Figure 4.17 : Flow chart for Xenon gas version.

Efficiencies of the system is one of the best evaluation of the system performance. Electrical efficiency refers to how much of the system's electrical power is converted into a product. Mass utilization efficiency shows how much of the system's propellant is ionized and actively used in propulsion production. In addition to mass utilization efficiency and electrical efficiency, thruster efficiency is how much of the output electrical power of the system can be converted to jet power. The total efficiency of the system is calculated as the combining of the electrical efficiency and the mass utilization efficiency of the system. All of these efficiencies are calculated for the Krypton and Xenon versions of the propulsion system as shown in Table 4.16.

Table 4.16 : Efficiencies of two versions of the thruster.

Efficiencies			
Krypton	Electrical efficiency	n_e	0.46
	Mass utilization eff.	n_m	0.8
	Thruster efficiency	n_{th}	0.77
	Total efficiency	n_T	0.34
Xenon	Electrical efficiency	n_e	0.68
	Mass utilization eff.	n_m	0.8
	Thruster efficiency	n_{th}	0.77
	Total efficiency	n_T	0.50

Although the Xenon gas version requires more electrical power to generate thrust, the input electrical power is more efficient than the Krypton gas version as seen Table 4.16 because Xenon has higher atomic mass than Krypton. Both systems have the same mass utilization efficiency and thruster efficiency. As a result, the Xenon gas version of the propulsion system is more efficient than Krypton version.

4.4 Structural and CAD Design of the Propulsion System

The 3D CAD design and structural design of the thruster to be used in the lunar mission, which was designed in detail in the previous sections, was made in this section. The drawing of the components required for the propulsion system, the dimensioning and material selection of the elements that form the thruster are made in this section. As already mentioned in the conceptual design section, a propulsion system generally consists of the following parts: discharge chamber, ion optics, RF coil, RF generator, propellant tank, mass flow control unit, power processing unit and neutralizer.

The discharge chamber, where the propellant is ionized by means of RF signals, is one of the most important parts of the thruster and 3D design has been started with the drawing of the discharge chamber. In accordance with the calculations made in the preliminary design section, it is appropriate that the discharge chamber diameter is in the range of 3-4 cm. Discharge chamber is made in 3D design with a diameter of 4 cm. Since the L / D ratio is 0.75, the horizontal length of the discharge chamber is 3 cm. Already in the Performance Calculations section, calculations were made considering these parameters and the results were drawn. The discharge chamber of thruster was designed as Figure 4.18.

The discharging chamber must be made of insulating material to minimize electrical power loss and ensure effective operation. Glass, ceramic and derivatives are generally used as insulating materials for these purposes. In this study, Borosilicate glass, which is frequently used in daily life, is preferred as material of the discharge chamber because of its heat resistant and low thermal expansion qualities [100].

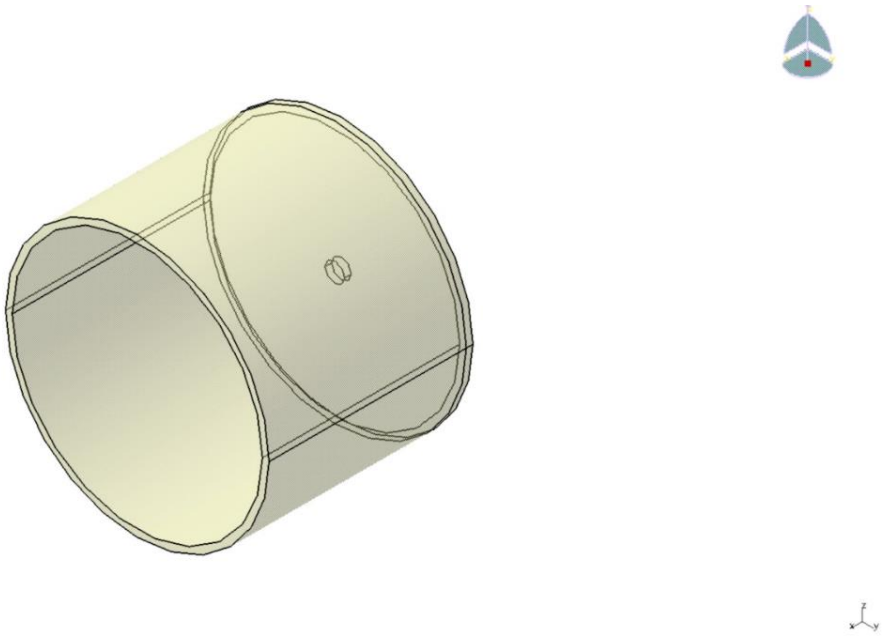

Figure 4.18 : CAD design of the discharge chamber.

In this study, it is stated in the conceptual design section that the thruster ion optics will have a three-grid configuration including screen grid, acceleration grid and deceleration grid. The aperture diameter, thickness, and distance of the grids from each grid were previously determined based on the work of Farnell. The diameter of the grids was determined as 4.5 cm by considering the thruster properties. These grids with a diameter of 4.5 cm are designed to have apertures of 3.5 cm in diameter. In grid design, the grid surface is divided into hexagonal imaginary cells, which are geometrically based on the distance of the centers of the apertures on the grid surface, and apertures are located in the middle of these imaginary hexagonal cells. In this study, center-to-center length of apertures was reported as 2.34 cm. According to the calculations, this grid is theoretically expected to have 202 apertures, but in CAD design 199 apertures can be fitted in this area. This difference can be negligible for performance calculation because its effects is very small. CAD design of the grid set of the systems are given in Figure 4.19.

There are many studies on grid materials. The reason why there are so many studies on this subject is that the properties of the materials used directly affect the values to be provided by the thruster. There are two major problems that may occur depending on material selection and directly affect thruster lifetime. The first is thermal expansion and the other is sputter erosion [101].

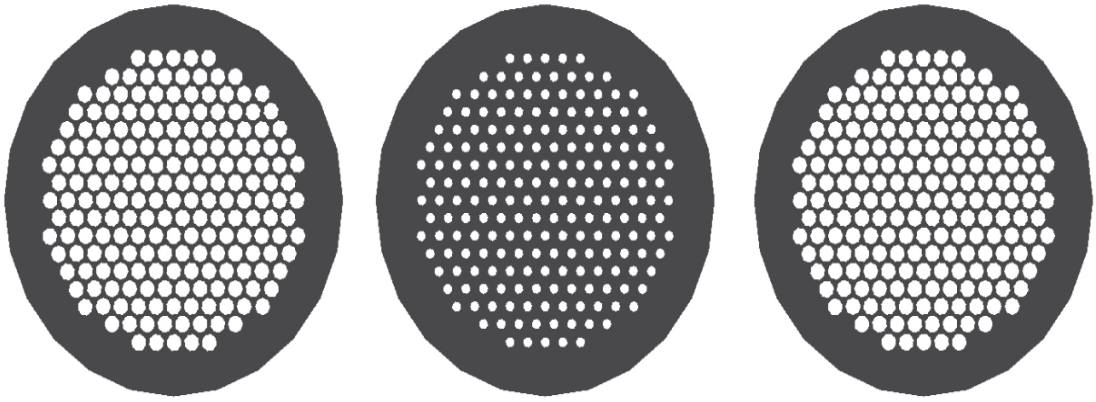

Figure 4.19 : CAD design of the screen, accel. and decel. grid respectively.

The screen grid and acceleration grid have almost 120° C temperature and alignment between the grids may break due to thermal expansion [102]. This affects the effective operation of the system in a very negative way. The goal of material selection is to minimize the effect of these two factors. For this purpose, molybdenum having low sputter erosion rate has been used as material in ion optic grids for many years. However, nowadays, since carbon-based materials are widespread and thermal expansion coefficients are much lower than metal materials; these materials have started to be used as grid materials [101]. In fact, thermal expansion coefficient can be considered as zero in carbon based materials compared to metal materials. Therefore, the use of such materials in ion optics grids has increased. The materials currently used for grids are molybdenum, graphite, carbon-carbon, pyrolytic graphite and stainless steel [101]. In this study, carbon-carbon was determined as the grid material due to the advantages of carbon-based materials.

In order to effectively contribute to thrust production, although grids have apertures of different sizes, these apertures must be aligned with each other. Therefore, the grids are designed to have the same aperture pattern as each other. Two spacers were used to maintain the distance between the grids and to insulate grids most importantly. For obtain the isolation between grids, PTFE was chosen as material of the spacer [70].

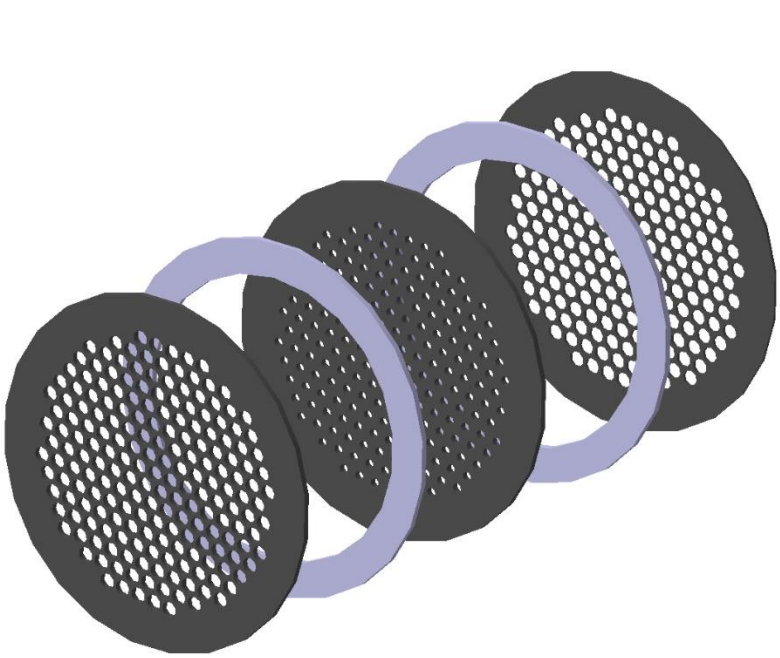

Figure 4.20 : CAD design of the grids and spacers.

The RF coil, which allows the ionization of the propellant in the discharge chamber, is designed as a coil consisting of 5 turns, 3 cm in length and 4.15 cm in diameter. In order to the RF coil transmitting RF signals with maximum efficiency, the coil must be made of a high conductivity material. Copper and copper alloys are the most widely used materials. This coil is available in copper wire or copper tube versions. It is designed to be 0.25 cm diameter copper wire for the RF coil shown in Figure 4.21. The shape of RF coil holder was inspired from a literature search [75].

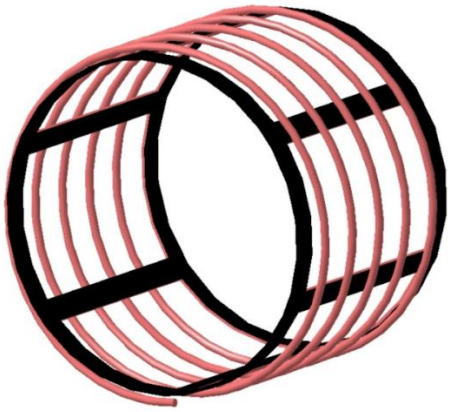

Figure 4.21 : CAD design of the RF coil.

Thruster and the whole propulsion system together in CAD design is as Figure 4.22. In this study, the 3D drawing of the remaining components is made as representative because the thruster design is made in detail.

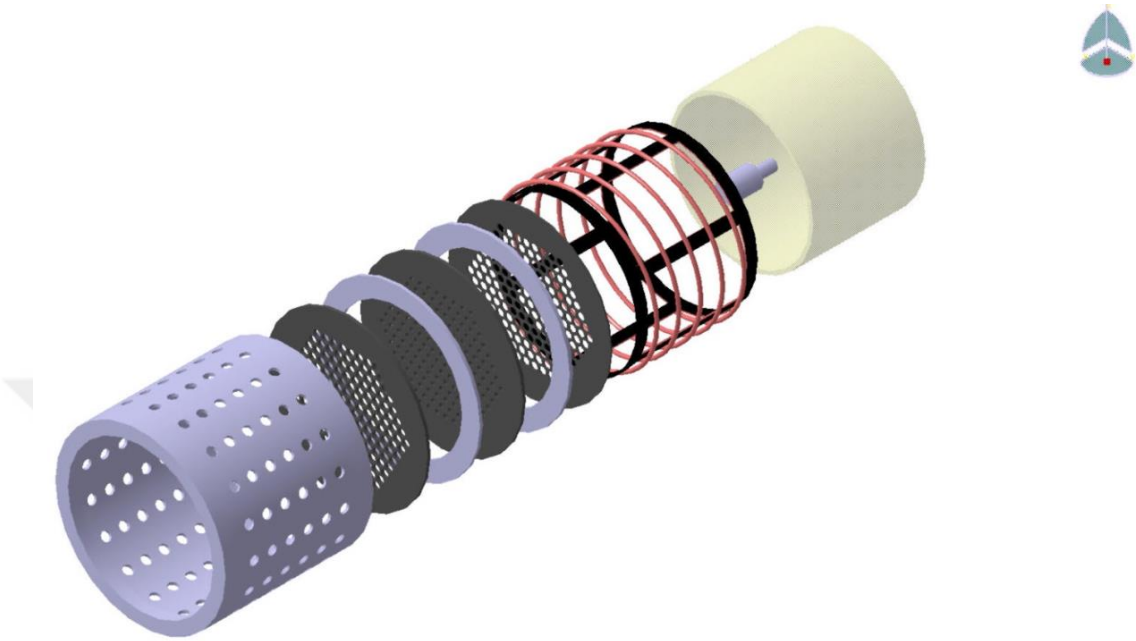

Figure 4.22 : CAD design of the whole thruster.

On the outside of the thruster components, there is a shell that holds them together as seen in Figure 4.22. This shell is also used to prevent RF signal leakages and protects other subsystems from radiation emitted by the discharge chamber. It should be made of aluminum for using as a radiation shielding. In addition to these, front side of the shell is taken out of the satellite as the thruster head and protects the ion optics. The shape of shell was inspired from a literature search [75]. The whole thruster has 4.7 cm diameter with this shell and 4.2 cm length. According to the literature review, wall temperature of the discharge chamber is approximately 230 °C, coil temperature is nearly 200 °C [102]. To protect other subsystems from this temperature and provide thermal balance, MLI and aerogel material should be used to separate propulsion system from other subsystems. In addition to this thermal measures, the energy that is not converted into kinetic energy is transformed into heat energy and it should be emitted into the space by surface of the thruster facing to space and radiator or fins. The bottom surface of the satellite can be extended by fins to emit more energy. There is sufficient area in the satellite for other thermal measures that can be applied.

In addition to the thruster design, the propellant tank concept design can be made within the preliminary design of propulsion system. Since both propellants, Xenon and Krypton, planned to be used are noble gas in nature, they should be stored in the pressurized tank in the satellite as highly compressed gas or cryogenic liquid. Propellant tanks, which are available to use in a satellite or already used in satellite, stores the Xenon gas at about 160-170 bar [103, 104, 105]. Considering the 6U CubeSat sizes, 1.25 kg Krypton and Xenon cannot be fitted as a compressed gas in the pressurized tank because of their low density. Therefore, this amount propellant should be stored in cryogenic tank, which has -150°C temperature [89]. In addition to 1.25 kg Xenon or Krypton propellants for thruster, there is an extra amount of propellant for neutralizer and for leaving a 10% margin to thruster propellant. Hence, liquid Xenon needs almost 468 cm^3 and liquid Krypton needs almost 570 cm^3 internal volume in the tank. To be on the safe side, propellant tank should be design according to the Krypton propellant since it needs more space than Xenon. For calculation dimensions of the inside of the tank, the shape of tank should be determined. There are several alternates for propellant tank as combination of cylindrical, spherical etc. shape. In this study, internal and external shapes of pressurized tank are determined as Cassini oval domes with a cylindrical intersection as seen in Figure 4.23. Based on this internal shape of the tank, the dimensions of the tank are calculated as 12.5 cm cylindrical height and 4 cm domes height with 3.5 cm radius. Therefore, total length and diameter of the internal tank is 16.5 cm x 7 cm. Taking into account remaining space for tank, external dimensions were arranged as 16 cm cylindrical height and 4 cm total domes height with 4.5 cm. Therefore, total length and diameter of the external tank is 20 cm x 9 cm. Between internal tank and external tank, isolation material should be covered because tank needs an isolation material to help to sustain this low temperature. Material of the internal and external of the tank are chosen titanium steel alloy (Ti-6Al-4V), graphite epoxy overwrapped as XIPS system of HS-601 HP satellite [104, 103]. As a result, the propellant tank needs less than 1.75 U space in satellite. The CAD design of the propellant tank is given in Figure 4.23.

After CAD design of all components (some of them are not detailed), the total area of the propulsion system is approximately 2.5U. The remaining 0.5U can be used for thermal and radiation measures. 3D design can be made more detailed by designing other systems. The thruster 3D design has been kept in the forefront as the most

mentioned and studied part is thruster in this study. The CAD design of the whole ion engine propulsion system is given in Figure 4.24

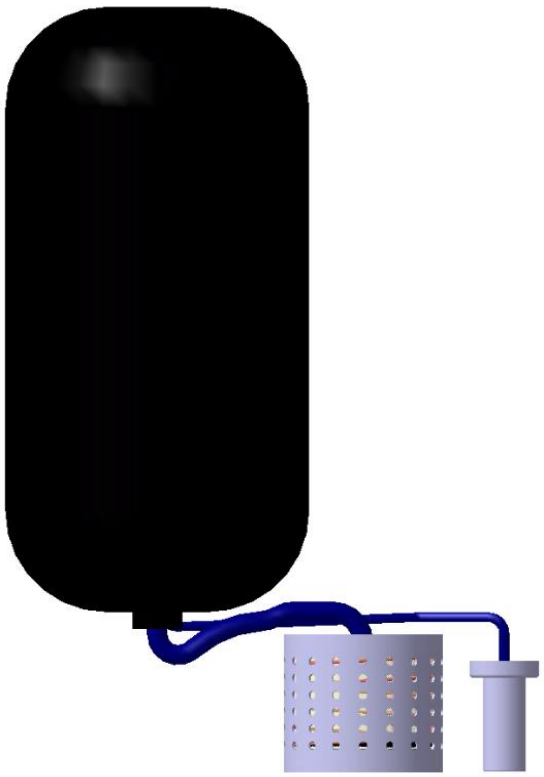

Figure 4.23 : CAD design of propellant tank of the system.

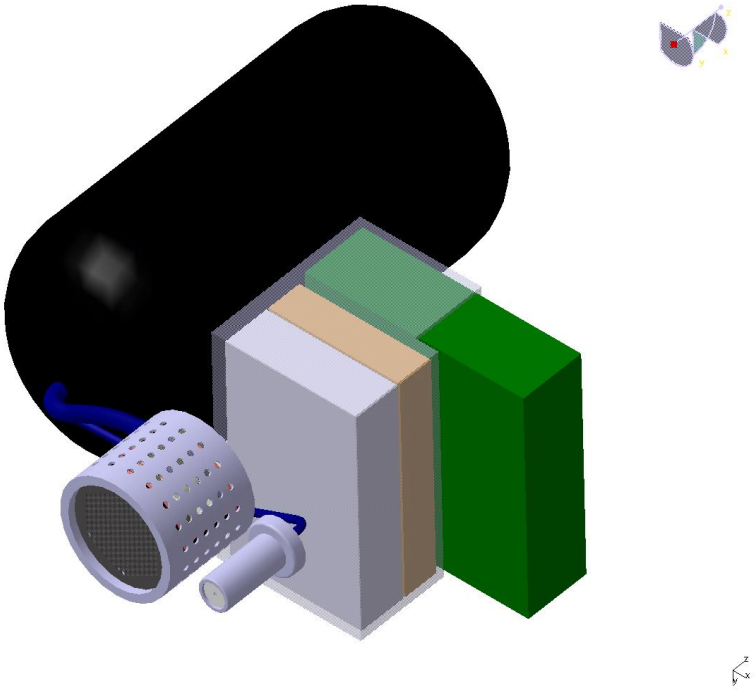

Figure 4.24 : CAD design of the whole propulsion system.

4.5 Summary

The performance results of Krypton version, which were discussed and evaluated in detail in the previous section, are summarized as in Table 4.17.

The CAD design of the 6U CubeSat, which is used in this lunar mission, and subsystems of the satellite are given in Figure 4.25. The designed propulsion system is shown in the satellite. The Figure 4.25 shows the whole satellite and its subsystem.

Table 4.17 : Preliminary designed Krypton RF ion thruster specifications.

RF ION THRUSTER SPECIFICATION			
Ion Beam Current	I_B	30	mA
Propellant Mass Flow Rate	$\dot{m}_p$	3.26E-08	kg/sec
		1.57	sccm
Accelerating Voltage	V_b	786.8	V
Ionization Cost	ε_b	1698	eV/ion
Supply Voltage	V	~30	VDC
Power Consumption	P_{in}	51	W
Specific Impulse	Isp	3420	$s$ec
Total Impulse Capability	I_t	41,925	N-sec
Thrust	T	1.09	mN
Exhaust Velocity	v	33.54	km/s
Electrical Efficiency	n_e	0.46	
Mass Efficiency	n_m	0.8	
Thruster Efficiency	n_{th}	0.77	
Total Efficiency	n_T	0.34	

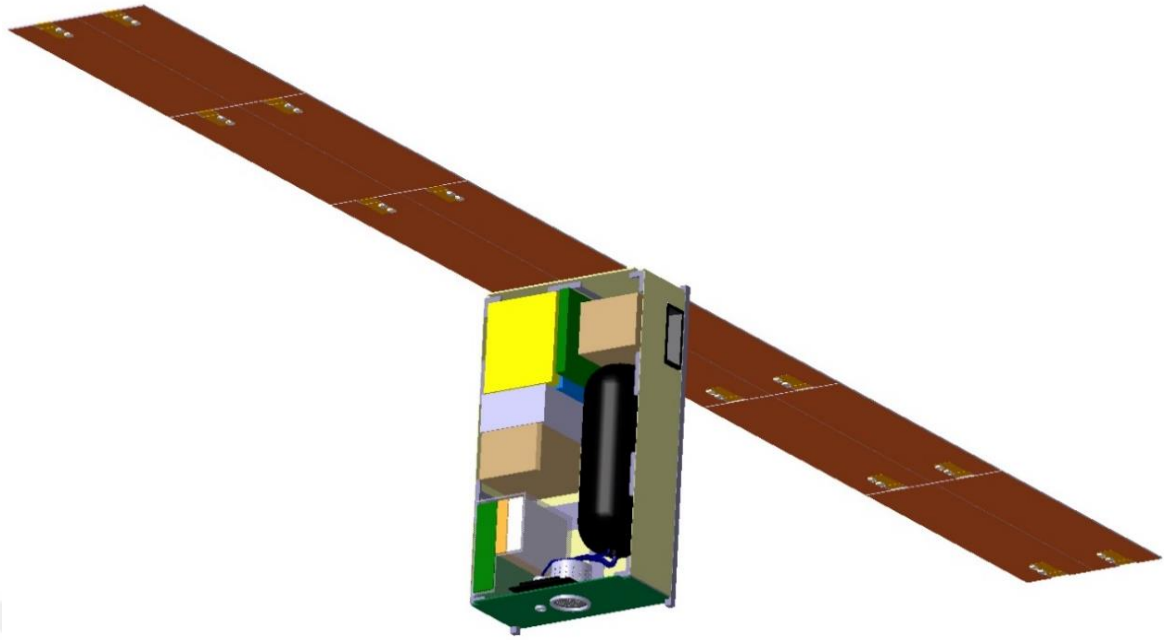

Figure 4.25 : 3D drawing of the Lunar mission 6U CubeSat with designed propulsion system.

5. CONCLUSIONS AND RECOMMENDATIONS

In this study, propulsion system types that can be used in small satellites were briefly mentioned and propulsion system was preliminary designed to meet the requirements of 6U CubeSat to be used in the lunar mission. The delta-V value that is needed in this type of mission was predicted and the specific impulse and exhaust values of the satellite, which are supposed to be necessary, were obtained by considering the satellite mass limitations. Propulsion system type, which provides these values and can be miniaturized for 6U CubeSat form, was determined as ion engine propulsion system. Comparing the types of ion engines, the RF ion thruster preliminary design was made according to the mentioned lunar mission, since the lifetime is longer because it does not contain cathodes. Working principle of the system was mentioned and formulas that is required for design of the thruster were given. The propellants that can be used in the thruster to be designed are evaluated considering the performance values and costs of propellant. The performance values of the experimentally Krypton gas version and traditionally Xenon gas version of the system were calculated. Structural and CAD design of the components of the propulsion system were made according to the calculations and assumptions. Thermal and radiation measures were defined due to the requirements. After the preliminary design, the Xenon gas version of the propulsion system requires more electrical power than the Krypton gas version to accelerate charged Xenon particles because of the large molecular mass of the Xenon as a result. Considering the current satellite form, panel layout and the power values that can be produced by the panels, the Xenon gas version is not suitable for the mission described in this study. In contrast to the Xenon gas version, the Krypton gas version requires approximately 51W electrical power. This required power value is appropriate considering the 50-60W power interval, which can be allocated for propulsion system. As disadvantages, the Krypton has storage problem because of its lower density. It was stored in a cryogenic tank to fit in 6U CubeSat. Therefore, it requires more space inside the satellite and extra thermal equipment. This propellant was chosen because of lower cost. However, this krypton gas version is no longer cheap due to its extra requirements. In addition, this version has longer burn time, since it generates smaller

thrust value than Xenon gas version. The Krypton gas version will complete the mission in a much longer.

The details not mentioned in the preliminary design may be included in the works planned for the future. These future works can be summarized as follows.

- The most effective grid can be designed by making optimization for ion optics of the thruster.
- The detailed design and calculations can be made for other components of the propulsion system such as neutralizer, RF generator etc.
- Plasma part, which is not examined in detail in the scope of system engineering, can be examined in detail and the performance of the system can be evaluated in this perspective.
- Cost analysis can be made.
- The preliminary design can be developed and tested in the laboratory and improvement studies can be performed according to the results.
- Because of the Xenon and Krypton version disadvantages, usage of the Iodine propellant should be tried, this version may provide more advantages.
- Structural and CAD design of the propellant tank should be detailed. Its requirements can be changed due to current situation.
- Thermal design may be detailed according to the changing requirements.
- In the light of given working principle and formulas, not only preliminary design for specified mission, but also preliminary design of propulsion system can be made with optimum requirements such as power consumption by approaching different angle.
- The Xenon gas version of the system can be utilized in bigger form CubeSats than 6U. In other way, propulsion system is designed to not exceed this limit based on the power consumption limitation and this version can be used for a mission, which has different delta-V and specific impulse requirements.
- By increasing scope of the study, a software can be developed to give preliminary design of propulsion system for different mission scenarios due to the delta-V and other mission requirements based on selected satellite form.

This software can determine required propulsion system type due to the mission and its requirements and make thruster sizing for all different propulsion system types.

REFERENCES

[1] **Mann A.** (2019). *What Was the Space Race?*. Retrieved August 18, 2019 from *https://www.space.com/space-race.html*.

[2] **Memiş, Ş.** (2018). *Soğuk Savaş Döneminde Uzay Yarışı: ABD ve Sovyetler Birliği.* Retrieved September 20, 2019 from http://bigenc.org/soguk-savas-doneminde-uzay-yarisi-abd-ve-sovyetler-birligi/.

[3] **Sandbrook, D., Bizony, P.** (2019). *The Space Race: how Cold War tensions put a rocket under the quest for the Moon.* Retrieved August 20, 2019 from *https://www.sciencefocus.com/space/the-space-race-how-cold-war-tensions-put-a-rocket-under-the-quest-for-the-moon/*.

[4]**<URL 1>** *History of CubeSat.* Retrieved July 3, 2019 from *https://spacemauritius.com/2019/04/16/history-of-the-cubesat/*.

[5] **Swartwout, M.** (2014). *The First 272 CubeSats.* IEEE Parts for Small Missions Workshop NASA Goddard Space Flight Center.

[6]**<URL 2>** *Mars Cube One (MarCO).* Retrieved June 28, 2019 from *https://www.jpl.nasa.gov/cubesat/missions/marco.php*.

[7] **Dunbar, B.** (2019). What is Artemis?. Retrieved August 30, 2019 from *https://www.nasa.gov/what-is-artemis.*

[8]<**URL3**> Retrieved date August 10, 2019 from *https://space.skyrocket.de/doc_sdat/smart-1.htm.*

[9] **Mann, A.** (2019). *China's Chang'e Program: Missions to the Moon*. Retrieved July 3, 2019 from *https://www.space.com/43199-chang-e-program.html.*

[10] **<URL 4>** *Isro lost Chandrayaan-2 lander Vikram contact 400 metres above Moon, not 2.1 kms.* Retrieved August 30, 2019 from *https://www.indiatoday.in/science/story/chandrayaan-2-lander-vikram-contact-lost-400-metres-moon-isro-1598004-2019-09-11*.

[11] **< URL 5>** *Space Launch System (SLS) Overview.* Retrieved August 1, 2019 from *https://www.nasa.gov/exploration/systems/sls/overview.html.*

[12] **Yost, B.** (2019). *State of the Art of Small Spacecraft Technology, 04. Propulsion.* National Astronautical Space Administration.

[13] **Aerojet Rocketdyne**. (n.d.). *MPS-120 Thruster Datasheet*. Retrieved December 3, 2018 from *https://www.rocket.com/sites/default/files/documents/CubeSat/MPS-120%20data%20sheet-single%20sheet.pdf.*

[14] **Moog Space and Defense Group.** (2018). *MONARC-1 Thruster Datasheet*. Retrieved November 18, 2018 from *https://www.moog.com/content/dam/moog/literature/Space_Defense/spaceliterature/propulsion/Moog-MonopropellantThrusters-Datasheet.pdf*

[15] **Ariane Group.** (n.d.). 1N *Monopropellant Hydrazine Thruster Datasheet.* Retrieved November 18, 2018 from *http://www.space-propulsion.com/brochures/hydrazine-thrusters/hydrazine-thrusters.pdf.*

[16] **Tummala, A. R., Dutta, A.** (2017). *An Overview of Cube-Satellite Propulsion Technologies and Trends.* Aerospace 4,58; doi:10.3390.

[17] **Lemmer, K**. (2017). *Propulsion for CubeSats.* Acta Astronautica 134.

[18] **Ecaps by Bradford.** (n.d.). *HPGP Thruster Datasheet.* Retrieved November 20, 2018 from *http://ecaps.space/products-1n.php.*

[19] **Busek Co.** (n.d.). *BGT-X5 Datasheet.* Retrieved December 20, 208 from *www.busek.com/index_htm.../70008517E.pdf.*

[20] **Aerojet Rocketdyne**. (n.d.). *MPS-130 Thruster Datasheet*. Retrieved December 3, 2018 from *https://www.rocket.com/sites/default/files/documents/CubeSat/MPS-130%20data%20sheet%20crop.pdf.*

[21] **Moratta Controls, Inc.** (n.d.). *MicroThruster Datasheet.* Retrieved December 15, 2018 from *http://marotta.com/cold-gas-microthruster/.*

[22] **<URL 5>** (2014). *Special Projects: Propulsion for Micro and Small Satellites.* Retrieved November 20, 2018 from *https://www.utias-sfl.net/?page_id=1274.*

[23] **Baumbarger, P. P.** (2013). *Analysis of a Minature Radio Frequency Ion Thruster with an Inductively Coupled Plasma Source* (Master's Thesis). Boise State University.

[24] **CU Aerospace, LLC**. (n.d.). CHIPS Thruster Datasheet. Retrieved December 15, 2018 from *http://www.cuaerospace.com/portals/2/sitecontent/pdfs/datasheets/chips/chips-brochure-170718.pdf?ver=2017-07-18-234056-717.*

[25] **Busek Co.** (n.d.). *Micro Resistojet Datasheet.* Retrieved December 17, 2018 from *http://www.busek.com/index_htm_files/70008518B.pdf*

[26] **CU Aerospace, LLC.** (n.d.). *PUC Datasheet.* Retrieved December 17, 2018 from *http://www.cuaerospace.com/Portals/2/SiteContent/pdfs/datasheets/PUC/PUC-184-SO2%20(Rev140716).pdf.*

[27] **Busek Co.** (n.d.). *BIT-1 Thruster Datasheet*. Retrieved December 20, 2018 from *http://busek.com/technologies__ion.htm.*

[28] **Busek Co.** (n.d.). *BIT-3 3cm RF Ion Thruster Datasheet.* Retrieved December 19, 2018 from *http://busek.com/technologies__ion.htm*.

[29]**<URL6>** Retrieved date December 10, 2018 from *https://www.nasa.gov/feature/mit-spl-delivers-the-scalable-ion-electrospray-propulsion-system-s-ieps-for-cubesats-to-nasa.*

[30]**Busek Co.** (n.d.). *Busek, BHT-200, Datasheet.* Retrieved December 1, 2018 from *http://busek.com/technologies__hall.htm.*

[31] **Busek Co.** (n.d.). *Busek, BHT-600, Datasheet.* Retrieved December 1, 2018 from *http://busek.com/technologies__hall.htm.*

[32] **Gupta, T., Jangid, S., Guven, U.** (2017). *Utilization of a 6U Nanosatellite for Lunar Sampling Mission.* International Journal of Engineering and Techniques.

[33]<**URL7**> Retrieved August 10, 2019 from *http://www.planetary.org/explore/space-topics/space-missions/missions-to-the-moon.html*

[34]<**URL8**> Retrieved date August 10, 2019 from *https://www.wikizero.com/en/Artemis_1*

[35]<**URL9**> Retrieved August 10, 2019 from *https://scipioamericanus.wordpress.com/tag/robert-heinlein/*

[36]<**URL10**> Retrieved August 11, 2019 from *https://www.wikizero.com/en/Comparison_of_orbital_launch_systems#cite_note-NASA-SLS-168.*

[37]<**URL11**> Retrieved August 10, 2019 from *https://sst-soa.arc.nasa.gov/10-integration-launch-and-deployment.*

[38]<**URL12**> Retrieved July 22, 2019 from *https://spacemauritius.com/2019/04/16/history-of-the-cubesat/.*

[39]<**URL13**> Retrieved August 11, 2019 from *https://static1.squarespace.com/static/5418c831e4b0fa4ecac1bacd/t/56e9b62337013b6c063a655a/1458157095454/cds_rev13_final2.pdf.*

[40]<**URL14**> Retrieved August 11, 2019 from *https://www.ecm-space.de/index.php/launch-adapters-h/cubesat-sizes.*

[41] **Clark, P.** (2018). *Cubesats in Cislunar Space.* 32nd Annual AIAA/USU Conference on Small Satellites.

[42]<**URL15**> Retrieved August 20, 2019 from *http://static1.squarespace.com/static/5418c831e4b0fa4ecac1bacd/t/573fa2fee321400346075f01/1463788288448/6U_CDS_2016-05-19_Provisional.pdf*

[43] <**URL16**> Retrieved September 3, 2019 from https://hyperscout.nl/product/.

[44] **Erdoğan, E.** (2019). *Nano Uydu ile Konsept Derin Uzay Görevi Tasarımı* (Master's thesis). Istanbul Technical University.

[45] **Tsay, M., Model, J., …, Feng, C.** (2017). *Integrated Testing of Iodine BIT-3 RF Ion Propulsion System for 6U Cubesat Applications.* 35th International Electric Propulsion Conference Georgia Institute of Technology, USA.

[46] **Biesbroek, R., Janin, G.** (2000). *Ways to the Moon?.* ESA bulletin 103, August.

[47] <**URL17**> (2007). *Luna T.I.C - Path to the Moon.* Retrieved July 16, 2019 from *http://propagation.ece.gatech.edu/ECE6390/project/Fall2007/LunaTIC/Luna%20TIC%20Project/launch/path.html.*

[48]<**URL18**> Retrieved July 13, 2019 from *https://www.wikizero.com/en/Orbit_of_the_Moon.*

[49]<**URL19**> Retrieved July 15, 2019 from *https://en.wikibooks.org/wiki/Astrodynamics/InPlane_Orbit_Changes#:~:targetText=Spiral%20transfer%5Bedit%5D,total%20%CE%94V%20than%20Hohmann%20transfers.*

[50] **Tsay, M.** (2015). *LunarCube: A Deep Space 6U CubeSat with Mission Enabling Ion Propulsion Technology.* 29th AIAA/USU Conference on Small Satellites North Logan, Utah August 8-13, 2015. (Presentation)

[51] **Walker, R.** (2015). *The European Student Moon Orbiter (ESMO) Project: Attracting and Training a Nes Generation of Lunar Explorers.* Education Projects Activities Unit, ESA Education Office, ESA/ESTEC, Keplerlaan 1, 2201 AZ Noordwijk, The Netherlands.

[52] **Belbruno, E. A., Carrico, J. P**. (2000). *Calculation of Weak Satbility Boundary Ballistic Lunar Transfer Trajectories.* AIAA/AAS Astrodynamics Specialist Conference, Denver, Colorado.

[53] **Martinez-Sanchez, M.** (n.d.). *Lecture 3: Approximate ΔV for Low-Thrust Spiral Climb,* 16.522, Space Propulsion.

[54] **Roncoli, R. B.** (2005). *Lunar Constants and Models Document.* Jet Propulsion Laboratory, California Institute of Technology.

[55] **Akin, D. L.** (2018). *Orbital Mechanics, ENAE 483/788D - Principles of Space Systems Design.* University of Maryland (presentation).

[56] **Ozimek, M. T.** (2010). *Low Thrust Trajectory Design and Optimization of Lunar South Pole Coverage Missions* (Doctoral dissertation). Purdeu University.

[57] **Choueiri, E. Y.** (2004). *A Critical History of Electric Propulsion: The First 50 Years (1906–1956).* Journal of Propulsion and Power, Vol. 20, No.2, March-April.

[58] **Lara, C. S.** (2016). *Design and Performance Analysis Study of an Ion Thruster* (Bachelor's Degree's Final Degree Project). Polytechnic University of Catalonia.

[59] **Bumbarger, P. P**. (2013). *Analysis of a Miniature Radio Frequency Ion Thruster with an Inductively Coupled Plasma Source.* Boise State Universtiy.

[60] **Goebel, D. M., Katz, I.** (2008). *Fundamentals of Electric Propulsion: Ion and Hall Thrusters.* Jet Propulsion Laboratory, California Institute of Technology.

[61] **Leiter, H., Kilinger, R., ..., Kukies, R.** (2001). *Development of the Radio Frequency Ion Thruster RIT XT – A Status Report.* Astrium GmbH, Germany.

[62] **Çelik, M., Turkoz, E.** (2013). *Prototype Design and Manufacturing Method of an 8 cm Diameter RF Ion Thruster.* Department of Mechanical Engineering, Bogazici University, Istanbul, Turkey.

[63] **Tsay, M., Frongillo, J., …, Paritsky, L**. (2016). *Flight Development of Iodine BIT-3 RF Ion Propulsion System for SLS EM-1 CubeSats.* 30th AIAA/USU Conference on Small Satellites, 6-11 August 2016, North Logan, Utah (Presentation).

[64] **Botha, J. R.** (2014). *Design of an RF Ion Thruster* (Master's thesis). Stellenbosh University.

[65] **Farnell, C.C.** (2007). *Performance and Lifetime Simulation of Ion Thruster Optics* (Doctoral dissertation). Colorado State University.

[66] **Dobkevicius, M.** (2017). *Modelling and Design of Inductively Coupled Radio Frequency Gridded Ion Thrusters with an Application to Ion Beam Shepherd Type Space Missions* (Doctoral dissertation). University of Suothampton.

[67] **Freg, B.** (2001). *Lecture Notes of Plasma Pysics.* University of Sydney NSW, AUSTRALIA.

[68]**<URL20>** Retrieved June 14, 2019 from *https://www.researchgate.net/publication/305112245_Effect_of_selfbias_on_the_elemental_composition_and_neutron_absorption_of_boron_carbide_films_deposited_by_RF_plasma_enhanced_CVD/figures.*

[69] **Liebermann, M. A., Liehtenberg, A. J.** (2005). *Principles of Plasma Discharges and Materials Processing.*

[70] **Andersen, H., Heigre, M. F., Sund, V.** (2016). *Design Proposal of Tigris - A CubeSat Ion Propulsion System.* Faculty of Engineering Science and Technology University of Tromso, The Arctic University of Norway.

[71] **Simon, J., Probst, U., Klar, P. J.** (2015). *Development of a Radio-Frequency Generator for RF Ion Thrusters.* Institute of Experimental Physics I, University of Giessen.

[72] **Dobkevicius, M., Feili, D., Müller, J.** (2015). *Comprehensive Radio – Frequency Ion Thruster Electromagnetic and Thermal Modelling.* 34th International Electric Propulsion Conference and 6th Nano-satellite Symposium,Hyogo-Kobe, Japan.

[73] **Simon, J., Volkmar, C., Proabst, U**. (n.d.). *High-Precision Power Measurement for Accurate Characterization of RF Ion Thruster.* Department of Electrical Engineering, Technische Hochschule Mittelhessen, University of Applied Seciences, Giessen, Germany.

[74] **Kindberg, P.** (n.d.). *Development of a Miniature Gridded Ion Thruster* (Master's thesis). SpaceMaster Program.

[75] **Çelik, M., Turan, N., Kokal, U., Kurt, H.** (n.d.). *Design Improvements and Experimental Measurements of BURFIT-80 RF Ion Thruster*. American Institute of Aeronautics and Astronautics.

[76] **Wang, J., Polk, J., Brophy, J., Katz, I.** (n.d). *Three Dimensional particle Simulations of NSTAR Ion Optics.* Jet Propulsion Laboratory, California Institute of Technology.

[77] **Holmes, A.J.T., & Thompson, E**. (1981). *Beam steering in tetrode extraction systems*. United States. doi:10.1063/1.1136568.

[78] **Beattie, J. R., Mattossian, J. N.** (1989). *Mercury Ion Thruster Technology*. Hughes Research Laboratories, National Aeronautics and Space Administration.

[79] **Sutton, G. P., Biblarz, O.** (2010). *Rocket Propulsion Elements.* Hoboken, New Jersey: John Wiley & Sons, Inc.

[80] **Hall, N.** (2015). *Specific Impulse.* Retrieved June 6, 2019 from *https://www.grc.nasa.gov/www/k-12/airplane/specimp.html.*

[81] **Chabert, P., Monreal, J., ..., Aanesland, A.** (2012). *Global Model of a Grided-ion Thruster Powered by a Radiofrequency Inductive Coil.* Physics of Plasma 19 .

[82] **Wade, M.** (1997-2019). *Electric / Mercury.* Retrieved June 9, 2019 from *http://www.astronautix.com/e/electricmercury.html.*

[83] **Rawlin, K., Patterson, M. J., Gruber, R. P.** (1990). *Xenon Ion Propulsion for Orbit Transfer.* Lewis Research Center, National Aeronautics and Space Administration.

[84] **Fearn, D. G.** (n.d.). *The UK-10 Ion Propulsion System – A Technology for Improving the Cost-Effectiveness of Communications Spacecraft.* Space Departments, Aerospace Establishment.

[85] **Wilbur, P. J., Rawlin, K., Beattie, J. R.** (1998). *Ion Thruster Development Trends and Status in the United States.* Journal of Propulsion and Power (Vol. 14, No. 5).

[86] **Sovey, J. S., Rawlin, V. K., Patterson, M. J.** (1999). *A Synopsis of Ion Propulsion Development projects in the United States: SERT I to Deep Space I.* Glenn Research Center, National Aeronautics and Space Administration.

[87]**<URL21>** Retrieved June 25, 2019 from *https://en.wikipedia.org/wiki/NEXT_**(ion_thruster).***

[88] **Leiter, J., Kukies, R.,..., Prost, P.** (2015). *Evolution of the AIRBUS DS GmbH Radio Frequency Ion Thruster Family.* Joint Conference of 30th International Symposium on Space Technology and Science 34th International Electric Propulsion Conference and 6th Nano-satellite Symposium, Hyogo-Kobe, Japan.

[89] **Nakles, M. R., ..., Corey, R. L.** (2011). A Performance Comparision of Xenon and Krypton Propellant on an SPT-100 Hall Thruster. *International Electric Propulsion Conferance.* Weisbaden, Germany.

[90] **Fazio, N., Gabriel, S. B., Golosnoy, I. O.** (2018). *Alternative Propellants for Gridded Ion Engines.* Univesity of Southampton.

[91] **Holste, K., ..., Schreiner, P. R.** (2015). In Search of Alternative Propellants for Ion Thrusters. *30th International Symposium on Space Technology and Secience, 34th International Electric Propulsion Conference and 6th Nano-satellite Symposium.* Hyogo-Kobe, Japan.

[92]**Propellant.** (n.d.). Retrieved June 9, 2019 from *https://www.buildtheenterprise.org/propellant/.*

[93]**<URL21>** Retrieved June 10, 2019 from *https://en.wikipedia.org/wiki/Variable_Specific_Impulse_Magnetoplasma_Rocket.*

[94] **Szabo, B., Freeman, C.** (2013). *Iodine Propellant Space Propulsion.* 33rd International Electric Propulsion Conference. Washington, DC., USA.

[95] **Busek Co.** (n.d.). *Busek, BHT-8000, Datasheet.* Retrieved December 1, 2018 from *http://busek.com/technologies__hall.htm.*

[96] **Clark, S**. (2019). *SpaceX releases new details on Starlink satellite design.* Retrieved June 9, 2019 from *https://spaceflightnow.com/2019/05/15/spacex-releases-new-details-on-starlink-satellite-design/.*

[97] **Busek Co.** (n.d.). *Busek, BHT-1500, Datasheet.* Retrieved December 1, 2018 from *http://busek.com/technologies__hall.htm.*

[98] **Meija J., ..., Prohaska, T.** (2015). *Atomic Weights of the Elements 2013 (IUPAC Technical Report).*

[99] **Petterson, M. J., Williams G. J.** (1992) *Krypton Ion Thruster.*

[100]**<URL21>** Retrieved September 11, 2019 from *https://www.wikizero.com/en/Borosilicate_glass.*

[101] **Sangregorio, M., Xie, K., …, Zhang, Z.** (2017). *Ion engine grids: Function, Main Parameters, Issues, Configurations, Geometries, Materials and Fabrication Methods.* Chinese Journal of Aeronautics.

[102] **Dobkevicius, M., Feili, D.** (2016). *A Coupled Performance and Thermal Model for Radio-frequency Gridded Ion Thrusters.* University of Southampton, Southampton.

[103]**<URL22>** Retrieved October 3, 2019 from *https://asri.technion.ac.il/node/462.*

[104]**<URL23>** Retrieved October 10, 2019 from *https://www.northropgrumman.com/Capabilities/PressurantTanks/Pages/default.aspx.*

[105]**<URL24>** Retrieved October 15, 2019 from *http://www.space-propulsion.com/brochures/.*

[106] **Yost, B.** (2019). *State of the Art of Small Spacecraft Technology, 07. Thermal Control.* National Astronautical Space Administration.

[107] **Levchenko, I., Xu, S., …, Keidat, M**. (n.d.) *Recent Progress and Perspective of Space Electric Propulsion Systems Based on Smart Nanomaterials.* Nature Communicaitons 9.

[108]**<URL25>** Retrieved November 5, 2019 from *https://www.nasa.gov/sites/default/files/trl.png*.

APPENDICES

APPENDIX A: Technology Readiness Levels are explained as Figure A.1.

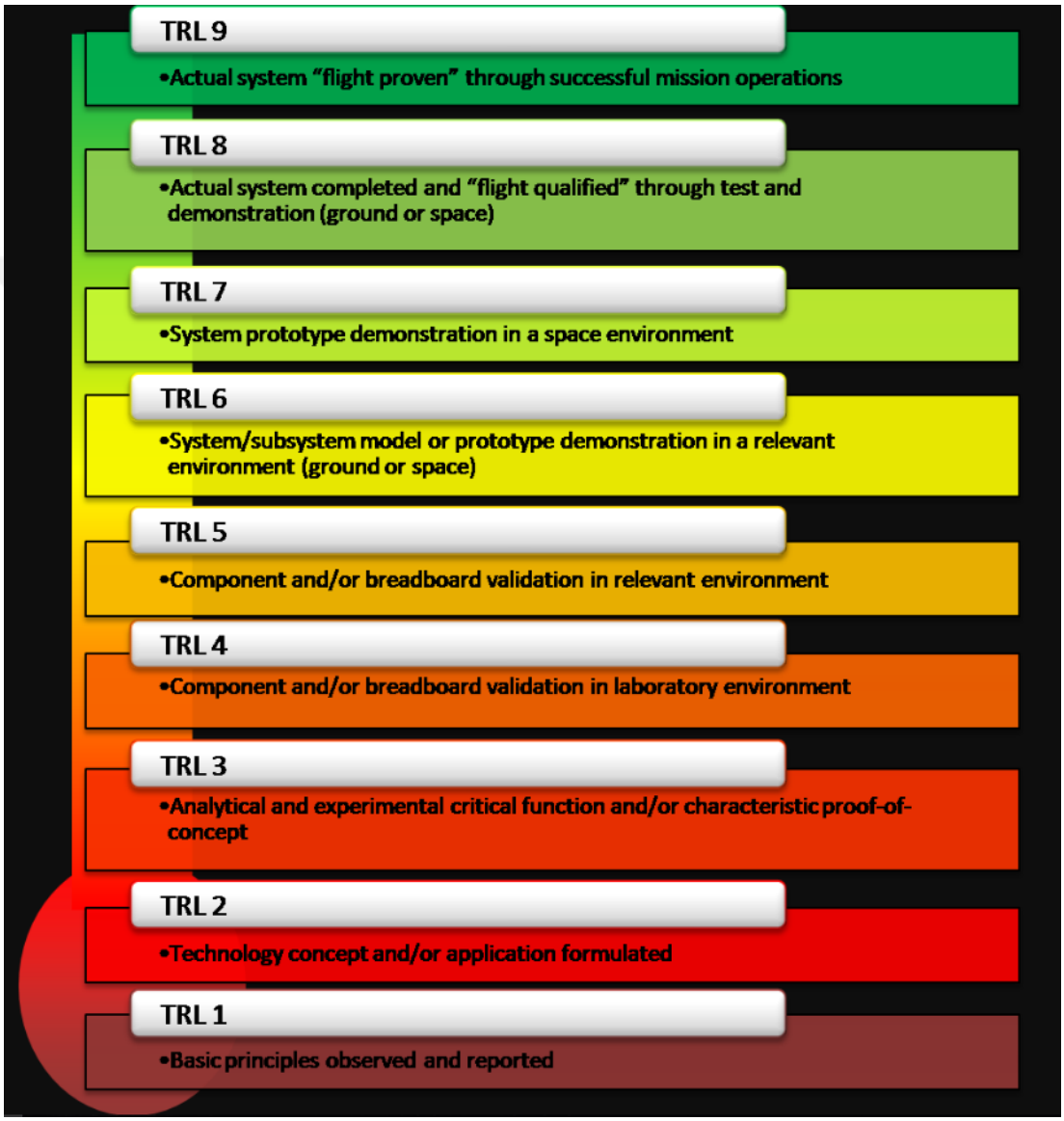

Figure A. 2: Technology Readiness Level Explanations [108].

CURRICULUM VITAE

Name Surname : Emine ÇALIK

Place and Date of Birth : Istanbul, 18.08.1994

E-Mail : emine.calik.tr@gmail.com

EDUCATION **:**

- **B.Sc.** **:** 2017, University of Turkish Aeronautical Association, Faculty of Aeronautics and Astronautics, Astronautical Engineering

PROFESSIONAL EXPERIENCE AND REWARDS:

- 2018 – Turkish Technic Inc., Tooling Engineer